ABSTRACT

OZBAG, FATIH. Stability Analysis of Combustion Waves in Porous Media. (Under the direction of Stephen Schecter.)

This thesis is devoted to the analysis of combustion waves that occur when air is injected into a porous medium containing initially some fuel. Our analysis consists of showing existence of traveling waves, studying stability of some of them, constructing possible generic wave sequences, showing numerical simulations and looking at an extension of the combustion system.

We begin by discussing the existence of various combustion waves for a system of three partial differential equations that give temperature, oxygen and fuel balance laws. After simplifying our model in a more convenient form, we use phase plane analysis to prove their existence.

Studying stability starts by determining the spectrum of the linearized system at a traveling wave. A weight function is required to stabilize the essential spectrum for certain waves. For the discrete spectrum, we perform a numerical computation of the Evans function for certain waves to show that there is no unstable discrete spectrum.

One problem during the stability analysis is that the system is partially parabolic so the linearized operator is not sectorial. We use recent results about partially parabolic systems to overcome this issue.

The thesis then identifies all possible generic wave sequences that solve boundary value problems. In addition, numerical simulations are presented for the generic wave sequences.

Lastly, extension to small diffusion of oxygen is studied to find a bound on the unstable eigenvalues by spectral energy estimates.

Stability Analysis of Combustion Waves in Porous Media

by
Fatih Ozbag

A dissertation submitted to the Graduate Faculty of
North Carolina State University
in partial fulfillment of the
requirements for the Degree of
Doctor of Philosophy

Applied Mathematics

Raleigh, North Carolina

2016

APPROVED BY:

Xiao-Biao Lin	Michael Shearer
Jesus Rodriguez	Stephen Schecter Chair of Advisory Committee

DEDICATION

To my parents Yasar Ozbag and Selver Ozbag

BIOGRAPHY

Fatih Ozbag was born in Kirikkale, Turkey on October 20th 1984. He earned his Bachelor of Science in Mathematics in 2006 from Gazi University in Ankara. He began his graduate work at Clemson University in 2008 and earned his Masters of Science in Mathematics in 2010. Then he joined PhD program at NCSU.

ACKNOWLEDGEMENTS

It is my honor to thank the many people who have helped me through this work.

First of all, I would like to express my deepest gratitude to my advisor Dr. Stephen Schecter for mentoring me throughout the whole time, and for his generous support and guidance. I truly appreciate his invaluable advice and the amount of time and effort he has invested in the development of this work.

Besides my advisor, i would like to sincerely thank Dr. Xiao-Biao Lin, Dr. Michael Shearer, Dr. Jesus Rodriguez for taking the time out of their schedules to be on my thesis advisory committee.

I would also like to thank Dr. Dan Marchesin (IMPA, Rio de Janeiro, Brazil) and Dr. Grigori Chapiro (UFJF, Juiz de Fora, Brazil) for their valuable contributions which added greatly to the thesis and for their kind hospitality while I was in Brazil. Special thanks to Dr. Grigori Chapiro for all his help and assistance in producing the numerical simulations that appear in chapter 8.

Thank you to Dr. Blake Barker, Dr. Jeffrey Humpherys and Dr. Kevin Zumbrun for providing the open source software STABLAB: a MATLAB-based numerical library for Evans function computation. I also wish to thank Dr. Blake Barker for valuable discussions regarding the Evans function computation that appear in chapter 6. I would also like to thank Dr. Jeffrey Humpherys for his valuable contributions and kind suggestions on spectral energy estimates.

Finally, I could not have completed this journey without my wonderful wife, Nazire. She has been the first to hear of my struggles and successes during the research for this dissertation. Thank you for the uncountable sacrifices that you made in helping to make this dream a reality. Thank you for your support through everything.

TABLE OF CONTENTS

LIST OF FIGURES . . . . . **vi**

Chapter 1 Introduction **1**

Chapter 2 Mathematical model and its traveling waves **4**

Chapter 3 Traveling wave equation and its equilibria **11**
3.1 Reduced traveling wave equation 11
3.2 Equilibria 14

Chapter 4 Existence of traveling waves **17**
4.1 Fast traveling waves ($0 < a < b < c$) 17
4.1.1 The curve C 18
4.1.2 Region 1 21
4.1.3 Region 2 23
4.1.4 Numerical results. 26
4.2 Slow traveling waves ($0 < c < a < b$) 27
4.3 Intermediate traveling waves ($0 < a < c < b$) 32

Chapter 5 Spectrum and exponential weight functions **39**

Chapter 6 Numerical results of Evans function for fast combustion waves **50**

Chapter 7 Stability analysis of combustion waves **56**
7.1 Assumptions 60
7.2 Eigenvalue problem 61
7.3 Hypotheses and proof of Theorem 7.0.1 62

Chapter 8 Contact discontinuities and wave sequences **65**
8.1 Right state of type FC 68
8.2 Right state of type OC 69
8.3 Right state of type TC 73

Chapter 9 Adding small diffusion to the model **81**
9.1 Spectral Energy Estimates 87

Chapter 10 Conclusion **94**

BIBLIOGRAPHY **96**

Appendix **100**
Appendix A Linear stability theorem 101

LIST OF FIGURES

Figure 4.1 Curve C, region 1 and region 2. 18
Figure 4.2 Phase portrait of (4.4)–(4.5) in P ($\rho \geq 0$) assuming $\frac{bY^+\rho^+}{(b-a)Y^++a\rho^+}+\theta^+ > 0$. In $\rho > 0$, $\dot{\rho} = 0$ for $\theta \leq 0$ and $\dot{\rho} > 0$ for $\theta > 0$. $\dot{\theta}$ changes from positive to negative when the null cline $(a\rho^+ + (b-a)Y^+)(\theta^+ - \theta) + bY^+(\rho^+ - \rho) = 0$ is crossed from left to right. 19
Figure 4.3 Phase portrait of (4.2)–(4.3) in P ($\rho \geq 0$) for (Y^+, c) in Region 1. The equilibrium $(\theta^+ + \frac{c}{c-a}\rho^+, 0)$ is a hyperbolic saddle. 22
Figure 4.4 Phase portrait of (4.14)–(4.15) in P ($\rho \geq 0$). 23
Figure 4.5 For (Y^+, c) in Region 2, phase portrait of (4.2)–(4.3) in P ($\rho \geq \rho^+ - \frac{c-b}{c}Y^+ > 0$, i.e., in $Y \geq 0$). 24
Figure 4.6 Curve C and $\tilde{C}$. 25
Figure 4.7 Phase portrait for (4.16)-(4.17). 25
Figure 4.8 Bifurcation diagram when $a = 0.5$, $b = 0.7$. 26
Figure 4.9 Bifurcation diagram when $a = b = 0.5$. 27
Figure 4.10 Bifurcation diagram when $a = 0.5$, $b = 0.55$. 27
Figure 4.11 a=b=0.5 28
Figure 4.12 a=0.5, b=0.7 28
Figure 4.13 For $0 < c < a$, phase portrait of (4.19)–(4.20). (a) $0 < c < \frac{\theta^+}{\theta^++\rho^+}a$. (b) $\frac{\theta^+}{\theta^++\rho^+}a < c < a$. 30
Figure 4.14 Phase portrait of (4.24)–(4.25). 31
Figure 4.15 After a small perturbation. 31
Figure 4.16 Phase portrait for (4.29)-(4.30). 33
Figure 4.17 Phase portrait for (4.35)-(4.36). 35
Figure 4.18 Phase portrait of (4.40)–(4.41) 37
Figure 4.19 After a small perturbation 37

Figure 6.1 Profile for the system (4.2)–(4.3) (left) and Evans function output for a semi-circular contour of radius 250 (right). We have $Y^+ = 8$. 52
Figure 6.2 Evans function of Figure 6.1, zoom in near 0, showing that 0 is inside the curve. 52
Figure 6.3 Profile for the system (4.2)–(4.3) (left) and Evans function output for a semi-circular contour of radius 250 (right). We have $Y^+ = 1.5$. . . . 53
Figure 6.4 Evans function of Figure 6.3, zoom in near 0, showing that 0 is inside the curve. 54
Figure 6.5 Profile for the system (4.2)–(4.3) (left) and Evans function output for a semi-circular contour of radius 2 (right). We have $Y^+ = 1.2$. 54
Figure 6.6 Evans function of Figure 6.5, zoom in near 0, showing that the curve winds twice around 0. 55

Figure 8.1 All possible generic wave sequences. Dashed and black arrows indicate dimension number 0 and 1 respectively. 69
Figure 8.2 Result of numerical simulation for the wave sequence $TC \xrightarrow{0} TC \cap FC \xrightarrow{a} FC \xrightarrow{b} FC$ with $a = 0.5$ and $b = 0.7$, demonstrating contact discontinuities of speed 0, a and b. Initial conditions (left) and simulation time 1000 (right). 70
Figure 8.3 Result of numerical simulation for the wave sequence $FC \xrightarrow{c_s} OC \xrightarrow{a} OC$ with $a = 0.5$, demonstrating a fuel-controlled to oxygen-controlled slow combustion wave followed by a contact discontinuity of speed a. Initial conditions (left) and simulation time 3500 (right). 71
Figure 8.4 Result of numerical simulation for the wave sequence $FC \xrightarrow{a} FC \xrightarrow{c_m} OC$ with $a = 0.5$, demonstrating a fuel-controlled to oxygen-controlled intermediate combustion wave that moves ahead of a contact discontinuity of speed 0. Initial conditions (left) and simulation time 3000 (right). 71
Figure 8.5 Result of numerical simulation for the wave sequence $TC \xrightarrow{0} TC \xrightarrow{c_s} OC \xrightarrow{a} OC$ with $a = 0.5$, demonstrating a temperature-controlled to oxygen-controlled slow combustion wave that moves ahead of a contact discontinuity of speed 0 and followed a contact discontinuity of speed a. Initial conditions (left) and simulation time 3500 (right). 72
Figure 8.6 Result of numerical simulation for the wave sequence $TC \xrightarrow{0} TC \xrightarrow{c_s} OC \xrightarrow{a} OC \cap TC \xrightarrow{b} TC$ with $a = 0.5$ and $b = 0.7$, demonstrating a temperature-controlled to oxygen-controlled slow combustion wave that moves ahead of a contact discontinuity of speed 0 and followed contact discontinuities of speed a and b. Initial conditions (left) and simulation time 3000 (right). 73
Figure 8.7 Result of numerical simulation for the wave sequence $TC \xrightarrow{0} TC \cap FC \xrightarrow{a} FC \xrightarrow{b} FC \xrightarrow{c_f} TC$ with $a = 0.5$ and $b = 0.7$, demonstrating a fuel-controlled to temperature-controlled fast combustion wave that moves ahead of contact discontinuities of speed a and b. Initial conditions (left) and simulation time 1900 (right). We take $Y^+ > Y_*^+$ to have FC to TC fast combustion wave as stated in Theorem 2.0.4(2). Once combustion starts, the produced high temperature zone remains behind the combustion front. 75
Figure 8.8 Result of numerical simulation for the wave sequence $TC \xrightarrow{0} TC \cap FC \xrightarrow{a} FC \xrightarrow{c_m} OC \xrightarrow{c_f} TC$ with a=0.5, demonstrating a fuel-controlled to oxygen-controlled intermediate combustion wave and oxygen controlled to temperature-controlled fast combustion wave that move ahead of contact discontinuities of speed 0 and a. Initial conditions (left) and simulation time 1600 (right). 75

Figure 8.9 Result of numerical simulation for the wave sequence $TC \xrightarrow{0} TC \cap FC \xrightarrow{a} FC \xrightarrow{c_m} TC \xrightarrow{b} TC$ with $a = 0.5$ and $b = 0.7$, demonstrating a fuel-controlled to temperature-controlled intermediate combustion wave that is preceded and followed by contact discontinuities of speed 0, a and b. Initial conditions (left) and simulation time 2500 (right). . 76
Figure 8.10 Result of numerical simulation for the wave sequence $FC \xrightarrow{c_s} OC \xrightarrow{a} OC \xrightarrow{c_f} TC$. with $a = 0.5$, demonstrating a fuel-controlled to oxygen-controlled slow combustion wave and oxygen-controlled to temperature-controlled fast combustion wave. Between these combustion waves there is a contact discontinuity of speed a. Initial conditions (left) and simulation time 1800 (right). 77
Figure 8.11 Result of numerical simulation for the wave sequence $FC \xrightarrow{a} FC \xrightarrow{c_m} OC \xrightarrow{c_f} TC$ with $a = 0.5$, demonstrating a fuel-controlled to oxygen-controlled intermediate combustion wave and oxygen-controlled to temperature controlled fast combustion wave that move ahead of contact discontinuity of speed a. Initial conditions (left) and simulation time 1750 (right). 78
Figure 8.12 Result of numerical simulation for the wave sequence $FC \xrightarrow{a} FC \xrightarrow{c_m} TC \xrightarrow{b} TC$ with $a = 0.5$ and $b = 0.7$, demonstrating a fuel-controlled to temperature-controlled intermediate combustion wave that is preceded and followed by contact discontinuities of speed a and b. Initial conditions (left) and simulation time 2500 (right). 79
Figure 8.13 Result of numerical simulation for the wave sequence $OC \xrightarrow{0} OC \xrightarrow{a} OC \xrightarrow{c_f} TC$ with $a = 0.5$, demonstrating an oxygen-controlled to temperature-controlled fast combustion wave that move ahead of contact discontinuities of speed 0 and a. Initial conditions (left) and simulation time 1500 (right). 80

Chapter 1

Introduction

Combustion waves are studied widely in heavy oil recovery techniques. There are several methods of enhanced oil recovery. The most commonly used approaches are air injection (in situ combustion), steam injection and water injection. In this paper we study combustion waves that occur when air is injected into a porous medium containing initially some fuel. The main goal behind in situ combustion (ISC) is to reduce the oil viscosity and enhance the oil flow. The recovery process with this method is hard to control and has explosion hazards. Due to safety risks use of this method is not widespread.

This thesis is devoted to the analysis of combustion waves in porous media. Combustion waves are continuous nontrivial traveling waves. A traveling wave is a solution of a partial differential equation that moves with constant velocity while maintaining its shape. Our analysis consists of showing existence of traveling waves, studying stability of some of them, constructing possible generic wave sequences, showing numerical simulations and looking at extension to small diffusion of oxygen.

We consider here a combustion system that is derived in [9]. It is a partly parabolic system which has diffusion in one equation and no diffusion in others. In chapter 2 we describe our model which consists of three equations that give temperature, oxygen and fuel balance laws. It is based on one proposed in [1] and expanded in [6], [7] and [9]. In our system we ignore the diffusion of oxygen and also have solid reactant that does not diffuse. In [9] oxygen and heat are both moving at exactly the same velocity of the moving gas. In this work we assume the oxygen is transported faster than the temperature which is physically more realistic. We define the generic boundary conditions and generic waves. Then we state our theorems about the existence of combustion waves.

We consider only combustion waves that approach both end states exponentially. We find six types of combustion waves in this pattern. We have two fast combustion waves that propagate faster than oxygen and temperature, and two slow combustion waves called "reaction-trailing smolder waves" [2] that propagate more slowly than oxygen and temperature. We also find two intermediate combustion waves that propagate more slowly than oxygen but faster than temperature. The intermediate combustion waves have been called "reaction-leading smolder waves" studied in [2] and [31].

In a fast combustion wave, combustion begins with both oxygen and fuel present at the right in a low temperature region. Once it starts, it runs to the right where oxygen and fuel are present. Since heat is transported at a lower velocity, the heat produced remains behind the combustion front. The reaction stops when either oxygen or fuel is exhausted. In a slow combustion wave, combustion begins when the moving gas transports oxygen into a region in which solid fuel and high temperature are present. Combustion occurs behind the incoming gas. It can not start ahead since there is no oxygen. The reaction stops once the solid fuel is exhausted or because the incoming gas is low temperature. Intermediate combustion waves are similar to the slow combustion waves. The main difference is that the oxygen velocity is greater than that of the flame front and temperature velocity is less than that of the flame front. Thus the high temperature region stays behind the wave. Combustion cannot occur ahead of the front since there is low temperature or no oxygen or both.

Our model can be simplified in a convenient form which allows us to prove the existence of traveling waves by a technique for studying the behavior of nonlinear systems that is called phase plane analysis. In section 3.1 the traveling wave system is reduced to two dimensions and then equilibria of the traveling wave equation are determined in section 3.2.

In section 4.1, 4.2 and 4.3 we prove the existence of fast, slow and intermediate combustion waves using phase plane analysis.

Once the existence of the combustion waves is proved, we focus on their stability. The first step of the stability analysis is to find the spectrum of the operator which we obtain from the linearization of the partial differential equation system about traveling wave. The spectrum of the operator will then provide information about stability of the wave. To find the spectrum, first we find essential spectrum which is done in chapter 5 by using Fourier transform. For the discrete spectrum, we study certain waves and

perform a numerical computation of the Evans function which is an analytic function whose zeros correspond to the isolated eigenvalues of the differential operator. It is used to show that there is no unstable discrete spectrum. However some of the waves turn out to be unstable.

In chapter 7 the stability of the combustion waves is studied. Stability of a traveling wave is sometimes called nonlinear stability which means that a small perturbation of the traveling wave stays close to the set of all translates of the traveling wave. We face some problems during the stability analysis. One of the problems is that the essential spectrum is *marginally* stable. For certain waves this problem can be cured by working in a weighted space. The other issue is that the system is partially parabolic so the linearized operator is not sectorial. We use recent results in [15] to overcome this issue.

Contact discontinuities and wave sequences are discussed in chapter 8. We only consider generic wave sequences; in particular the reaction does not occur for one reason only at both end states. Moreover we give our theorems that state only certain contact discontinuities can appear in generic wave sequences. Lastly numerical simulations are presented for the generic wave sequences that we expect to occur for large time.

Finally, in chapter 9 we show that adding small diffusion to the oxygen equation does not change the traveling waves. However it can cause some difference on the continuous spectrum. Therefore we find the spectrum for the system with diffusion added. In section 9.1, with this new system, we are able to find a bound on the eigenvalues by using the similar study of [12].

Chapter 2

Mathematical model and its traveling waves

The original model was proposed in [1]. In this chapter we present the simplified version of this model used in [9]. We consider combustion waves that occur when air is injected into a porous medium containing initially solid fuel that is immobile and does not vaporize.

In time–space coordinate the model includes the heat balance equation (2.1), the molar balance equations for fuel (2.2) and oxygen (2.3). We ignore gas diffusion as in [1]. Same notation and assumptions are used as in [6]. The balance equations for energy, fuel and oxygen are:

$$\begin{aligned} \frac{\partial((C_m + \varphi c_g \rho_g)(T - T_{res}))}{\partial t} + \frac{\partial(c_g \rho_g u (T - T_{res}))}{\partial x} &= \lambda \frac{\partial^2 T}{\partial x^2} + Q_r \rho Y W_r, \quad (2.1) \\ \frac{\partial \rho}{\partial t} &= -\mu_f \rho Y W_r, \quad (2.2) \\ \varphi \frac{\partial(Y \rho_g)}{\partial t} + \frac{\partial(Y \rho_g u)}{\partial x} &= -\mu_o \rho Y W_r \quad (2.3) \end{aligned}$$

where T $[K]$ is the temperature, Y $[mole/mole]$ is the oxygen molar fraction in the gas, ρ $[mole/m^3]$ is the molar concentration of immobile fuel. We assume that rest of the quantities are constant as in [1]: C_m $[J/m^3K]$, heat capacity of the porous medium; c_g $[J/mole\,K]$, heat capacity of the gas; T_{res} $[K]$, initial reservoir temperature; λ $[J/(m\,s\,K)]$, thermal conductivity of the porous medium; Q_r $[J/mole]$, the immobile fuel combustion enthalpy at T_{res}; ρ_g $[mole/m^3]$, molar density of gas; u $[m/s]$, gas injection rate; φ $[m^3/m^3]$, porosity of the medium.

In the reaction, we assume that one mole of immobile fuel reacts with one mole of oxygen to generate one mole of gaseous products that yields the scalar stoichiometric coefficients $\mu_f = \mu_o = 1$. The reaction rate is usually governed by the Arrhenius' law as $W_r = k_p \exp(-E/RT)$. Instead we use shifted Arrhenius' law as

$$W_r = \begin{cases} k_p \exp\left(\frac{-E}{R(T-T_{ign})}\right), & T > T_{ign}, \\ 0, & T \leq T_{ign}, \end{cases} \tag{2.4}$$

where E is the activation energy; R is the ideal gas constant; T_{ign} is the ignition temperature; and k_p is the pre-exponential factor.

In order to derive the nondimensionalized version of the equations (2.1)–(2.4), we present the dimensionless dependent and independent variables (denoted by tildes) as ratios of the dimensional quantities and reference quantities (denoted by stars):

$$\tilde{t} = \frac{t}{t^*}, \quad \tilde{x} = \frac{x}{x^*}, \quad \tilde{\theta} = \frac{T - T_{ign}}{\Delta T^*}, \quad \tilde{\rho} = \frac{\rho}{\rho^*}, \quad \tilde{Y} = \frac{Y}{Y^*}. \tag{2.5}$$

To simplify the equations (2.1)–(2.4), we choose the reference quantities as

$$\Delta T^* = \frac{E}{R}, \;\; t^* = \frac{\varphi Q_r \rho_g}{k_p C_m^* \Delta T^*}, \;\; Y^* = \frac{1}{k_p t^*}, \;\; \rho^* = \frac{\varphi \rho_g}{k_p t^*}, \;\; x^* = \sqrt{\frac{\lambda t^*}{C_m^*}}, \tag{2.6}$$
$$C_m^* = C_m + \varphi c_g \rho_g.$$

We nondimensionalize the equations (2.1)–(2.4) by using (2.5)–(2.6). Omitting the tildes, we have the following model that is described by three dependent variables that are temperature θ ($\theta = 0$ corresponds to $T = T_{ign}$), oxygen fraction Y and fuel concentration ρ:

$$\partial_t \theta + a \partial_x \theta = \partial_{xx} \theta + \rho Y \Phi, \tag{2.7}$$

$$\partial_t \rho = -\rho Y \Phi, \tag{2.8}$$

$$\partial_t Y + b \partial_x Y = -\rho Y \Phi, \tag{2.9}$$

$$\Phi = \begin{cases} e^{(-1/\theta)}, & \theta > 0 \\ 0, & \theta \leq 0 \end{cases} \tag{2.10}$$

where a and b are dimensionless thermal and oxygen wave speeds given by:

$$a = \frac{c_g \rho_g u t^*}{x^* C_m^*}, \quad b = \frac{u t^*}{\varphi x^*}. \tag{2.11}$$

We assume $a < b$ which is correct in rock porous media since the thermal capacity of the gas c_g is much less than the thermal capacity of the substrate C_m. See [9] for more information for the derivation of the model.

Combustion can occur at an ignition temperature when air is injected into a porous medium containing initially solid fuel. We normalize so that $\theta = 0$ corresponds to ignition temperature where reaction can not occur when the temperature is below the ignition temperature. The first equation (2.7) is the heat balance equation represents transport and diffusion of temperature and production of energy in the chemical reaction. Equation (2.8) is the immobile fuel balance equation that represents consumption of the solid fuel. Equation (2.9) is the oxygen balance equation that consists of transport and consumption of oxygen. We neglect the diffusion of oxygen until chapter 9.

We only consider the solutions such that both solid fuel and the oxygen are nonnegative everywhere. We have constant boundary conditions for (2.7)–(2.9) on $-\infty < x < \infty$, $t \geq 0$

$$(\theta, \rho, Y)(-\infty) = (\theta^L, \rho^L, Y^L), \qquad (\theta, \rho, Y)(\infty) = (\theta^R, \rho^R, Y^R). \tag{2.12}$$

Reaction can not occur at the boundaries since the reaction ceases due to low temperature $\theta \leq 0$ (temperature control or TC), lack of fuel $\rho = 0$ (fuel control or FC) or lack of oxygen $Y = 0$ (oxygen control or OC). Two or all three of these conditions can exist simultaneously. For example, there can be neither oxygen nor fuel at the left state. We only consider the generic boundary conditions: only one of the following conditions holds at the left state: $\theta^L \leq 0$, or $\rho^L = 0$, or $Y^L = 0$ and at the right state: $\theta^R \leq 0$, or $\rho^R = 0$, or $Y^R = 0$. The other two components are positive for left and right state.

A wave with velocity c can be denoted by $(\theta^-, \rho^-, Y^-) \xrightarrow{c} (\theta^+, \rho^+, Y^+)$ where (θ^-, ρ^-, Y^-) is left state and (θ^+, ρ^+, Y^+) is right state. For example, a wave of velocity c from a left state of type $TC \cap FC$ to a right state of type OC can be indicated $TC \cap FC \xrightarrow{c} OC$. Since we are only interested in generic wave sequences, TC, FC, and OC can be the first or last state of a wave sequence. For example $TC \cap OC$ can not be the first and last state of a wave sequences but it can appear between left and right end states.

We only consider the waves with $\rho \geq 0$ and $Y \geq 0$. We also limit our attention to waves that approach end states exponentially, except that we sometimes discuss other waves in order to explain how these fit together. Only combustions waves with velocity $c > 0$ are considered.

Theorem 2.0.1. *There exist two types of fast combustion waves with velocity* $c_f > b > a$

- $FC \xrightarrow{c_f} TC$.
- $OC \xrightarrow{c_f} TC$.

Right end state has low-temperature in a fast combustion wave. Once the reaction occurs, combustion front moves to the right by leaving the high temperature zone behind. Behind the combustion front the reaction ceases due to lack of fuel or lack of oxygen or both. In section 4.1 we prove the existence of these fronts.

Theorem 2.0.2. *There exist two types of slow combustion waves with velocity* $b > a > c_s$

- $FC \xrightarrow{c_s} OC$.
- $TC \xrightarrow{c_s} OC$.

There is no oxygen at right state in a slow combustion wave. Therefore reaction can not start ahead of the incoming gas. Once the combustion begins behind the incoming gas, generated high temperature zone is transported ahead of the combustion front since $c < a < b$. The reaction ceases due to lack of fuel or low temperature. In section 4.2 we prove the existence of these fronts.

Theorem 2.0.3. *There exist two types of intermediate combustion wave with velocity* $b > c_m > a$

- $FC \xrightarrow{c_m} OC$.
- $FC \xrightarrow{c_m} TC$.

Intermediate combustion wave is slightly different than slow ones. In an intermediate combustion wave, heat produced by the combustion stays behind the combustion front since $a < c < b$. Behind the front the reaction stops because the fuel is entirely consumed.

Theorem 2.0.4. *Fast Combustion Waves.*

1. *$FC \cap OC \xrightarrow{c_f} TC$ Waves. Fix $b > a > 0$. Let $\theta^+ \leq 0$, $\rho^+ > 0$ with $(b-a)\theta^+ + b\rho^+ > 0$. Then there are numbers $\theta^- > 0$, $c_f > b > a$ and unique $Y_*^+ > 0$, such that there is a combustion wave of type $FC \cap OC \xrightarrow{c_f} TC$, i.e. $(\theta^-, \rho^- = 0, Y^- = 0) \xrightarrow{c_f} (\theta^+, \rho^+, Y^+)$. Moreover*

$$\theta^- = \theta^+ + \frac{bY_*^+\rho^+}{(b-a)Y_*^+ + a\rho^+}, \quad c_f = \frac{bY_*^+}{Y_*^+ - \rho^+}.$$

   These waves approach only their right state exponentially.

2. *$FC \xrightarrow{c_f} TC$ and $OC \xrightarrow{c_f} TC$ Waves. Fix $b > a > 0$. Let $\theta^+ \leq 0$ and $\rho^+ > 0$. If $Y^+ > Y_*^+$,*

   (a) *there exists a combustion wave of type $FC \xrightarrow{c_f} TC$, i.e. $(\theta^-, \rho^- = 0, Y^-) \xrightarrow{c_f} (\theta^+, \rho^+, Y^+)$ where $\theta^- > 0$, $Y^- > 0$ and $c_f > b > a$. θ^-, Y^- and c_f are related by the formulas*

$$\theta^- = \theta^+ + \frac{b\rho^+(Y^+ - Y^-)}{(b-a)(Y^+ - Y^-) + a\rho^+}, \quad c_f = \frac{b(Y^+ - Y^-)}{Y^+ - Y^- - \rho^+}.$$

   (b) *there exists a combustion wave of type $OC \xrightarrow{c_f} TC$, i.e. $(\theta^-, \rho^-, Y^- = 0) \xrightarrow{c_f} (\theta^+, \rho^+, Y^+)$ where $\theta^- > 0$, $\rho^- > 0$ and $c_f > b > a$. θ^-, ρ^- and c_f are related by the formulas*

$$\theta^- = \theta^+ + \frac{bY^+(\rho^+ - \rho^-)}{(b-a)Y^+ + a(\rho^+ - \rho^-)}, \quad c_f = \frac{bY^+}{Y^+ + \rho^- - \rho^+}.$$

   These waves approach both end states exponentially.

Other than possible non uniqueness of the waves described in parts 2a and 2b, there are no other combustion waves with $c_f > b > a$ and $\theta^+ + \frac{bY^+\rho^+}{(b-a)Y^+ + a\rho^+} > 0$ that approach the right state exponentially.

If $\theta^+ + \frac{bY^+\rho^+}{(b-a)Y^+ + a\rho^+} \leq 0$, there are no traveling waves with right state (θ^+, ρ^+, Y^+). For given θ^+ and ρ^+, if the right state has sufficient amount of oxygen, then reaction can occur until all the oxygen is consumed or all the fuel is consumed.

Theorem 2.0.5. *Slow Combustion Waves.*

1. *FC* $\xrightarrow{c_s}$ *OC and* $FC \cap TC \xrightarrow{c_s}$ *OC Waves. Fix* $b > a > 0$. *Let* $(\theta^-, 0, Y^-)$ *have* $\theta^- \geq 0$ *and* $Y^- > 0$. *Then for each* $\rho^+ > 0$, *such that* $(a-b)Y^- + a\rho^+ > 0$, *there are numbers* $\theta^+ > 0$ *and* c_s, $0 < c_s < a < b$, *such that there exists a combustion wave of velocity* c_s *from* $(\theta^-, 0, Y^-)$ *to* $(\theta^+, \rho^+, 0)$. *In fact,*

$$\theta^+ = \theta^- + \frac{bY^-\rho^+}{(a-b)Y^- + a\rho^+}, \quad c_s = \frac{bY^-}{\rho^+ + Y^-}. \tag{2.13}$$

   These waves approach their right state exponentially, and approach their left state exponentially if and only if $\theta^- > 0$, *i.e., if and only if the left state is of type FC.*

2. *TC* $\xrightarrow{c_s}$ *OC Waves. Fix* $b > a > 0$. *Let* $\theta^- < 0$, Y^- *with* $\theta^- + \frac{b}{a}Y^- > 0$, *and* $\rho^+ > 0$ *be given. Then there are numbers* $\rho^- > 0$, $\theta^+ > 0$, *and* c_s, $0 < c_s < a < b$, *such that there exists a combustion wave of velocity* c_s *from* (θ^-, ρ^-, Y^-) *to* $(\theta^+, \rho^+, 0)$. *Moreover* $\theta^+ = \theta^- + \frac{b(\rho^+ - \rho^-)Y^-}{a(\rho^+ - \rho^-) - (b-a)Y^-}$, *and the quantities* c_s *and* ρ^- *are related by the formula*

$$c_s = \frac{bY^-}{Y^- - \rho^- + \rho^+}.$$

   These waves approach both end states exponentially.

3. *There are no other combustion waves* $0 \leq c \leq a \leq b$. *In particular, there are no slow combustion waves with* $\theta^- + \frac{b(\rho^+ - \rho^-)Y^-}{a(\rho^+ - \rho^-) - (b-a)Y^-} \leq 0$.

Theorem 2.0.6. *Intermediate Combustion Waves.*

1. *FC* $\xrightarrow{c_m}$ *OC Waves. Fix* $b > a > 0$. *Let* $\theta^+ > 0$ *and* $\rho^+ > 0$. *Then for each* $Y^- > 0$, *such that* $(a-b)Y^- + a\rho^+ < 0$, *there are numbers* $\theta^- > 0$ *and* c_m, $0 < a < c_m < b$, *such that there exists a combustion wave of velocity* c_m *from* $(\theta^-, 0, Y^-)$ *to* $(\theta^+, \rho^+, 0)$. *In fact,*

$$\theta^- = \theta^+ + \frac{bY^-\rho^+}{(b-a)Y^- - a\rho^+}, \quad c_m = \frac{bY^-}{\rho^+ + Y^-}. \tag{2.14}$$

   These waves approach their right and left state exponentially.

2. *FC* $\xrightarrow{c_m}$ $OC \cap TC$ *Waves. Fix* $b > a > 0$. *Let* $\theta^+ = 0$ *and* $\rho^+ > 0$. *Then for each* $Y^- > 0$, *such that* $(a-b)Y^- + a\rho^+ < 0$, *there are numbers* $\theta^- > 0$ *and* c_m,

$0 < a < c_m < b$, *such that there exists a combustion wave of velocity* c_m *from* $(\theta^-, 0, Y^-)$ *to* $(0, \rho^+, 0)$. *In fact,*

$$\theta^- = \frac{b\rho^+ Y^-}{(b-a)Y^- - a\rho^+}, \quad c_m = \frac{bY^-}{Y^- + \rho^+}. \tag{2.15}$$

These waves approach only their left state exponentially.

3. *FC* $\xrightarrow{c_m}$ *TC Waves. Fix* $b > a > 0$. *Let* $\theta^+ < 0$ *and* $\rho^+ > 0$. *Then for each* $Y^- > 0$, *such that* $(a-b)Y^- + a\rho^+ < 0$, *there are numbers* $\theta^- > 0$, $Y^+ > 0$ *and* c_m, $0 < a < c_m < b$, *such that there exists a combustion wave of velocity* c_m *from* $(\theta^-, 0, Y^-)$ *to* (θ^+, ρ^+, Y^+). *In fact,*

$$\theta^- = \theta^+ + \frac{b\rho^+(Y^+ - Y^-)}{(b-a)(Y^+ - Y^-) + a\rho^+}, \quad c_m = \frac{b(Y^+ - Y^-)}{Y^+ - Y^- - \rho^+}. \tag{2.16}$$

These waves approach their right and left state exponentially.

Chapter 3

Traveling wave equation and its equilibria

In this chapter we derive the traveling wave equation for our model, reduce it to two dimensions and study equilibria.

3.1 Reduced traveling wave equation

First we add equation (2.8) to (2.7), then replace (2.8). Next we substract equation (2.8) from (2.9), then replace (2.9). We obtain

$$\partial_t\theta + a\partial_x\theta = \partial_{xx}\theta + \rho Y\Phi(\theta), \tag{3.1}$$

$$\partial_t(\theta+\rho) + a\partial_x\theta = \partial_{xx}\theta, \tag{3.2}$$

$$\partial_t(Y-\rho) + b\partial_x Y = 0. \tag{3.3}$$

In (3.1)–(3.3), we replace the spatial coordinate x with the moving coordinate $\xi = x - ct$ with velocity c. We obtain

$$\partial_t\theta = (c-a)\partial_\xi\theta + \partial_{\xi\xi}\theta + \rho Y\Phi(\theta), \tag{3.4}$$

$$\partial_t(\theta+\rho) = (c-a)\partial_\xi\theta + \partial_{\xi\xi}\theta + c\partial_\xi\rho, \tag{3.5}$$

$$\partial_t(Y-\rho) = (c-b)\partial_\xi Y - c\partial_\xi\rho. \tag{3.6}$$

We can find a traveling wave solution of (2.7)–(2.9) with velocity c by considering a stationary solution of (3.4)–(3.6). Stationary solutions of (3.4)–(3.6) satisfy the system of ODEs

$$0 = (c-a)\partial_\xi\theta + \partial_{\xi\xi}\theta + \rho Y\Phi(\theta), \tag{3.7}$$

$$0 = (c-a)\partial_\xi\theta + \partial_{\xi\xi}\theta + c\partial_\xi\rho, \tag{3.8}$$

$$0 = (c-b)\partial_\xi Y - c\partial_\xi\rho. \tag{3.9}$$

In (3.7), let $v_1 = \partial_\xi\theta$, and integrate (3.8)–(3.9). Note that dot denotes the derivative with respect to ξ. Then we obtain the system

$$\dot{\theta} = v_1, \tag{3.10}$$

$$\dot{v}_1 = (a-c)v_1 - \rho Y\Phi(\theta), \tag{3.11}$$

$$w_1 = (c-a)\theta + v_1 + c\rho, \tag{3.12}$$

$$w_2 = (c-b)Y - c\rho, \tag{3.13}$$

where w_1 and w_2 are constants. We will show below (Proposition 3.1.1) that there are no traveling waves when $c = a$ and $c = b$. We therefore assume $c \neq a$ and $c \neq b$. In (3.10)–(3.11) we substitute for v_1 using (3.12) and for Y using (3.13). We obtain the reduced traveling wave system

$$\dot{\theta} = (a-c)\theta - c\rho + w_1, \tag{3.14}$$

$$\dot{\rho} = \frac{c\rho + w_2}{c(c-b)}\rho\Phi(\theta), \tag{3.15}$$

where (w_1, w_2) is a vector of parameters.

The system (3.14)–(3.15) has two invariant lines $\rho = 0 \quad \text{and} \quad \rho = -\frac{w_2}{c}$. The invariant line $\rho = -\frac{w_2}{c}$ corresponds to $Y = 0$ since $Y = \frac{c\rho + w_2}{c-b}$.

The phase space for (3.14)–(3.15) is the set $P = \{(\theta, \rho) : \rho \geq 0 \quad \text{and} \quad Y \geq 0\}$. We will always restrict to $(\theta, \rho) \in P$. From (3.13), we have three cases

1. if $0 < c < a < b$, $Y \geq 0$ if and only if $\rho \leq -\frac{w_2}{c}$,
2. if $0 < a < c < b$, $Y \geq 0$ if and only if $\rho \leq -\frac{w_2}{c}$,
3. if $c > b > a$, $Y \geq 0$ if and only if $\rho \geq -\frac{w_2}{c}$.

In the first and second case, P is nonempty if $w_2 \leq 0$; $P = \{(\theta, \rho) : 0 \leq \rho \leq -\frac{w_2}{c}\}$. In the third case, $P = \{(\theta, \rho) : \rho \geq \max(0, -\frac{w_2}{c})\}$. In both cases P is invariant.

We now show:

Proposition 3.1.1. *Consider the system* (2.7)–(2.9)

1. *Suppose $c = a$. Then there are no traveling waves for the system* (2.7)–(2.9).

2. *Suppose $c = b$. Then there are no traveling waves for the system* (2.7)–(2.9).

Proof. For case (1), let $c = a$ in (3.10)–(3.13). We have

$$\dot{\theta} = v_1, \tag{3.16}$$

$$\dot{v}_1 = -\rho Y \Phi(\theta), \tag{3.17}$$

$$w_1 = v_1 + c\rho, \tag{3.18}$$

$$w_2 = (c - b)Y - c\rho, \tag{3.19}$$

where w_1 and w_2 are constants.

In (3.16)–(3.17) we substitute for v_1 using (3.18) and for Y using (3.19). We obtain the reduced system.

$$\dot{\theta} = -c\rho + w_1, \tag{3.20}$$

$$\dot{\rho} = \frac{c\rho + w_2}{c(c - b)} \rho \Phi(\theta), \tag{3.21}$$

$\dot{\theta} = 0$ is the line $\rho = \frac{w_1}{c}$ and the set $\dot{\rho} = 0$ consists of two lines $\rho = 0$ and $\rho = \frac{-w_2}{c}$ and the half-space $\theta \leq 0$. The system (3.20)–(3.21) has a set of equilibrium points which is $\{(\theta, \rho) : \theta \leq 0 \text{ and } \quad \rho = \frac{w_1}{c}\}$. It is clear to see that there is no possibility to have a traveling wave with velocity $c > 0$.

For case (2), let $c = b$ in (3.10)–(3.13). After simplification, we have

$$\dot{\theta} = w_1 + w_2 + (a - c)\theta, \tag{3.22}$$

$$\dot{v_1} = (a - c)v_1 + \frac{w_2}{c} Y\Phi(\theta), \tag{3.23}$$

$$w_1 = (c - a)\theta + v_1 - w_2, \tag{3.24}$$

where w_1 and w_2 are constants.

In (3.22) we can solve for θ since w_1 and w_2 are constants and θ is the only variable. The solution of (3.22) is $\theta(\xi) = \frac{w_1+w_2}{c-a} + ke^{(a-c)\xi}$ where k is constant. Once we know θ, we substitute it into (3.24) then determine v_1. Therefore in (3.23) we can solve for Y. We find that the only solutions of (3.22) that approach constants at $\pm\infty$ are themselves constant. The result follows.

□

3.2 Equilibria

To find all equilibria of (3.14)–(3.15) we set $\dot{\theta} = 0$ and $\dot{\rho} = 0$. If an equilibrium is a FC equilibrium, then it has no fuel ($\rho = 0$), does have oxygen ($Y > 0$) and positive temperature ($\theta > 0$), i.e.

$$FC = \{(\theta, \rho) \in P : \theta > 0,\ \rho = 0,\ c\rho + w_2 \neq 0,\ \text{and}\ (a - c)\theta - c\rho + w_1 = 0\}.$$

If an equilibrium is an OC equilibrium, then it has no oxygen ($Y = 0$) and does have fuel ($\rho > 0$) and positive temperature ($\theta > 0$), i.e.

$$OC = \{(\theta, \rho) \in P : \theta > 0,\ \rho > 0,\ c\rho + w_2 = 0,\ \text{and}\ (a - c)\theta - c\rho + w_1 = 0\}.$$

If an equilibrium is a $FC \cap OC$ equilibrium, then it has no oxygen ($Y = 0$), no fuel ($\rho = 0$) and does have positive temperature ($\theta > 0$), i.e.

$$FC \cap OC = \{(\theta, \rho) \in P : \theta > 0,\ \rho = 0,\ c\rho + w_2 = 0,\ \text{and}\ (a - c)\theta - c\rho + w_1 = 0\}.$$

If an equilibrium is a TC equilibrium, then it has fuel ($\rho > 0$), oxygen ($Y > 0$) and low temperature ($\theta \leq 0$), i.e.

$$TC = \{(\theta, \rho) \in P : \theta \leq 0, \rho > 0, c\rho + w_2 > 0 \text{ and } (a-c)\theta - c\rho + w_1 = 0\}.$$

If an equilibrium is a $FC \cap TC$ equilibrium, then it has no fuel ($\rho = 0$) and does have oxygen($Y > 0$) and low temperature ($\theta \leq 0$), i.e.

$$FC \cap TC = \{(\theta, \rho) \in P : \theta \leq 0,\ \rho = 0,\ c\rho + w_2 > 0,\ \text{and } (a-c)\theta - c\rho + w_1 = 0\}.$$

If an equilibrium is an $OC \cap TC$ equilibrium, then it has no oxygen ($Y = 0$) and does have fuel ($\rho > 0$) and low temperature ($\theta \leq 0$), i.e.

$$OC \cap TC = \{(\theta, \rho) \in P : \theta \leq 0,\ \rho > 0,\ c\rho + w_2 = 0,\ \text{and } (a-c)\theta - c\rho + w_1 = 0\}.$$

If an equilibrium is a $FC \cap TC \cap OC$ equilibrium, then it has no fuel ($\rho = 0$), no oxygen ($Y = 0$) and low temperature ($\theta \leq 0$), i.e.

$$FC \cap TC \cap OC = \{(\theta, \rho) \in P : \theta \leq 0,\ \rho = 0,\ c\rho + w_2 = 0,\ \text{and } (a-c)\theta - c\rho + w_1 = 0\}.$$

The last four subsets are called low-temperature equilibria.

The set of equilibria of (3.14)–(3.15) is the union of these seven subsets. Let H be the line defined by $(a-c)\theta - c\rho + w_1 = 0$. It contains all equilibria. The invariant lines $\rho = -\frac{w_2}{c}$ and $\rho = 0$ each contain only one equilibrium.

The linearization of (3.14)–(3.15) at a point (θ, ρ) has the matrix

$$\begin{pmatrix} a-c & -c \\ \dfrac{c\rho + w_2}{c(c-b)}\rho\Phi'(\theta) & \dfrac{2c\rho + w_2}{c(c-b)}\Phi(\theta) \end{pmatrix}. \tag{3.25}$$

If (θ, ρ) is a low-temperature equilibrium, (3.25) becomes

$$\begin{pmatrix} a-c & -c \\ 0 & 0 \end{pmatrix}. \tag{3.26}$$

Proposition 3.2.1. *If an equilibrium is a low-temperature equilibrium, then one eigenvalue is $a-c$, with eigenvector $(1, 0)$; the other eigenvalue is 0 with eigenvector $(c, a-c)$.*

If $(\theta, \rho) \in FC$ or $FC \cap OC$, (3.25) becomes

$$\begin{pmatrix} a-c & -c \\ 0 & \dfrac{w_2}{c(c-b)}\Phi(\theta) \end{pmatrix}. \tag{3.27}$$

In FC, $Y > 0$ and $\rho = 0$, so $w_2 = (c-b)Y - c\rho = (c-b)Y$ has the sign of $c-b$. If $Y = 0$ and $\rho = 0$ that is $FC \cap OC$, then $w_2 = 0$. Therefore:

Proposition 3.2.2. *If an equilibrium is in FC or $FC \cap OC$, then one eigenvalue is $a-c$, with eigenvector $(1,0)$. This eigenvector points along the invariant line $\rho = 0$. The other eigenvalue is positive if $Y > 0$ and is 0 if $Y = 0$.*

If $(\theta, \rho) \in OC$, (3.25) becomes

$$\begin{pmatrix} a-c & -c \\ 0 & \dfrac{w_2}{c(b-c)}\Phi(\theta) \end{pmatrix}. \tag{3.28}$$

In OC, $Y = 0$ and $\rho > 0$, so $c\rho + w_2 = 0$ and $w_2 < 0$. Therefore:

Proposition 3.2.3. *If an equilibrium is in OC, then one eigenvalue is $a-c$, with eigenvector $(1,0)$. This eigenvector points along the invariant line $\rho = -w_2/c$, which corresponds to $Y = 0$.*

We are concerned only with the solutions of (3.14)–(3.15) that approach their end states exponentially. Therefore from the propositions of this section, we only consider the following three cases:

- $0 < a < b < c$, left state in FC or OC, right state in one of the low-temperature equilibria.
- $0 < a < c < b$, left state in FC, right state in OC or one of the low-temperature equilibria.
- $0 < c < a < b$, left state in FC or one of the low-temperature equilibria, right state in OC.

Chapter 4

Existence of traveling waves

4.1 Fast traveling waves $(0 < a < b < c)$

In this section we study fast traveling waves which have TC right state and prove Theorem 2.0.4.

We assume that the right state of a traveling wave for (2.7)–(2.9) is TC that is (θ^+, ρ^+, Y^+) with $\theta^+ \leq 0$, $\rho^+ > 0$ and $Y^+ > 0$.
In (3.14)–(3.15) the right state (θ^+, ρ^+, Y^+) corresponds to $(\theta, v_1, \rho, Y) = (\theta^+, 0, \rho^+, Y^+)$. The constants w_1 and w_2 are

$$(w_1, w_2) = ((c-a)\theta^+ + c\rho^+, (c-b)Y^+ - c\rho^+). \tag{4.1}$$

We substitute (w_1, w_2) into (3.14)–(3.15) and obtain

$$\dot{\theta} = (a-c)(\theta - \theta^+) - c(\rho - \rho^+), \tag{4.2}$$

$$\dot{\rho} = \left(\frac{\rho - \rho^+}{c-b} + \frac{Y^+}{c}\right)\rho\Phi(\theta). \tag{4.3}$$

The system (4.2)–(4.3) has two invariant lines $\rho = 0$ and $\rho = \rho^+ - \frac{c-b}{c}Y^+$. The latter corresponds to $Y = 0$. If $\rho^+ = \frac{c-b}{c}Y^+$, i.e., $c = \frac{bY^+}{Y^+ - \rho^+}$, the lines $\rho = 0$ and $Y = 0$ coincide. The line $\rho = \rho^+ - \frac{c-b}{c}Y^+$ lies above $\rho = 0$ provided $\rho^+ > \frac{c-b}{c}Y^+$ and lies below provided $\rho^+ < \frac{c-b}{c}Y^+$. Moreover it lies below $\rho = \rho^+$ since we assume $c > b > a$.

For fixed $b > 0$ and $\rho^+ > 0$, we define a curve and two regions

$$C = \{(Y^+, c) : \rho^+ < Y^+ < \infty \text{ and } c = \frac{bY^+}{Y^+ - \rho^+}\},$$
$$\text{Region } 1 = \{(Y^+, c) : \rho^+ < Y^+ < \infty \text{ and } c > \frac{bY^+}{Y^+ - \rho^+}\},$$
$$\text{Region } 2 = \{(Y^+, c) : Y^+ > 0,\ c > b, \text{and } (Y^+, c) \notin C \cup \text{Region } 1\}.$$

See Figure 4.1.

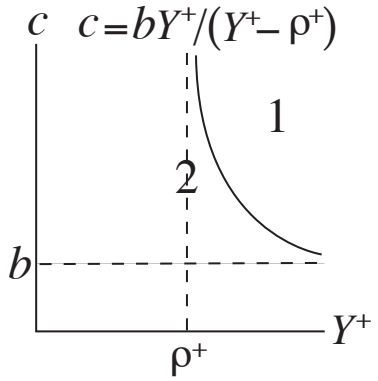

Figure 4.1 Curve C, region 1 and region 2.

4.1.1 The curve C

On the curve C, we have $c = \frac{bY^+}{Y^+ - \rho^+}$. By substituting this into (4.2)–(4.3) and multiplying the right hand side by $b\rho^+(Y^+ - \rho^+) > 0$, we obtain

$$\dot{\theta} = b\rho^+\big((a\rho^+ + (b-a)Y^+)(\theta^+ - \theta) + bY^+(\rho^+ - \rho)\big), \tag{4.4}$$
$$\dot{\rho} = (Y^+ - \rho^+)^2\rho^2\Phi(\theta). \tag{4.5}$$

See Figure 4.2. The equilibrium (θ^+, ρ^+) has a 1-dimensional stable manifold.

If $\frac{bY^+\rho^+}{(b-a)Y^+ + a\rho^+} + \theta^+ \leq 0$, there are no traveling waves with right state (θ^+, ρ^+). If $\frac{bY^+\rho^+}{(b-a)Y^+ + a\rho^+} + \theta^+ > 0$, then in $\rho > 0$ the equilibrium $(\frac{bY^+\rho^+}{(b-a)Y^+ + a\rho^+} + \theta^+, 0)$ has a unique 1-dimensional center manifold $W^c(\frac{bY^+\rho^+}{(b-a)Y^+ + a\rho^+} + \theta^+, 0)$.

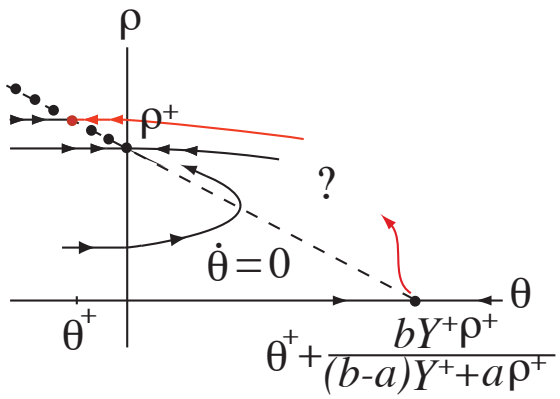

Figure 4.2 Phase portrait of (4.4)–(4.5) in P ($\rho \geq 0$) assuming $\frac{bY^+\rho^+}{(b-a)Y^+ + a\rho^+} + \theta^+ > 0$. In $\rho > 0$, $\dot{\rho} = 0$ for $\theta \leq 0$ and $\dot{\rho} > 0$ for $\theta > 0$. $\dot{\theta}$ changes from positive to negative when the null cline $(a\rho^+ + (b-a)Y^+)(\theta^+ - \theta) + bY^+(\rho^+ - \rho) = 0$ is crossed from left to right.

Proposition 4.1.1. *Let $\theta^+ \leq 0$. Suppose $(b-a)\theta^+ + b\rho^+ > 0$ then there are two possibilities*

1. *Suppose $\rho^+ \geq \frac{-a\rho^+\theta^+}{\theta^+(b-a)+b\rho^+}$. Then there is a unique Y_*, $\rho^+ < Y_* < \infty$ such that, for (4.4)–(4.5), the stable manifold of (θ^+, ρ^+) contains a branch of the center manifold of $(\frac{bY_*\rho^+}{(b-a)Y_* + a\rho^+} + \theta^+, 0)$. For $\rho^+ < Y^+ < Y_*$, the former lies above the latter; for $Y_* < Y^+ < \infty$, the former lies below the latter.*

2. *Suppose $\rho^+ < \frac{-a\rho^+\theta^+}{\theta^+(b-a)+b\rho^+}$. Then there is a unique Y_*, $\frac{-a\rho^+\theta^+}{\theta^+(b-a)+b\rho^+} < Y_* < \infty$ such that, for (4.4)–(4.5), the stable manifold of (θ^+, ρ^+) contains a branch of the center manifold of $(\frac{bY_*\rho^+}{(b-a)Y_* + a\rho^+} + \theta^+, 0)$. For $\frac{-a\rho^+\theta^+}{\theta^+(b-a)+b\rho^+} < Y^+ < Y_*$, the former lies above the latter; for $Y_* < Y^+ < \infty$, the former lies below the latter.*

The connection in Proposition(4.1.1) corresponds to a traveling wave of (2.7)–(2.9) of type $FC \cap OC \xrightarrow{c_f} TC$ that does not approach its left state exponentially.

Proof. In case one, we consider $Y^+ > \rho^+$; in case two, we consider $\frac{-a\rho^+\theta^+}{\theta^+(b-a)+b\rho^+} < Y^+$. In both cases, $\frac{-a\rho^+\theta^+}{\theta^+(b-a)+b\rho^+} < Y^+$, so there may be traveling waves with right state (θ^+, ρ^+) and the phase portrait is given by Figure 4.2.

For the first case, consider the limit $Y^+ = \rho^+$ of (4.4)–(4.5). We obtain

$$\dot{\theta} = b^2(\rho^+)^2\big((\theta^+ - \theta) + (\rho^+ - \rho)\big), \tag{4.6}$$

$$\dot{\rho} = 0. \tag{4.7}$$

The stable manifold of (θ^+, ρ^+) lies above the center manifold of $(\frac{bY^+\rho^+}{(b-a)Y^+ + a\rho^+} + \theta^+, 0)$ for Y^+ a little larger than ρ^+.

For the second case, consider the limit $Y^+ = \frac{-a\rho^+\theta^+}{\theta^+(b-a)+b\rho^+}$. We obtain

$$\dot{\theta} = \frac{ab^2(\rho^+)^2}{\theta^+(b-a) + b\rho^+}(\theta^+\rho - \rho^+\theta), \tag{4.8}$$

$$\dot{\rho} = \left(\frac{-b\rho^+(\theta^+ + \rho^+)}{\theta^+(b-a) + b\rho^+}\right)^2 \rho^2\phi(\theta). \tag{4.9}$$

The stable manifolds of equilibria on the line $\rho\theta^+ - \theta\rho^+ = 0$ are horizontal lines. In particular, the stable manifold of (θ^+, ρ^+) is the line $\rho = \rho^+$, and the center manifold of $(\frac{bY^+\rho^+}{(b-a)Y^+ + a\rho^+} + \theta^+, 0) = (0, 0)$ is the line $\rho\theta^+ - \theta\rho^+ = 0$, $\theta^+ < \theta$. It follows that for Y^+ a little larger than ρ^+, the former lies above the latter.

Next we show that for large Y^+, the former lies below the latter. For fixed ϵ, $0 < \epsilon < \rho^+$, consider the region $-\theta^+ + \epsilon \le \theta \le -\theta^+ + 2\epsilon, \quad \rho^+ - \epsilon \le \rho \le \rho^+$. On this region, we have

$$\frac{d\theta}{d\rho} = \frac{b\rho^+}{(Y^+ - \rho^+)^2} \cdot \frac{\big((b-a)Y^+ + a\rho^+\big)(\theta^+ - \theta) + bY^+(\rho^+ - \rho)}{\rho^2\Phi(\theta)}.$$

Therefore, say $\frac{b\rho^+}{(Y^+ - \rho^+)^2} = K > 0$

$$K \cdot \frac{\big((b-a)Y^+ + a\rho^+\big)(2\theta^+ - 2\epsilon)}{(\rho^+ - \epsilon)^2\Phi(-\theta^+ + \epsilon)} \le \frac{d\theta}{d\rho} \le K \cdot \frac{\big((b-a)Y^+ + a\rho^+\big)(2\theta^+ - \epsilon) + bY^+\epsilon}{(\rho^+ - \epsilon)^2\Phi(-\theta^+ + \epsilon)}.$$

For large Y^+, the lower bound is negative and upper bound is positive. Both lower and upper bound approach 0 as $Y^+ \to \infty$. The result follows.

Therefore, for (4.4)–(4.5), there exists Y_*, with $\rho^+ < Y_* < \infty$ in case (1) and $\frac{-a\rho^+\theta^+}{\theta^+(b-a)+b\rho^+} < Y_* < \infty$ in case (2), such that, for (4.4)–(4.5), the stable manifold of (θ^+, ρ^+) contains a branch of the center manifold of $(\frac{bY^+\rho^+}{(b-a)Y^+ + a\rho^+} + \theta^+, 0)$.

The breaking of these manifolds for (4.4)–(4.5) as Y^+ varies is obtained by a Melnikov

integral. Let $X(\theta,\rho) = (X_1(\theta,\rho), X_2(\theta,\rho))$ be the vector field given by the right hand side of (4.4)–(4.5). Let Y^+ be a value for which the connection exists, let $(\theta,\rho)(\tau)$ be the connecting orbit, and let $r(\tau) = \mathrm{div}X(\theta,\rho)(\tau)$. Then the Melnikov integral is given by

$$\begin{aligned} M &= \int_{-\infty}^{\infty} \exp\left(-\int_0^\tau r(\eta)\,d\eta\right)\begin{pmatrix}-\dot\rho & \dot\theta\end{pmatrix}\frac{\partial}{\partial Y^+}\begin{pmatrix}X_1\\X_2\end{pmatrix}d\tau \\ &= \int_{-\infty}^{\infty} \exp\left(-\int_0^\tau r(\eta)\,d\eta\right)\begin{pmatrix}-\dot\rho & \dot\theta\end{pmatrix}\begin{pmatrix}b\rho^+\big((b-a)(\theta^+-\theta)+b(\rho^+-\rho)\big)\\ 2(Y^+-\rho^+)\rho^2\Phi(\theta)\end{pmatrix}d\tau. \end{aligned}$$

We have $\theta^+ - \theta < 0$, $\rho^+ - \rho > 0$, $\dot\theta < 0$ and $\dot\rho > 0$. Since $Y^+ > \rho^+$ and $\dot\theta < 0$, we have

$$0 < \frac{(b-a)Y^+ + a\rho^+}{bY^+} < \frac{(b-a)(Y^+ + \rho^+) + 2a\rho^+}{b(Y^+ + \rho^+)}, \tag{4.10}$$

$$\frac{(b-a)Y^+ + a\rho^+}{bY^+}(\theta^+ - \theta) + (\rho^+ - \rho) < 0. \tag{4.11}$$

After plugging $\dot\theta$ and $\dot\rho$ into the Melkinov integral and by using (4.10) and (4.11), we obtain

$$\Big(b\rho^+(Y^+-\rho^+)\Big)\Big(\big((b-a)(Y^+ + \rho^+) + 2a\rho^+\big)(\theta^+-\theta) + b(Y^+ + \rho^+)(\rho^+ - \rho)\Big) < 0.$$

It follows that $M < 0$. Therefore the center manifold of $(\frac{bY^+\rho^+}{(b-a)Y^+ + a\rho^+} + \theta^+, 0)$ crosses from below to above the stable manifold of (θ^+, ρ^+) as Y^+ increases past Y_*. Since this is true for any Y_* where the manifolds meet, it follows that Y_* is unique. □

4.1.2 Region 1

In Region 1, we have $c > \frac{bY^+}{Y^+ - \rho^+}$ so the line $Y = 0$ lies below $\rho = 0$. The equilibrium (θ^+, ρ^+) has a stable manifold and $(\theta^+ + \frac{c}{c-a}\rho^+, 0)$ has an unstable manifold. A traveling wave exists if there is a connection from left state $(\theta^+ + \frac{c}{c-a}\rho^+, 0)$ to right state (θ^+, ρ^+).

Proposition 4.1.2. *Let $b > a > 0$ and $\theta^+ \le 0$. Let Y_* given by Proposition 4.1.1.*

1. *Suppose $\rho^+ \ge -\theta^+$. For $Y_* < Y^+ < \infty$, all points (Y^+, c) in Region 1 have $\theta^+ + \frac{c}{c-a}\rho^+ > 0$, so the phase portrait of (4.2)–(4.3) is given by Figure 4.3. For each such Y^+ there exists a c, $\frac{bY^+}{Y^+-\rho^+} < c < \infty$, such that the unstable manifold of the saddle $(\theta^+ + \frac{c}{c-a}\rho^+, 0)$ meets the stable manifold of the degenerate equilibrium (θ^+, ρ^+).*

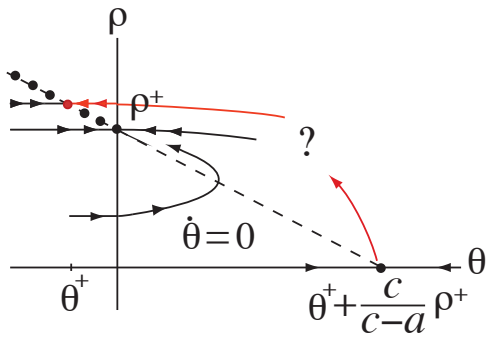

Figure 4.3 Phase portrait of (4.2)–(4.3) in P ($\rho \geq 0$) for (Y^+, c) in Region 1. The equilibrium $(\theta^+ + \frac{c}{c-a}\rho^+, 0)$ is a hyperbolic saddle.

2. *Suppose* $\rho^+ < -\theta^+$. *For* $Y_* < Y^+ < \infty$, *points* (Y^+, c) *in Region 1 have* $\theta^+ + \frac{c}{c-a}\rho^+ > 0$ *(so the phase portrait of* (4.2)–(4.3) *is given by Figure 4.3) if and only if* $\frac{bY^+}{Y^+-\rho^+} < c < \frac{a\theta^+}{\theta^++\rho^+}$. *For each such* Y^+ *there exists a* c, $\frac{bY^+}{Y^+-\rho^+} < c < \frac{a\theta^+}{\theta^++\rho^+}$, *such that the unstable manifold of the saddle* $(\theta^+ + \frac{c}{c-a}\rho^+, 0)$ *meets the stable manifold of the degenerate equilibrium* (θ^+, ρ^+).

In both cases there are no points (Y^+, c) *in Region 1 with* $Y^+ < Y_*$ *for which the unstable manifold of the saddle* $(\theta^+ + \frac{c}{c-a}\rho^+, 0)$ *meets the stable manifold of the degenerate equilibrium* (θ^+, ρ^+).

In Proposition 4.1.2 the connections that exist are combustion waves for (2.7)–(2.9) of type $FC \xrightarrow{c_f} TC$. These traveling waves have left state $(\theta^-, \rho^-, Y^-) = (\theta^+ + \frac{c}{c-a}\rho^+, 0, Y^+ - \frac{c}{(c-b)}\rho^+)$ and right state (θ^+, ρ^+, Y^+). Y^- can be determined by using the fact that w_2 given by (3.13) is constant on solutions.

Proof. Fix $Y^+ > Y_*$.

For the first case, consider the limit $c \to \infty$, divide the right hand side of (4.2)–(4.3) by c and let $c \to \infty$. Then we obtain

$$\dot{\theta} = -(\theta - \theta^+) - (\rho - \rho^+), \tag{4.12}$$

$$\dot{\rho} = 0. \tag{4.13}$$

This is the same system (4.8)–(4.9) divided by $(b\rho^+)^2$. By the proof of Proposition 4.1.1,

the stable manifold of (θ^+, ρ^+) lies above the unstable manifold of $(\theta^+ + \rho^+, 0)$ for large c.

For the second case, we substitute $c = \frac{a\theta^+}{\theta^+ + \rho^+}$ into (4.2)–(4.3) and multiply the right hand side of (5.2) by $-(\theta^+ + \rho^+) > 0$, which yields

$$\dot{\theta} = -a\rho^+(\theta - \theta^+) + a\theta^+(\rho - \rho^+), \tag{4.14}$$

$$\dot{\rho} = (\theta^+ + \rho^+)\left(\frac{\rho - \rho^+}{(a-b)\theta^+ - b\rho^+} + \frac{Y^+}{a\theta^+}\right)\rho\Phi(\theta). \tag{4.15}$$

See Figure 4.4. The stable manifold of (θ^+, ρ^+) lies above the center manifold of the origin.

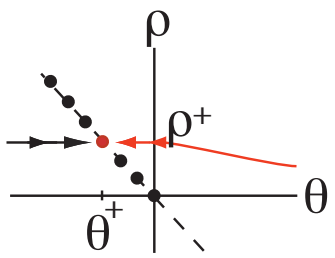

Figure 4.4 Phase portrait of (4.14)–(4.15) in P ($\rho \geq 0$).

For $Y_* < Y^+ < \infty$, by Proposition 4.1.1 the structure of invariant manifolds on C and at large c are reverse in both cases. This shows the existence of c.

□

4.1.3 Region 2

In Region 2, a point (Y^+, c) is neither on C nor in region 1, so the line $Y = 0$ lies above $\rho = 0$ and lies below $\rho = \rho^+$. See Figure 4.5. The equilibrium $(\theta^+ + \frac{c-b}{c-a}Y^+, \rho^+ - \frac{c-b}{c}Y^+)$ has an unstable manifold and the degenerate equilibrium (θ^+, ρ^+) has a stable manifold. A traveling wave exists if there is a connection from left state $(\theta^+ + \frac{c-b}{c-a}Y^+, \rho^+ - \frac{c-b}{c}Y^+)$ to right state (θ^+, ρ^+).

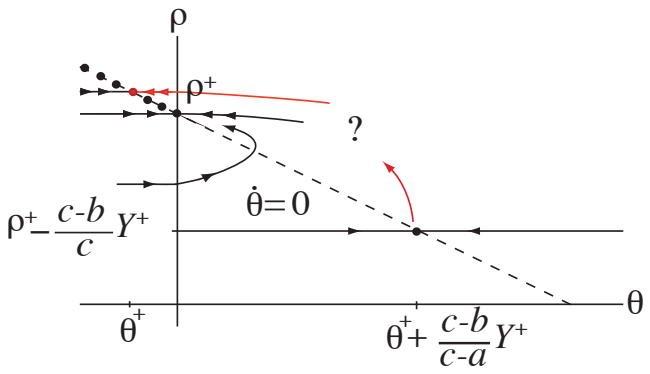

Figure 4.5 For (Y^+, c) in Region 2, phase portrait of (4.2)–(4.3) in P ($\rho \geq \rho^+ - \frac{c-b}{c}Y^+ > 0$, i.e., in $Y \geq 0$).

Proposition 4.1.3. *For $b > a > 0$, $\theta^+ \leq 0$ and $Y_* < Y^+$ given by Proposition 4.1.1, there is a speed $c > b > a$ such that $\frac{a\theta^+ + bY^+}{\theta^+ + Y^+} < c < \frac{bY^+}{Y^+ - \rho^+}$ the point (Y^+, c) lies in Region 2, and the stable manifold of (θ^+, ρ^+) contains part of the unstable manifold of $(\theta^+ + \frac{c-b}{c-a}Y^+, \rho^+ - \frac{c-b}{c}Y^+)$.*

In Proposition 4.1.3 the connection that exists is a combustion wave for (2.7)–(2.9) of type $OC \xrightarrow{c_f} TC$. It has left state $(\theta^-, \rho^-, Y^-) = (\theta^+ + \frac{c-b}{c-a}Y^+, \rho^+ - \frac{c-b}{c}Y^+, 0)$ and right state (θ^+, ρ^+, Y^+).

Proof. (1) Fix $Y^+ > Y_*$.

$\theta^- = \theta^+ + \frac{c-b}{c-a}Y^+$ is positive as required provided $c > \frac{a\theta^+ + bY^+}{\theta^+ + Y^+} > b$. Consider the new curve $c = \frac{a\theta^+ + bY^+}{\theta^+ + Y^+}$ and call it $\tilde{C}$ which is below the curve C. See Figure 4.6.

We consider the limit $c = \frac{a\theta^+ + bY^+}{\theta^+ + Y^+}$. Substitute it into (4.2)–(4.3) and multiply the right hand side by $\theta^+ + Y^+ > 0$ which yields

$$\dot{\theta} = (a-b)Y^+(\theta - \theta^+) - (a\theta^+ + bY^+)(\rho - \rho^+), \tag{4.16}$$

$$\dot{\rho} = (\theta^+ + Y^+)^2\left(\frac{\rho - \rho^+}{(a-b)\theta^+} + \frac{Y^+}{a\theta^+ + bY^+}\right)\rho\Phi(\theta). \tag{4.17}$$

See Figure 4.7. The stable manifold of (θ^+, ρ^+) lies above the center manifold of $(0, \rho^+ + \frac{(b-a)\theta^+ Y^+}{a\theta^+ + bY^+})$ which perturbs to the unstable manifold of $(\theta^+ + \frac{c-b}{c-a}Y^+, \rho^+ - \frac{c-b}{c}Y^+)$ when c is increased.

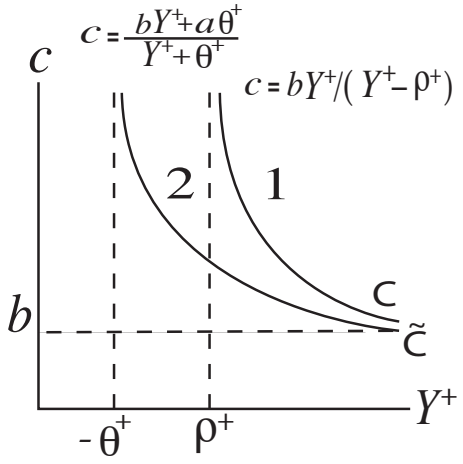

Figure 4.6 Curve C and $\tilde{C}$.

For $Y_* < Y^+ < \infty$, by Proposition 4.1.1 the structure of invariant manifolds on C and $\tilde{C}$ are reverse. This shows the existence of c. □

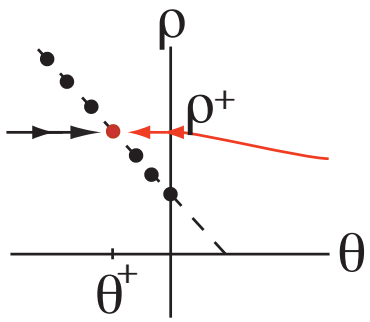

Figure 4.7 Phase portrait for (4.16)-(4.17).

Now we can prove Theorem 2.0.4. Proposition 4.1.1 implies Theorem 2.0.4 (1).

Proof of Theorem 2.0.4 (2):

Proof. (a) The formula for c follows from the equations $w_2 = (c-b)Y^+ - c\rho^+$ and $w_2 = (c-b)Y^- - c\rho^- = (c-b)Y^-$. The formula for θ^+ follows from the equations

$w_1 = (c-a)\theta^+ + c\rho^+$ and $w_1 = (c-a)\theta^- + c\rho^- = (c-a)\theta^-$, together with the formula for c. Existence of the wave follows from Proposition 4.1.2.

(b) The formula for c follows from the equations $w_2 = (c-b)Y^+ - c\rho^+$ and $w_2 = (c-b)Y^- - c\rho^- = -c\rho^-$. The formula for θ^+ follows from the equations $w_1 = (c-a)\theta^+ + c\rho^+$ and $w_1 = (c-a)\theta^- + c\rho^-$, together with the formula for c. Existence of the wave follows from Proposition 4.1.3.

□

4.1.4 Numerical results.

In previous subsections, we prove the existence of a traveling wave for values of c in region 1 and region 2 for large Y^+. Now we try to see how c changes as we vary Y^+. We set $a = 0.5$, $b = 0.7$, $\theta^+ = -0.1$, $\rho^+ = 2$, $Y^+ = 8$ and found a value of c for which a traveling wave exists. Starting from this point (Y^+, c), we then used AUTO to plot a curve of values (Y^+, c) for which a traveling wave exists. Figure 4.8 shows the result. The solutions labeled from 12 to 18 are in region 1 and after that, solutions cross to region 2. While the curve is in region 2, Y^+ reaches a minimum value Y^+_{**}; the curve turns at Y^+_{**}, and later stays in region 2.

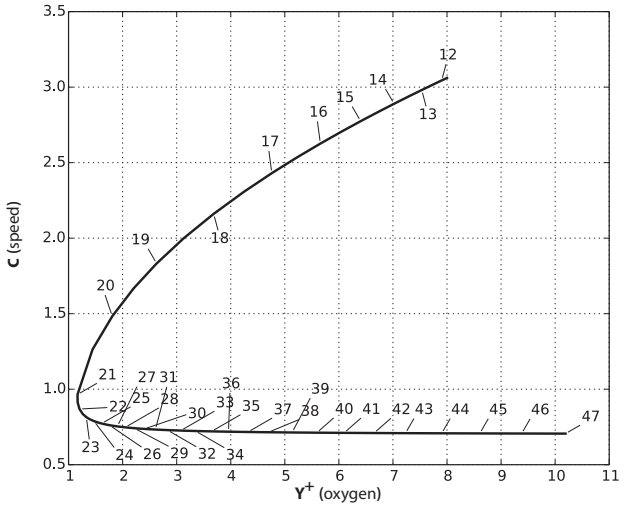

Figure 4.8 Bifurcation diagram when $a = 0.5$, $b = 0.7$.

Next we consider the case when $a = b = 0.5$ which is studied in [9]. In [9] oxygen (b) and heat (a) are both moving at exactly the same velocity of the moving gas. Figure 4.9 shows how c changes as we vary Y^+ when $a = b$. This figure is consistent with [9], which shows that when $a = b$, traveling waves in region 2 must exist for $Y^+ < Y^+_*$, not for $Y^+_* < Y^+$ as in the present paper. We obtain the Figure 4.10 when we make a small change on b. A little change on b causes the curve of c parameters turn and c values approach to 0.55 as we decrease Y^+.

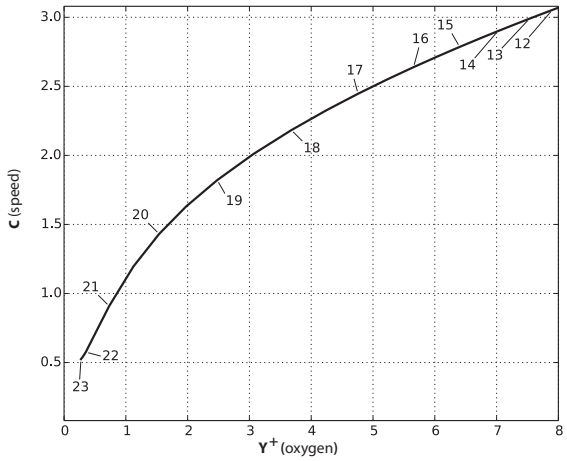

Figure 4.9 Bifurcation diagram when $a = b = 0.5$.

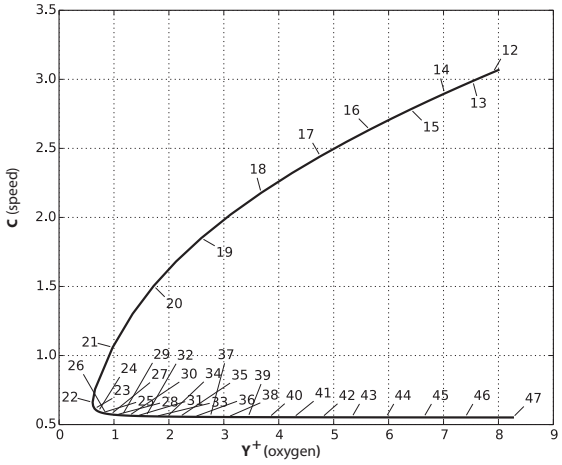

Figure 4.10 Bifurcation diagram when $a = 0.5$, $b = 0.55$.

Figure 4.12 shows the bifurcation diagram for $a = 0.5$ and $b = 0.7$ along with the curve C and $\tilde{C}$. Bifurcation solution for region 2 is between the curve C and $\tilde{C}$ as we state in Proposition 4.1.3. Additionally, Figure 4.11 shows the bifurcation diagram when $a = b$ along with the curve C.

4.2 Slow traveling waves $(0 < c < a < b)$

In this section we study slow traveling waves which have OC right state and prove Theorem 2.0.5.

We assume that $0 < c < a < b$ and the right state of a traveling wave for (2.7)–(2.9)

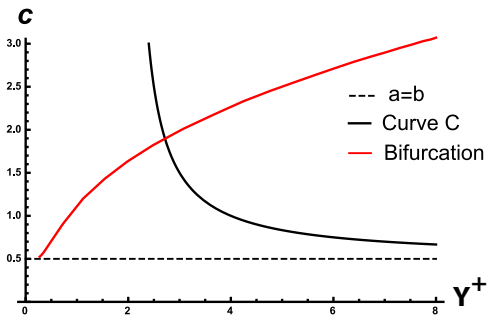

Figure 4.11 a=b=0.5

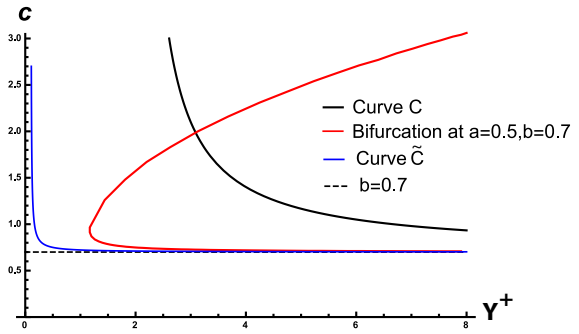

Figure 4.12 a=0.5, b=0.7 .

is OC that is (θ^+, ρ^+, Y^+) with $\theta^+ > 0$, $\rho^+ > 0$ and $Y^+ = 0$. The constants w_1 and w_2 are

$$(w_1, w_2) = ((c-a)\theta^+ + c\rho^+, -c\rho^+). \tag{4.18}$$

We substitute (w_1, w_2) into (3.14)–(3.15) and obtain

$$\dot{\theta} = (a-c)(\theta - \theta^+) - c(\rho - \rho^+), \tag{4.19}$$

$$\dot{\rho} = \frac{\rho^+ - \rho}{b-c}\rho\Phi(\theta). \tag{4.20}$$

The invariant line $Y = 0$ corresponds to $\rho = \rho^+$. P is the region $0 \le \rho \le \rho^+$.

Let $\theta^\sharp = \theta^+ - \frac{c}{a-c}\rho^+ < \theta^+$, $\rho^\dagger = \rho^+ - \frac{a-c}{c}\theta^+ < \rho^+$. Recall from section 3.2 the line H defined by $(a-c)\theta - c\rho + w_1 = 0$, which contains all equilibria.

Proposition 4.2.1. *Let $b > a > 0$, $\theta^+ > 0$, and $\rho^+ > 0$. For each c with $0 < c < a < b$, one equilibrium of (4.19)–(4.20) is the saddle (θ^+, ρ^+), which corresponds to $(\theta, \rho, Y) = (\theta^+, \rho^+, 0)$. In addition:*

1. *If $0 < c < \frac{\theta^+}{\theta^+ + \rho^+}a$, then $\theta^\sharp > 0$, $\rho^\dagger < 0$, $(\theta^\sharp, 0)$ is a repeller, and there is unique connecting orbit from $(\theta^\sharp, 0)$ to (θ^+, ρ^+), of type $FC \xrightarrow{cs} OC$. The line H does not intersect the part of P with $\theta \le 0$, so the set TC is empty. There are no other connecting orbits in P.*

2. *If $c = \frac{\theta^+}{\theta^+ + \rho^+}a$, then $\theta^\sharp = \rho^\dagger = 0$, $(0,0)$ has one positive and one zero eigenvalue, and there is unique connecting orbit from $(0,0)$ to (θ^+, ρ^+), of type $TC \cap FC \xrightarrow{cs} OC$.*

The intersection of the line H and P is the origin. There are no other connecting orbits in P.

3. *If $\frac{\theta^+}{\theta^+ + \rho^+} a < c < a$, then $\theta^\sharp < 0$, $\rho^\dagger > 0$, and H meets P in the line segment of equilibria*

$$TC = \{(\theta, \rho) : \theta^\sharp \leq \theta \leq 0 \text{ and } \rho = \rho^+ + \frac{a-c}{c}(\theta - \theta^+)\}.$$

The endpoints of TC are $(\theta^\sharp, 0)$ and $(0, \rho^\dagger)$. The equilibria in TC have one 0 eigenvalue and one positive eigenvalue.

In cases (1) and (2) the connecting orbit approaches the right state exponentially; in case (1), but not case (2), it also approaches the left state exponentially.

Proof. We give a sketch of the easy proof of this proposition.

To prove the first part of the Proposition 4.2.1, consider the region

$$R = \{(\theta, \rho) : \theta^\sharp \leq \theta \leq \theta^+,\ 0 \leq \rho \leq \rho^+,\ (\theta, \rho) \text{ is below or on H } \}.$$

In backward time, the orbit starts from the unstable manifold of (θ^+, ρ^+) can not cross this compact region R. It has to stay in this region and go to its α-limit points. The only possible limit point is the equilibrium of the unstable node $(\theta^\sharp, 0)$. Second part can be proved with similar argument. For proof of the last part, see Figure 4.13. □

Now we can prove the Theorem 2.0.5.

Proof of Theorem 2.0.5 (1):

Proof. The formula for c follows from the equations

$$w_2 = (c-b)Y^+ - c\rho^+ = -c\rho^+ \quad \text{and} \quad w_2 = (c-b)Y^- - c\rho^- = (c-b)Y^-.$$

Therefore we have $c = \frac{bY^-}{\rho^+ + Y^-}$. Now we show that $0 < c < a < b$. It suffices to show that $0 < \frac{bY^-}{\rho^+ + Y^-} < a$ which is true by the assumption $(a-b)Y^- + a\rho^+ > 0$.

The formula for θ^+ follows from the equations

$$w_1 = (c-a)\theta^+ + c\rho^+ \quad \text{and} \quad w_1 = (c-a)\theta^- + c\rho^- = (c-a)\theta^-,$$

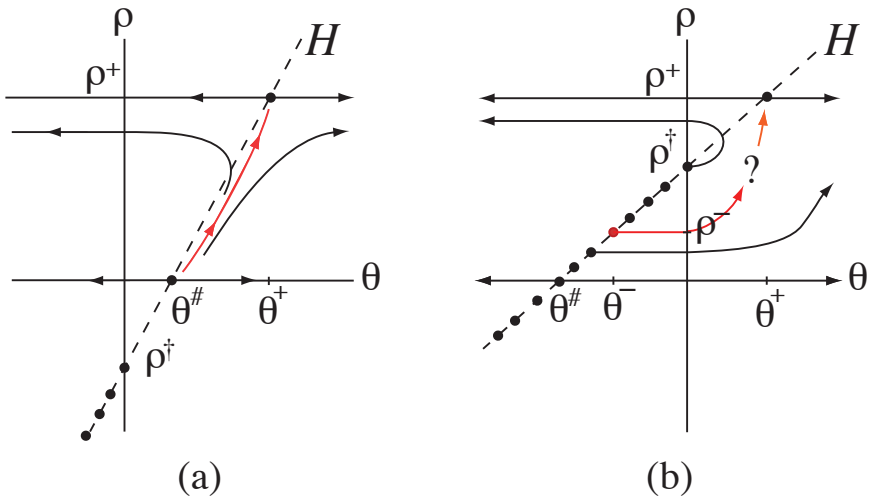

Figure 4.13 For $0 < c < a$, phase portrait of (4.19)–(4.20). (a) $0 < c < \frac{\theta^+}{\theta^+ + \rho^+} a$. (b) $\frac{\theta^+}{\theta^+ + \rho^+} a < c < a$.

together with the formula for c. Since $\theta^+ > 0$ and $0 < c < a < b$, the existence and uniqueness of the wave follow from Proposition 4.2.1 (1). □

Proof of Theorem 2.0.5 (2):

Proof. Since w_1 (resp. w_2) is equal at $(\theta, v_1, \rho, Y) = (\theta^-, 0, \rho^-, Y^-)$ and $(\theta^+, 0, \rho^+, 0)$, we obtain the equations

$$(c-a)\theta^- + c\rho^- = (c-a)\theta^+ + c\rho^+, \quad (c-b)Y^- - c\rho^- = -c\rho^+.$$

Solving for (ρ^-, θ^+), we obtain

$$\rho^- = \rho^+ - \frac{b-c}{c} Y^-, \quad \theta^+ = \theta^- + \frac{b-c}{a-c} Y^-. \tag{4.21}$$

Both are positive as required provided $\frac{Y^-}{\rho^+ + Y^-} b < c < a < b$. By Proposition 4.2.1 (3), for $\frac{Y^-}{\rho^+ + Y^-} b < c < a$, the phase portrait is given by Figure 4.13 (b).

We rewrite (4.19)–(4.20) in terms of the parameters $(\theta^-, Y^-, \rho^+, c)$ by making the

substitutions (4.21), which yields

$$\dot{\theta} = (a-c)(\theta - (\theta^- + \frac{b-c}{a-c}Y^-)) - c(\rho - \rho^+), \tag{4.22}$$

$$\dot{\rho} = \frac{\rho^+ - \rho}{b-c}\rho\Phi(\theta). \tag{4.23}$$

We consider this system for $\frac{Y^-}{\rho^+ + Y^-}b < c < a$.

We find the limit $c \to a$ and we obtain

$$\dot{\theta} = -(b-a)Y^- - a(\rho - \rho^+), \tag{4.24}$$

$$\dot{\rho} = \frac{(\rho^+ - \rho)}{b-a}\rho\Phi(\theta). \tag{4.25}$$

The flow is given by Figure 4.14. After a small perturbation, we have Figure 4.15.

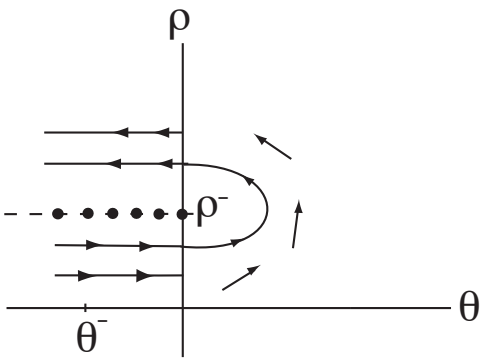

Figure 4.14 Phase portrait of (4.24)–(4.25).

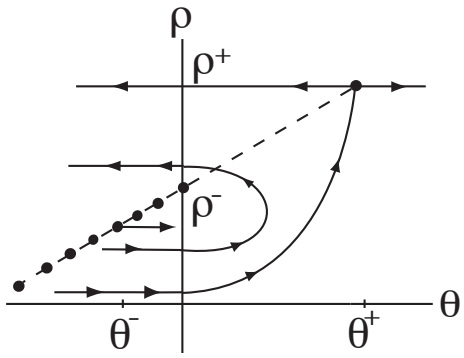

Figure 4.15 After a small perturbation.

By Figures 4.14–4.15, unstable manifold of the point (θ^-, ρ^-) is above the stable manifold of (θ^+, ρ^+).

To study $c = \frac{Y^-}{\rho^+ + Y^-}b$, we substitute this value into (4.22)–(4.23), multiply by $\rho^+ + Y^-$

which is positive and simplify, which yields

$$\dot{\theta} = ((a-b)Y^- + a\rho^+)(\theta - \theta^-) - bY^-\rho, \tag{4.26}$$

$$\dot{\rho} = \frac{(\rho^+ + Y^-)^2}{b\rho^+}(\rho^+ - \rho)\rho\Phi(\theta). \tag{4.27}$$

For this system, the point on TC with $\theta = \theta^-$ is just $(\theta^-, 0)$. Its unstable manifold is the θ-axis, above which is the stable manifold of (θ^+, ρ^+).

From the previous two paragraphs we deduce the existence of the combustion wave for some c in the interval $\frac{Y^-}{\rho^+ + Y^-}b < c < a < b$. □

4.3 Intermediate traveling waves ($0 < a < c < b$)

We assume $0 < a < c < b$. From Section 3.2, we assume that the right state of a traveling wave of (2.7)–(2.9) is of type OC or TC.

If the right state is OC, i.e., an equilibrium $(\theta^+, \rho^+, 0)$ with $\theta^+ > 0$ and $\rho^+ > 0$ then the constants w_1 and w_2 are

$$(w_1, w_2) = ((c-a)\theta^+ + c\rho^+, -c\rho^+), \tag{4.28}$$

We substitute (w_1, w_2) into (3.14)–(3.15) and obtain

$$\dot{\theta} = (a-c)(\theta - \theta^+) - c(\rho - \rho^+), \tag{4.29}$$

$$\dot{\rho} = \frac{\rho^+ - \rho}{b-c}\rho\Phi(\theta). \tag{4.30}$$

The invariant line $Y = 0$ corresponds to $\rho = \rho^+$. P is the region $0 \le \rho \le \rho^+$. Let $\theta^\sharp = \theta^+ - \frac{c}{a-c}\rho^+ > \theta^+$, $\rho^\dagger = \rho^+ - \frac{a-c}{c}\theta^+ > \rho^+$. Recall from section 3.2 the line H defined by $(a-c)\theta - c\rho + w_1 = 0$, which contains all equilibria.

Proposition 4.3.1. *Let $b > a > 0$, $\theta^+ > 0$, and $\rho^+ > 0$. For each c with $0 < a < c < b$, one equilibrium of (4.29)–(4.30) is the saddle $(\theta^\sharp, 0)$. In addition (θ^+, ρ^+) is the stable node which corresponds to $(\theta, \rho, Y) = (\theta^+, \rho^+, 0)$ and there is unique connecting orbit from $(\theta^\sharp, 0)$ to (θ^+, ρ^+), of type $FC \xrightarrow{c_m} OC$. The line H does not intersect the part of*

P with $\theta \leq 0$, so the set TC is empty. There are no other connecting orbits in P. These waves approach both end state exponentially.

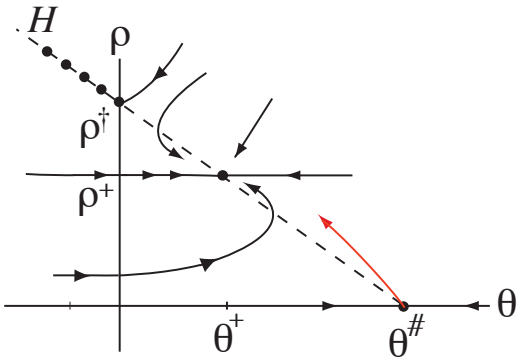

Figure 4.16 Phase portrait for (4.29)-(4.30).

Proof. The idea of the proof is similar to the proof of Proposition 4.2.1.

Consider the region

$$R = \{(\theta, \rho) : \theta^+ \leq \theta \leq \theta^\sharp,\ 0 \leq \rho \leq \rho^+,\ (\theta, \rho) \text{ is above or on H}\}.$$

In forward time, the orbit starts from the unstable manifold of $(\theta^\sharp, 0)$ can not leave the compact region R. It has to stay in this region and go to its ω-limit set. The only possible limit point is the equilibrium of the stable node (θ^+, ρ^+). See Figure 4.16. There are no other connecting orbits in P. □

If the right state is $OC \cap TC$ with an equilibrium (θ^+, ρ^+, Y^+) with $\theta^+ = 0$, $\rho^+ > 0$ and $Y^+ = 0$ then the constants w_1 and w_2 are

$$(w_1, w_2) = (c\rho^+, -c\rho^+). \tag{4.31}$$

We substitute (w_1, w_2) into (3.14)–(3.15) and obtain

$$\dot{\theta} = (a-c)\theta - c(\rho - \rho^+), \tag{4.32}$$

$$\dot{\rho} = \frac{\rho^+ - \rho}{b-c}\rho\Phi(\theta). \tag{4.33}$$

The invariant line $Y = 0$ corresponds to $\rho = \rho^+$. P is the region $0 \le \rho \le \rho^+$. Let $\theta^\sharp = \frac{c}{c-a}\rho^+ > 0$, $\rho^\dagger = \rho^+ > 0$. Recall from section 3.2 the line H defined by $(a-c)\theta - c\rho + w_1 = 0$, which contains all equilibria.

Proposition 4.3.2. *Let $b > a > 0$, $\theta^+ = Y^+ = 0$, and $\rho^+ > 0$. For each c with $a < c < b$, one equilibrium of (4.32)–(4.33) is the saddle $(\theta^\sharp, 0)$. In addition $(0, \rho^+)$ has one negative and one zero eigenvalue, and there is unique connecting orbit from $(\theta^\sharp, 0)$ to $(0, \rho^+)$, of type $FC \xrightarrow{c_m} OC \cap TC$. The intersection of the line H and P is the point $(0, \rho^+)$. There are no other connecting orbits in P. These waves approach only their left state exponentially.*

Proof of Proposition (4.3.2) is similar to proof of Proposition (4.3.1). Only difference is that we have the degenerate equilibrium $(0, \rho^+)$ which does not effect the proof.

Note that for $\theta^+ < 0$, the degenerate equilibrium (θ^+, ρ^+) lies in the invariant line $\rho = \rho^+$. Then the orbit starts from the unstable manifold of $(\theta^\sharp, 0)$ can not meet the stable manifold of the degenerate equilibrium (θ^+, ρ^+). Therefore $FC \xrightarrow{c_m} OC \cap TC$ waves do not exist with $\theta^+ < 0$ and $Y^+ = 0$.

If the right state is TC, i.e., an equilibrium (θ^+, ρ^+, Y^+) with $\theta^+ < 0$, $\rho^+ > 0$ and $Y^+ > 0$ then the constants w_1 and w_2 are

$$(w_1, w_2) = ((c-a)\theta^+ + c\rho^+, (c-b)Y^+ - c\rho^+). \tag{4.34}$$

We substitute (w_1, w_2) into (3.14)–(3.15) and obtain

$$\dot{\theta} = (a-c)(\theta - \theta^+) - c(\rho - \rho^+), \tag{4.35}$$

$$\dot{\rho} = (\frac{\rho^+ - \rho}{b-c} + \frac{Y^+}{c})\rho\Phi(\theta). \tag{4.36}$$

The invariant line $Y = 0$ corresponds to $\rho = \rho^+ + \frac{b-c}{c}Y^+$. Let $\theta^\sharp = \theta^+ - \frac{c}{a-c}\rho^+$, $\rho^\dagger = \rho^+ - \frac{a-c}{c}\theta^+ < \rho^+$. Recall from section 3.2 the line H defined by $(a-c)\theta - c\rho + w_1 = 0$,

which contains all equilibria. The equilibrium (θ^+, ρ^+) has a stable manifold and $(\theta^\sharp, 0)$ has an unstable manifold. A traveling wave exists if there is a connection from left state $(\theta^\sharp, 0)$ to right state (θ^+, ρ^+).

Proposition 4.3.3. *Let $b > a > 0$, $\theta^+ < 0$, and $\rho^+ > 0$.*

1. *Suppose $\rho^+ \geq -\theta^+$. Then $\theta^\sharp > 0$, $\rho^\dagger > 0$.*

2. *Suppose $\rho^+ < -\theta^+$. If $\frac{a\theta^+}{\theta^+ + \rho^+} > c > a$, then $\theta^\sharp > 0$, $\rho^\dagger > 0$.*

   For both cases, H meets P in a line segment of equilibria

$$TC = \{(\theta, \rho) : \theta^+ - \frac{b-c}{c-a} Y^+ \leq \theta \leq 0 \text{ and } \rho = \rho^+ + \frac{a-c}{c}(\theta - \theta^+)\}.$$

   The endpoints of TC are $(\theta^+ - \frac{b-c}{c-a} Y^+, 0)$ and $(0, \rho^\dagger)$. The equilibria in TC have one 0 eigenvalue and one negative eigenvalue.

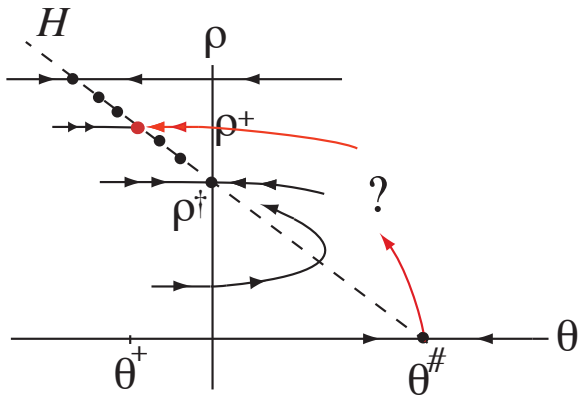

Figure 4.17 Phase portrait for (4.35)-(4.36).

Proof. See Figure 4.17. □

Now we can prove the Theorem 2.0.6.

Proof of Theorem 2.0.6(1) :

Proof. The formula for c follows from the equations

$$w_2 = (c-b)Y^+ - c\rho^+ = -c\rho^+ \quad \text{and} \quad w_2 = (c-b)Y^- - c\rho^- = (c-b)Y^-.$$

Therefore we have $c = \frac{bY^-}{\rho^+ + Y^-}$. Now we show that c is between a and b. It suffices to show that $a < \frac{bY^-}{\rho^+ + Y^-} < b$ which is true by the assumption $(a-b)Y^- + a\rho^+ < 0$.

The formula for θ^- follows from the equations

$$w_1 = (c-a)\theta^+ + c\rho^+ \quad \text{and} \quad w_1 = (c-a)\theta^- + c\rho^- = (c-a)\theta^-,$$

together with the formula for c. Since $\theta^+ > 0$, $\rho^+ > 0$ and $0 < a < c < b$, the existence of the wave follows from Proposition 4.3.1. □

Proof of Theorem 2.0.6(2) :

Proof. The formula for c follows from the equations

$$w_2 = (c-b)Y^+ - c\rho^+ = -c\rho^+ \quad \text{and} \quad w_2 = (c-b)Y^- - c\rho^- = (c-b)Y^-.$$

Hence we have $c = \frac{bY^-}{\rho^+ + Y^-}$ which is between a and b by the assumption $(a-b)Y^- + a\rho^+ < 0$.

The formula for θ^- follows from the equations

$$w_1 = (c-a)\theta^+ + c\rho^+ = c\rho^+ \quad \text{and} \quad w_1 = (c-a)\theta^- + c\rho^- = (c-a)\theta^-,$$

together with the formula for c. Since $\theta^+ = Y^+ = 0$, $\rho^+ > 0$ and $0 < a < c < b$, the existence of the wave follows from Proposition 4.3.2. □

Proof of Theorem 2.0.6(3) :

Proof. Since w_1 (resp. w_2) is equal at $(\theta, v_1, \rho, Y) = (\theta^-, 0, 0, Y^-)$ and $(\theta^+, 0, \rho^+, Y^+)$, we obtain the equations

$$(c-a)\theta^- = (c-a)\theta^+ + c\rho^+, \quad (c-b)Y^- = (c-b)Y^+ - c\rho^+.$$

Solving for (θ^-, Y^+), we obtain

$$\theta^- = \theta^+ + \frac{c}{c-a}\rho^+, \quad Y^+ = Y^- + \frac{c}{c-b}\rho^+. \tag{4.37}$$

Y^+ is positive as required provided $b > \frac{bY^-}{\rho^+ + Y^-} > c$. θ^- is positive as required provided $\rho^+ \geq -\theta^+$ and $c > a$, or $-\theta^+ > \rho^+$ and $\frac{a\theta^+}{\rho^+ + \theta^+} > c > a$. By Proposition 4.3.3, for $b > \frac{bY^-}{\rho^+ + Y^-} > c > a$, the phase portrait is given by Figure 4.17.

We rewrite (4.35)–(4.36) in terms of the parameters $(Y^-, \theta^+, \rho^+, c)$ by making the substitutions (4.37), which yields

$$\dot{\theta} = (a - c)(\theta - \theta^+) - c(\rho - \rho^+), \tag{4.38}$$

$$\dot{\rho} = (\frac{\rho}{c - b} + \frac{Y^-}{c})\rho\Phi(\theta). \tag{4.39}$$

We consider this system for $b > \frac{bY^-}{\rho^+ + Y^-} > c > a$.

We find the limit $c \to a$ and we obtain

$$\dot{\theta} = -a(\rho - \rho^+), \tag{4.40}$$

$$\dot{\rho} = (\frac{\rho}{a - b} + \frac{Y^-}{a})\rho\Phi(\theta). \tag{4.41}$$

The flow is given by Figure 4.18. After a small perturbation, we have the Figure 4.19. By

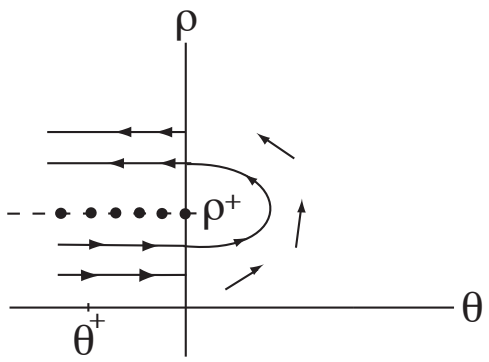

Figure 4.18 Phase portrait of (4.40)–(4.41)

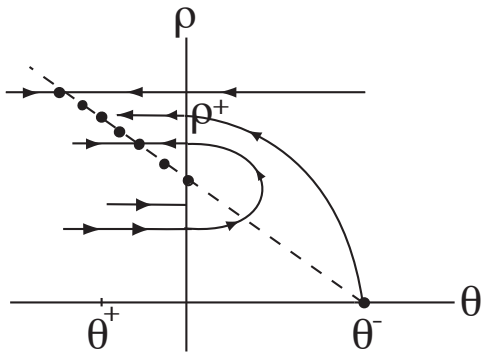

Figure 4.19 After a small perturbation

the Figures 4.18–4.19, unstable manifold of the point $(\theta^-, 0)$ is above the stable manifold of (θ^+, ρ^+).

To study $c = \frac{bY^-}{\rho^+ + Y^-}$, we substitute this value into (4.38)–(4.39), multiply by $\rho^+ + Y^-$

which is positive and simplify, which yields

$$\dot{\theta} = ((a-b)Y^- + a\rho^+)(\theta - \theta^+) - bY^-(\rho - \rho^+), \tag{4.42}$$

$$\dot{\rho} = \frac{(\rho^+ + Y^-)^2}{b\rho^+}(\rho^+ - \rho)\rho\Phi(\theta). \tag{4.43}$$

For this system, $\rho = \rho^+$ is the invariant line and the point on TC with $\theta = \theta^+$ is (θ^+, ρ^+). Its stable manifold is the line $\rho = \rho^+$, below which is the unstable manifold of $(\theta^-, 0)$.

From the previous two paragraphs we deduce the existence of the combustion wave for some c in the interval $b > \frac{bY^-}{\rho^+ + Y^-} > c > a$. □

Chapter 5

Spectrum and exponential weight functions

After proving the existence of the traveling waves, we are interested in investigating the stability of these traveling waves. For stability analysis, the first and natural approach is to linearize the system about the traveling wave and then study the spectrum of the operator $\mathcal{L}$. The spectrum of $\mathcal{L}$ which we denote $Sp(\mathcal{L})$ consists of the discrete spectrum $Sp_d(\mathcal{L})$ and the essential spectrum $Sp_{ess}(\mathcal{L})$. The discrete spectrum is the set of all eigenvalues of $\mathcal{L}$ with finite multiplicity that are isolated in the spectrum and the essential spectrum is complement of the discrete spectrum.

Replacing the spatial coordinate x by the moving coordinate $\xi = x - ct$ in (2.7)–(2.9), we obtain

$$\partial_t \theta = \partial_{\xi\xi}\theta + (c-a)\partial_\xi \theta + F, \tag{5.1}$$

$$\partial_t \rho = c\partial_\xi \rho - F, \tag{5.2}$$

$$\partial_t Y = (c-b)\partial_\xi Y - F, \tag{5.3}$$

where $F = \rho Y \Phi$. The traveling wave $T^*(\xi) = (\theta^*(\xi), \rho^*(\xi), Y^*(\xi))$ is a stationary solution of (5.1)–(5.3) with

$$\lim_{\xi\to-\infty} T^*(\xi) = T^-, \qquad \lim_{\xi\to+\infty} T^*(\xi) = T^+.$$

We always consider traveling waves that approach their end states $T^\pm$ at an exponential rate.

The stability of the wave $T^*(\xi)$ can be proven by taking a small perturbation of T^* of the form $T = T^* + \tilde{T}$ then proving that it converges to some shift of T^*. Therefore we linearize (5.1)–(5.3) in moving coordinates at a traveling wave $T^*(\xi)$.

$$\partial_t\tilde{\theta} = \partial_{\xi\xi}\tilde{\theta} + (c-a)\partial_\xi\tilde{\theta} + F_\theta(T^*(\xi))\tilde{\theta} + F_\rho(T^*(\xi))\tilde{\rho} + F_Y(T^*(\xi))\tilde{Y}, \tag{5.4}$$

$$\partial_t\tilde{\rho} = c\partial_\xi\tilde{\rho} - F_\theta(T^*(\xi))\tilde{\theta} - F_\rho(T^*(\xi))\tilde{\rho} - F_Y(T^*(\xi))\tilde{Y}, \tag{5.5}$$

$$\partial_t\tilde{Y} = (c-b)\partial_\xi\tilde{Y} - F_\theta(T^*(\xi))\tilde{\theta} - F_\rho(T^*(\xi))\tilde{\rho} - F_Y(T^*(\xi))\tilde{Y}. \tag{5.6}$$

To find the spectrum of (5.4)–(5.6), we write the right hand side as $\mathcal{A}_t = \mathcal{L}\mathcal{A}$ where

$$\mathcal{L} = \begin{pmatrix} \partial_{\xi\xi} + (c-a)\partial_\xi + F_\theta(T^*(\xi)) & F_\rho(T^*(\xi)) & F_Y(T^*(\xi)) \\ -F_\theta(T^*(\xi)) & c\partial_\xi - F_\rho(T^*(\xi)) & -F_Y(T^*(\xi)) \\ -F_\theta(T^*(\xi)) & -F_\rho(T^*(\xi)) & (c-b)\partial_\xi - F_Y(T^*(\xi)) \end{pmatrix}. \tag{5.7}$$

There are two related constant coefficient linear partial differential equations $\mathcal{A}_t = \mathcal{L}_\pm\mathcal{A}$, obtained by linearizing (5.1)-(5.3) at $T^\pm$. The spectrum of $\mathcal{L}_\pm$ can be computed using the Fourier transform

$$\hat{\mathcal{L}}_\pm = \begin{pmatrix} -\mu^2 + i\mu(c-a) + F_\theta(T^*(\pm\infty)) & F_\rho(T^*(\pm\infty)) & F_Y(T^*(\pm\infty)) \\ -F_\theta(T^*(\pm\infty)) & i\mu c - F_\rho(T^*(\pm\infty)) & -F_Y(T^*(\pm\infty)) \\ -F_\theta(T^*(\pm\infty)) & -F_\rho(T^*(\pm\infty)) & i\mu(c-b) - F_Y(T^*(\pm\infty)) \end{pmatrix} \tag{5.8}$$

The right hand boundary of the essential spectrum of $\mathcal{L}$ is the union of the right hand boundary of $Sp(\mathcal{L}_-)$ and $Sp(\mathcal{L}_+)$.

Definition 5.0.1. *If the spectrum of* $\mathcal{L}_\pm$

- *lies in the half-plane* $\{Re\lambda \leq -\nu\}$ *for some* $\nu > 0$*, then* $T^\pm$ *is called stable.*
- *lies in the half-plane* $\{Re\lambda \leq 0\}$ *and touches the imaginary axis, then* $T^\pm$ *is called marginally stable.*
- *contains points with* $Re\lambda > 0$*, then* $T^\pm$ *is called unstable.*

Definition 5.0.2. *The traveling wave $T^*(\xi)$ is spectrally stable in a space $\mathcal{X}$ if*

1. *0 is a simple eigenvalue of $\mathcal{L}$, and*
2. *the rest of the spectrum of the linearized system (5.4)–(5.6) lies in $Re\lambda < -\mu$, $\mu > 0$.*

There is always an eigenvalue 0 with eigenfunction $T^{*\prime}(\xi)$.

Definition 5.0.3. *The traveling wave $T^*(\xi)$ is linearly stable in a space $\mathcal{X}$ if every solution of (5.4)–(5.6) decays exponentially to a multiple of $T^{*\prime}(\xi)$.*

Since there exist three different type of combustion waves, we determine the spectrum of each type.

- Spectrum of fast combustion waves ($a < b < c_f$)

  We have two types of fast combustion waves; $FC \xrightarrow{c_f} TC$ and $OC \xrightarrow{c_f} TC$. Since the right state has same type TC, first we compute the spectrum of $\hat{\mathcal{L}}_+$ at the right end state (θ^+, ρ^+, Y^+) where $\theta^+ \leq 0$, $\rho^+ > 0$ and $Y^+ > 0$. We obtain

$$\hat{\mathcal{L}}_+ = \begin{pmatrix} -\mu^2 + i\mu(c_f - a) & 0 & 0 \\ 0 & i\mu c_f & 0 \\ 0 & 0 & i\mu(c_f - b) \end{pmatrix}. \tag{5.9}$$

  The spectrum of $\hat{\mathcal{L}}_+$ is the set of the lambdas that are eigenvalues of (5.9) for some μ in $\mathbb{R}$.

$$\lambda(\mu) = -\mu^2 + i\mu(c_f - a), \quad \lambda(\mu) = i\mu c_f, \quad \lambda(\mu) = i\mu(c_f - b).$$

  At (θ^+, ρ^+, Y^+), the spectrum of the linearization is a parabola in the left-half plane that touches the origin and the imaginary axis.

  1. FC left state

     We determine the spectrum of $\hat{\mathcal{L}}_-$ at the point (θ^-, ρ^-, Y^-) where $\theta^- > 0$, $\rho^- = 0$ and $Y^- > 0$. We obtain

$$\hat{\mathcal{L}}_- = \begin{pmatrix} -\mu^2 + i\mu(c_f - a) & Y^-\Phi(\theta^-) & 0 \\ 0 & i\mu c_f - Y^-\Phi(\theta^-) & 0 \\ 0 & Y^-\Phi(\theta^-) & i\mu(c_f - b) \end{pmatrix}. \tag{5.10}$$

The spectrum of $\hat{\mathcal{L}}_-$ is the set of the lambdas that are eigenvalues of (5.10) for some μ in $\mathbb{R}$.

$$\lambda(\mu) = -\mu^2 + i\mu(c_f - a), \quad \lambda(\mu) = i\mu c_f - Y^-\Phi(\theta^-), \quad \lambda(\mu) = i\mu(c_f - b).$$

Similarly, the spectrum of the linearization is a parabola in the left-half plane that touches the origin, a vertical line in the left-half plane and the imaginary axis.

2. OC left state

   We determine the spectrum of $\hat{\mathcal{L}}_-$ at the point (θ^-, ρ^-, Y^-) where $\theta^- > 0$, $\rho^- > 0$ and $Y^- = 0$. We obtain

$$\hat{\mathcal{L}}_- = \begin{pmatrix} -\mu^2 + i\mu(c_f - a) & 0 & \rho^-\Phi(\theta^-) \\ 0 & i\mu c_f & -\rho^-\Phi(\theta^-) \\ 0 & 0 & i\mu(c_f - b) - \rho^-\Phi(\theta^-) \end{pmatrix}. \tag{5.11}$$

   The spectrum of $\hat{\mathcal{L}}_-$ is the set of the lambdas that are eigenvalues of (5.11) for some μ in $\mathbb{R}$.

$$\lambda(\mu) = -\mu^2 + i\mu(c_f - a), \quad \lambda(\mu) = i\mu(c_f - b) - \rho^-\Phi(\theta^-), \quad \lambda(\mu) = i\mu c_f.$$

   The spectrum consists of a curve, a vertical line in the left half-plane and imaginary axis.

- Spectrum of slow combustion waves ($c_s < a < b$)

  We have two types of slow combustion waves; $FC \xrightarrow{c_s} OC$ and $TC \xrightarrow{c_s} OC$. Since the right state has same type OC, first we compute the spectrum of $\hat{\mathcal{L}}_+$ at the right end state (θ^+, ρ^+, Y^+) where $\theta^+ > 0$, $\rho^+ > 0$ and $Y^+ = 0$. We obtain

$$\hat{\mathcal{L}}_+ = \begin{pmatrix} -\mu^2 + i\mu(c_s - a) & 0 & \rho^+\Phi(\theta^+) \\ 0 & i\mu c_s & -\rho^+\Phi(\theta^+) \\ 0 & 0 & i\mu(c_s - b) - \rho^+\Phi(\theta^+) \end{pmatrix}. \tag{5.12}$$

  The spectrum of $\hat{\mathcal{L}}_+$ is the set of the lambdas that are eigenvalues of (5.12) for some μ in $\mathbb{R}$.

$$\lambda(\mu) = -\mu^2 + i\mu(c_s - a), \quad \lambda(\mu) = i\mu c_s, \quad \lambda(\mu) = i\mu(c_s - b) - \rho^+\Phi(\theta^+).$$

The spectrum of the linearization is a parabola in the left-half plane that touches the origin, a vertical line in the left-half plane and the imaginary axis.

1. FC left state

   Similarly,

   $$\lambda(\mu) = -\mu^2 + i\mu(c_s - a), \quad \lambda(\mu) = i\mu c_s - Y^-\Phi(\theta^-), \quad \lambda(\mu) = i\mu(c_s - b).$$

   The spectrum of the linearization is a parabola in the left-half plane that touches the origin, a vertical line in the left-half plane and the imaginary axis.

2. TC left state

   $$\lambda(\mu) = -\mu^2 + i\mu(c_s - a), \quad \lambda(\mu) = i\mu c_s, \quad \lambda(\mu) = i\mu(c_s - b).$$

   The spectrum of the linearization is a parabola in the left-half plane that touches the origin and the imaginary axis.

- Spectrum of intermediate combustion waves ($a < c_m < b$)

  We have two types of intermediate combustion waves; $FC \xrightarrow{c_m} OC$ and $FC \xrightarrow{c_m} TC$. Since the left state has same type FC, we compute the spectrum of $\hat{\mathcal{L}}_-$ at the left end state (θ^-, ρ^-, Y^-) where $\theta^- > 0$, $\rho^- = 0$ and $Y^- > 0$. We obtain the spectrum of $\hat{\mathcal{L}}_-$ which is a parabola in the left-half plane that touches the origin, a vertical line in the left-half plane and the imaginary axis.

  $$\lambda(\mu) = -\mu^2 + i\mu(c_m - a), \quad \lambda(\mu) = i\mu c_m - Y^-\Phi(\theta^-), \quad \lambda(\mu) = i\mu(c_m - b).$$

1. TC right state

   $$\lambda(\mu) = -\mu^2 + i\mu(c_m - a), \quad \lambda(\mu) = i\mu c_m, \quad \lambda(\mu) = i\mu(c_m - b).$$

   The spectrum of the linearization is a parabola in the left-half plane that touches the origin and the imaginary axis.

2. OC right state

$$\lambda(\mu) = -\mu^2 + i\mu(c_m - a), \quad \lambda(\mu) = i\mu c_m, \quad \lambda(\mu) = i\mu(c_m - b) - \rho^+\Phi(\theta^+).$$

The spectrum consists of a curve, a vertical line in the left half-plane and the imaginary axis.

We don't have spectral stability for any type of the combustion wave since the spectrum of $\mathcal{L}_+$ and $\mathcal{L}_-$ for fast, slow and intermediate combustion waves touches the imaginary axis. Spectral stability can be obtained if these spectra can be moved to the left of the imaginary axis by working in a space with weighted norm. We introduce a weight function such that for $\alpha = (\alpha_-, \alpha_+) \in \mathbb{R}^2$, $\gamma_\alpha : \mathbb{R} \to \mathbb{R}$

$$\gamma_\alpha(\xi) = \begin{cases} e^{\alpha_-\xi}, & \xi \leq 0 \\ e^{\alpha_+\xi}, & \xi \geq 0 \end{cases} \tag{5.13}$$

Let $\mathcal{X}_0$ denote one of the standard Banach spaces $L^2(\mathbb{R})^n$, $H^1(\mathbb{R})^n$ or $BUC(\mathbb{R})^n$ with norm $\| \ \|_0$. Let $\mathcal{X}_\alpha$ denote the weighted space for a fixed weight $\gamma_\alpha(\xi)$ such that for $x(\xi) \in \mathcal{X}_\alpha$, $\gamma_\alpha(\xi)x(\xi) \in \mathcal{X}_0$ with norm $\|x\|_\alpha = \|\gamma_\alpha(\xi)x(\xi)\|_0$.

We need to find $Sp(\mathcal{L})$ on $\mathcal{X}_\alpha$ to determine weight functions for fast, slow and intermediate combustion waves at the left and right end states.

To study the spectrum of $\mathcal{A}_t = \mathcal{L}\mathcal{A}$ as an operator on $\mathcal{X}_\alpha$, let $\mathcal{A} = (\tilde{\theta}(\xi), \tilde{\rho}(\xi), \tilde{Y}(\xi)) \in \mathcal{X}_\alpha$ such that $\gamma_\alpha(\xi)\mathcal{A} = \mathcal{B}$, $\mathcal{B} = (u(\xi), v(\xi), z(\xi)) \in \mathcal{X}_0$. Then we have $\gamma_\alpha^{-1}\mathcal{B}_t = \mathcal{L}\gamma_\alpha^{-1}\mathcal{B}$ and multiply both sides by γ_α. We obtain $\mathcal{B}_t = \gamma_\alpha\mathcal{L}\gamma_\alpha^{-1}\mathcal{B}$ where $\gamma_\alpha\mathcal{L}\gamma_\alpha^{-1}$ is a linear operator on $\mathcal{X}_0$. To find the spectrum of $\mathcal{L}$ on $\mathcal{X}_\alpha$, instead find the spectrum of $\gamma_\alpha\mathcal{L}\gamma_\alpha^{-1}$ on $\mathcal{X}_0$. Let $\mathcal{L}_\alpha = \gamma_\alpha\mathcal{L}\gamma_\alpha^{-1}$. Therefore we have

$$\mathcal{B}_t = \mathcal{L}_\alpha\mathcal{B}. \tag{5.14}$$

By taking $\xi \to \pm\infty$, (5.14) yields constant-coefficient linear differential expressions

$$\mathcal{B}_t = \mathcal{L}_{\alpha_\pm}\mathcal{B} \tag{5.15}$$

where

$$\mathcal{L}_{\alpha_\pm} = \begin{pmatrix} \partial_{\xi\xi} + (c-a-2\alpha_\pm)\partial_\xi + \alpha_\pm^2 + a\alpha_\pm - c\alpha_\pm + F_\theta(T^*) & F_\rho(T^*) & F_Y(T^*) \\ -F_\theta(T^*) & c\partial_\xi - c\alpha_\pm - F_\rho(T^*) & -F_Y(T^*) \\ -F_\theta(T^*) & -F_\rho(T^*) & (c-b)(\partial_\xi - \alpha_\pm) - F_Y(T^*) \end{pmatrix}. \tag{5.16}$$

The right hand boundary of the essential spectrum of $\mathcal{L}_\alpha$ is the union of the right hand boundary of $Sp(\mathcal{L}_{\alpha_-})$ and $Sp(\mathcal{L}_{\alpha_+})$.

- Weight function for fast combustion waves $(a < b < c_f)$

  Since the right state has same type TC for fast combustion waves, we compute the spectrum of $\mathcal{L}_{\alpha_+}$ at the right end state (θ^+, ρ^+, Y^+) where $\theta^+ \leq 0$, $\rho^+ > 0$ and $Y^+ > 0$. We obtain

$$\mathcal{L}_{\alpha_+} = \begin{pmatrix} -\mu^2 + (c_f - a - 2\alpha_+)i\mu + \alpha_+^2 + (a-c_f)\alpha_+ & 0 & 0 \\ 0 & i\mu c_f - c_f\alpha_+ & 0 \\ 0 & 0 & i\mu(c_f - b) - (c_f - b)\alpha_+ \end{pmatrix}. \tag{5.17}$$

  The spectrum of $\mathcal{L}_{\alpha_+}$ is the set of the lambdas that are eigenvalues of (5.17) for some μ in $\mathbb{R}$.

$$\lambda(\mu) = -\mu^2 + (c_f - a - 2\alpha_+)i\mu + \alpha_+^2 + (a-c_f)\alpha_+,$$

$$\lambda(\mu) = i\mu c_f - c_f\alpha_+,$$

$$\lambda(\mu) = i\mu(c_f - b) - (c_f - b)\alpha_+.$$

  To move the spectrum to the left half plane, we require that real part of the eigenvalues to be negative. Therefore if $0 < \alpha_+ < c_f - a$ is provided, then the spectra lies in the left half plane.

  1. FC left state

     By similar computation, we determine the spectrum of $\mathcal{L}_{\alpha_-}$ at the point (θ^-, ρ^-, Y^-) where $\theta^- > 0$, $\rho^- = 0$ and $Y^- > 0$. We require $0 < \alpha_- < c_f - a$ to move the spectra to the left half plane.

  2. OC left state

     Similarly we determine the spectrum of $\mathcal{L}_{\alpha_-}$ at the point (θ^-, ρ^-, Y^-) where

$\theta^- > 0$, $\rho^- > 0$ and $Y^- = 0$. Again we require $0 < \alpha_- < c_f - a$ to move the spectra to the left half plane.

- Weight function for slow combustion waves ($c_s < a < b$)

  Since the right state has same type OC for slow combustion waves, we compute the spectrum of $\mathcal{L}_{\alpha_+}$ at the right end state (θ^+, ρ^+, Y^+) where $\theta^+ > 0$, $\rho^+ > 0$ and $Y^+ = 0$. We obtain

$$\mathcal{L}_{\alpha_+} = \begin{pmatrix} -\mu^2 + (c_s - a - 2\alpha_+)i\mu + \alpha_+^2 + (a - c_s)\alpha_+ & 0 & \rho^+\Phi(\theta^+) \\ 0 & i\mu c_s - c_s\alpha_+ & -\rho^+\Phi(\theta^+) \\ 0 & 0 & i\mu(c_s - b) - (c_s - b)\alpha_+ - \rho^+\Phi(\theta^+) \end{pmatrix}. \tag{5.18}$$

  The spectrum of $\mathcal{L}_{\alpha_+}$ is the set of the lambdas that are eigenvalues of (5.18) for some μ in $\mathbb{R}$.

$$\lambda(\mu) = -\mu^2 + (c_s - a - 2\alpha_+)i\mu + \alpha_+^2 + (a - c_s)\alpha_+, \tag{5.19}$$

$$\lambda(\mu) = i\mu c_s - c_s\alpha_+, \tag{5.20}$$

$$\lambda(\mu) = i\mu(c_s - b) - (c_s - b)\alpha_+ - \rho^+\Phi(\theta^+). \tag{5.21}$$

  To move the spectrum to the left half plane, real part of the eigenvalues needs to be negative. From (5.20) and (5.21), $0 < \alpha_+ < \frac{\rho^+\Phi(\theta^+)}{b - c_s}$. By (5.19), $c_s - a < \alpha_+ < 0$. α_+ can not be both negative and positive at the same time. Therefore, there is no α_+ which makes the real part of the eigenvalues be negative.

  1. FC left state

     We determine the spectrum of $\mathcal{L}_{\alpha_-}$ at the point (θ^-, ρ^-, Y^-) where $\theta^- > 0$, $\rho^- = 0$ and $Y^- > 0$.

$$\mathcal{L}_{\alpha_-} = \begin{pmatrix} -\mu^2 + (c_s - a - 2\alpha_-)i\mu + \alpha_-^2 + (a - c_s)\alpha_- & Y^-\Phi(\theta^-) & 0 \\ 0 & i\mu c_s - c_s\alpha_- - Y^-\Phi(\theta^-) & 0 \\ 0 & -Y^-\Phi(\theta^-) & i\mu(c_s - b) - (c_s - b)\alpha_- \end{pmatrix} \tag{5.22}$$

     The spectrum of $\mathcal{L}_{\alpha_-}$ is the set of the lambdas that are eigenvalues of (5.22) for some μ in $\mathbb{R}$.

$$\lambda(\mu) = -\mu^2 + (c_s - a - 2\alpha_-)i\mu + \alpha_-^2 + (a - c_s)\alpha_-, \tag{5.23}$$

$$\lambda(\mu) = i\mu c_s - c_s\alpha_- - Y^-\Phi(\theta^-), \tag{5.24}$$

$$\lambda(\mu) = i\mu(c_s - b) - (c_s - b)\alpha_-. \tag{5.25}$$

From (5.24) and (5.25), we get $\frac{-\Phi(\theta^-)Y^-}{c_s} < \alpha_- < 0$. By (5.23), $c_s - a < \alpha_- < 0$. To move the spectrum to the left half plane, we choose α_- such that

(1) if $\frac{-\Phi(\theta^-)Y^-}{c_s} < c_s - a$, then we pick $c_s - a < \alpha_- < 0$

(2) if $\frac{-\Phi(\theta^-)Y^-}{c_s} > c_s - a$, then we pick $\frac{-\Phi(\theta^-)Y^-}{c_s} < \alpha_- < 0$

2. TC left state

We determine the spectrum of $\mathcal{L}_{\alpha_-}$ at the point (θ^-, ρ^-, Y^-) where $\theta^- \leq 0$, $\rho^- > 0$ and $Y^- > 0$.

$$\mathcal{L}_{\alpha_-} = \begin{pmatrix} -\mu^2 + (c_s - a - 2\alpha_-)i\mu + \alpha_-^2 + (a - c_s)\alpha_- & 0 & 0 \\ 0 & i\mu c_s - c_s\alpha_- & 0 \\ 0 & 0 & i\mu(c_s - b) - (c_s - b)\alpha_- \end{pmatrix}. \tag{5.26}$$

The spectrum of $\mathcal{L}_{\alpha_-}$ is the set of the lambdas that are eigenvalues of (5.26) for some μ in $\mathbb{R}$.

$$\lambda(\mu) = -\mu^2 + (c_s - a - 2\alpha_-)i\mu + \alpha_-^2 + (a - c_s)\alpha_-, \tag{5.27}$$

$$\lambda(\mu) = i\mu c_s - c_s\alpha_-, \tag{5.28}$$

$$\lambda(\mu) = i\mu(c_s - b) - (c_s - b)\alpha_-. \tag{5.29}$$

We need α_- be positive for (5.28) and negative for (5.29) to make the real part of the eigenvalues be negative. α_- can not be both negative and positive at the same time. Therefore, there is no α_- which moves the spectra to the left half plane.

- Weight function for intermediate combustion waves ($a < c_m < b$)

Since the left state has same type FC for intermediate combustion waves, we compute the spectrum of $\mathcal{L}_{\alpha_-}$ at the left end state (θ^-, ρ^-, Y^-) where $\theta^- > 0$, $\rho^- = 0$ and $Y^- > 0$. We obtain

$$\mathcal{L}_{\alpha_-} = \begin{pmatrix} -\mu^2 + (c_m - a - 2\alpha_-)i\mu + \alpha_-^2 + (a - c_m)\alpha_- & Y^-\Phi(\theta^-) & 0 \\ 0 & i\mu c_m - c_m\alpha_- - Y^-\Phi(\theta^-) & 0 \\ 0 & -Y^-\Phi(\theta^-) & (i\mu - \alpha)(c_m - b) \end{pmatrix}. \tag{5.30}$$

The spectrum of $\mathcal{L}_{\alpha_-}$ is the set of the lambdas that are eigenvalues of (5.30) for some μ in $\mathbb{R}$.

$$\lambda(\mu) = -\mu^2 + (c_m - a - 2\alpha_-)i\mu + \alpha_-^2 + (a - c_m)\alpha_-, \tag{5.31}$$

$$\lambda(\mu) = i\mu c_m - c_m\alpha_- - Y^-\Phi(\theta^-), \tag{5.32}$$

$$\lambda(\mu) = i\mu(c_m - b) - (c_m - b)\alpha_-. \tag{5.33}$$

From (5.32) and (5.33), we get $\frac{-\Phi(\theta^-)Y^-}{c_m} < \alpha_- < 0$. By (5.31), $0 < \alpha_-$. α_- can not be both negative and positive at the same time. Therefore, there is no α_- which makes the real part of the eigenvalues be negative.

1. TC right state

   We determine the spectrum of $\mathcal{L}_{\alpha_+}$ at the point (θ^+, ρ^+, Y^+) where $\theta^+ < 0$, $\rho^+ > 0$ and $Y^+ > 0$.

$$\mathcal{L}_{\alpha_+} = \begin{pmatrix} -\mu^2 + (c_m - a - 2\alpha_+)i\mu + \alpha_+^2 + (a - c_m)\alpha_+ & 0 & 0 \\ 0 & i\mu c_m - c_m\alpha_+ & 0 \\ 0 & 0 & i\mu(c_m - b) - (c_m - b)\alpha_+ \end{pmatrix}. \tag{5.34}$$

   The spectrum of $\mathcal{L}_{\alpha_+}$ is the set of the lambdas that are eigenvalues of (5.34) for some μ in $\mathbb{R}$.

$$\lambda(\mu) = -\mu^2 + (c_m - a - 2\alpha_+)i\mu + \alpha_+^2 + (a - c_m)\alpha_+, \tag{5.35}$$

$$\lambda(\mu) = i\mu c_m - c_m\alpha_+, \tag{5.36}$$

$$\lambda(\mu) = i\mu(c_m - b) - (c_m - b)\alpha_+. \tag{5.37}$$

   We need α_+ be positive for (5.36) and negative for (5.37) to make the real part of the eigenvalues be negative. α_+ can not be both negative and positive at the same time. Therefore, there is no α_+ which moves the spectra to the left half plane.

2. OC right state

   We need to determine the spectrum of $\mathcal{L}_{\alpha_+}$ at the right end state (θ^+, ρ^+, Y^+) where $\theta^+ > 0$, $\rho^+ > 0$ and $Y^+ = 0$. The spectrum of $\mathcal{L}_{\alpha_+}$ is

$$\lambda(\mu) = -\mu^2 + (c_m - a - 2\alpha_+)i\mu + \alpha_+^2 + (a - c_m)\alpha_+, \tag{5.38}$$

$$\lambda(\mu) = i\mu c_m - c_m\alpha_+, \tag{5.39}$$

$$\lambda(\mu) = i\mu(c_m - b) - (c_m - b)\alpha_+ - \rho^+\Phi(\theta^+). \tag{5.40}$$

To move the spectrum to the left half plane, real part of the eigenvalues needs to be negative. From (5.39) and (5.40), $0 < \alpha_+ < \frac{\rho^+\Phi(\theta^+)}{b-c_m}$. By (5.38), $0 < \alpha_+ < c_m - a$. Therefore we choose α_+ such that

(1) if $\frac{\Phi(\theta^+)\rho^+}{b-c_m} < c_m - a$, then we pick $0 < \alpha_+ < \frac{\Phi(\theta^+)\rho^+}{b-c_m}$.

(2) if$\frac{\Phi(\theta^+)\rho^+}{b-c_m} > c_m - a$, then we pick $0 < \alpha_+ < c_m - a$.

Chapter 6

Numerical results of Evans function for fast combustion waves

The Evans function is an analytic function that can be used to locate the discrete spectrum of the differential operator L. It can be solved analytically for simple systems but in general, it is difficult to calculate explicitly for a given PDE. Hence numerical computation is required.

In this section we show the numerical result of Evans function for fast combustion waves. In previous section we have shown that the spectrum of $\mathcal{L}_+$ and $\mathcal{L}_-$ for fast combustion waves touches the imaginary axis. We fixed this problem by introducing the weight function such that for $\alpha = (\alpha_-, \alpha_+) \in \mathbb{R}^2$, $0 < \alpha_\pm < c_f - a$ is required to move the spectrum to the left half plane. In addition that to determine the stability one needs to trace the position of the point spectrum. Evans function is used to locate the point spectrum. We can count the eigenvalues in the right half plane by calculating the winding number.

We write the eigenvalue problem of (5.15). The eigenvalue problem reads

$$\begin{aligned}
\lambda u &= u_{\xi\xi} + (c - a - 2\alpha_\pm)u_\xi + (\alpha_\pm^2 + a\alpha_\pm - c\alpha_\pm)u + F_\theta(T^*)u + F_\rho(T^*)v + F_Y(T^*)z, \\
\lambda v &= cv_\xi - c\alpha_\pm v - F_\theta(T^*)u - F_\rho(T^*)v - F_Y(T^*)z, \\
\lambda z &= (c - b)z_\xi - (c - b)\alpha_\pm z - F_\theta(T^*)u - F_\rho(T^*)v - F_Y(T^*)z.
\end{aligned} \tag{6.1}$$

We can write (6.1) as a first order system, let $w = u_\xi$

$$\begin{aligned}
u_\xi &= w, \\
w_\xi &= \lambda u - (c - a - 2\alpha_\pm)w - (\alpha_\pm^2 + a\alpha_\pm - c\alpha_\pm)u - F_\theta(T^*)u - F_\rho(T^*)v - F_Y(T^*)z, \\
v_\xi &= \frac{1}{c}(\lambda v + c\alpha_\pm v + F_\theta(T^*)u + F_\rho(T^*)v + F_Y(T^*)z), \\
z_\xi &= \frac{1}{c-b}(\lambda z + (c-b)\alpha_\pm z + F_\theta(T^*)u + F_\rho(T^*)v + F_Y(T^*)z).
\end{aligned} \tag{6.2}$$

We obtain the system of ODE in the form

$$Z_\xi = A(\xi, \lambda)Z. \tag{6.3}$$

We note that the limit matrices $A_\pm(\lambda) = \lim_{\xi\to\pm\infty} A(\xi, \lambda)$ where A is analytic in λ. Also we know that the dimension of the unstable subspace U_- of A_- and the stable subspace $S_+$of A_+ are three and one respectively which sum to four, the dimension of the entire phase space. Then we run (6.3) at $-\infty$ with three vectors spanning the unstable subspace and with one vector spanning the stable subspace at $+\infty$ and compute them toward $\xi = 0$. This gives the analytic basis Z_1^-, Z_2^-, Z_3^- and Z_4^+ spanning the manifolds $Z^\pm$ of solutions of (6.3) that decay as $\xi \to \pm\infty$. Then Evans function can be defined as

$$D(\lambda) = det(Z_1^- Z_2^- Z_3^- Z_4^+)_{|\xi=0}.$$

Hence there is an eigenvalue if and only if $D(\lambda) = 0$, and order of root corresponds to algebraic multiplicity of eigenvalue.

We use STABLAB to compute the Evans function. First, we numerically solve the profile equations for the system (4.2)–(4.3). We have $a = 0.5$ and $b = 0.7$. For the right end state, we set $\theta^+ = -0.1$, $\rho^+ = 2$ and $Y^+ = 8$. For the left end state, first we take $\rho^- = 0$ which corresponds to $FC \xrightarrow{c_f} TC$ wave. These parameters yield the output shown in the left of the Figure 6.1. The picture in the right of the Figure 6.1 has winding number one about 0 indicating the simple eigenvalue at 0. Figure 6.2 shows that the Evans function output winds around 0. The parameters we take are the same parameters with the bifurcation diagram Figure 4.8. By varying Y^+ we plot a curve of values (Y^+, c). The solution labeled from 12 to 18 are in region 1 and we also computed their Evans function by decreasing Y^+ until solution labeled 18. We saw that they also

have the winding number one about 0 indicating the simple eigenvalue at 0. In all Evans function computation, we try to use large semi-circle since we are not able to rule out large eigenvalues. We could use it to plausibly conclude that the simple eigenvalue 0 is the only element in $\{\lambda : Re\lambda \geq 0\}$ for $FC \xrightarrow{c_f} TC$ waves.

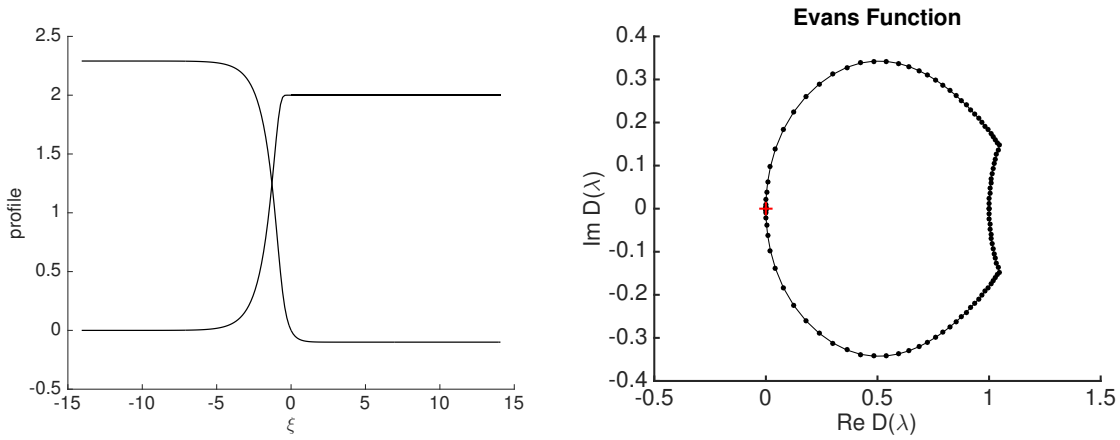

Figure 6.1 Profile for the system (4.2)–(4.3) (left) and Evans function output for a semi-circular contour of radius 250 (right). We have $Y^+ = 8$.

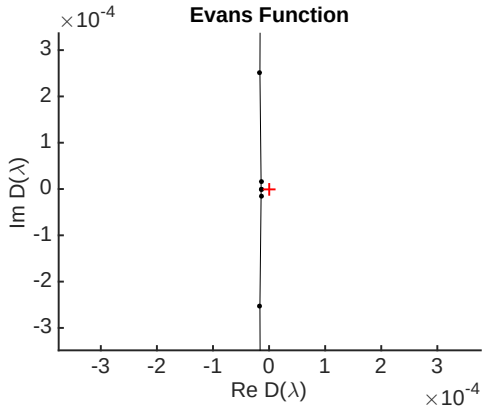

Figure 6.2 Evans function of Figure 6.1, zoom in near 0, showing that 0 is inside the curve.

Now we take $Y^- = 0$ which corresponds to $OC \xrightarrow{c_f} TC$ wave and decrease Y^+ to 1.5. These parameters yield the output shown in the left of the Figure 6.3. The picture in the right of the Figure 6.3 has winding number one about 0 indicating the simple eigenvalue at 0. Figure 6.4 shows that the Evans function output winds around 0. By Figure 4.8 the solutions labeled from 18 to 21 are in region 2 and we also computed their Evans function by decreasing Y^+ until solution labeled 21. We saw that they also have the winding number one about 0 indicating the simple eigenvalue at 0. Evans function computations are performed for large semi-circle since we do not have bound on the eigenvalues. Therefore we could use it to reasonably conclude that the simple eigenvalue 0 is the only element in $\{\lambda : Re\lambda \geq 0\}$ for $OC \xrightarrow{c_f} TC$ waves between the solutions label 18 and 21.

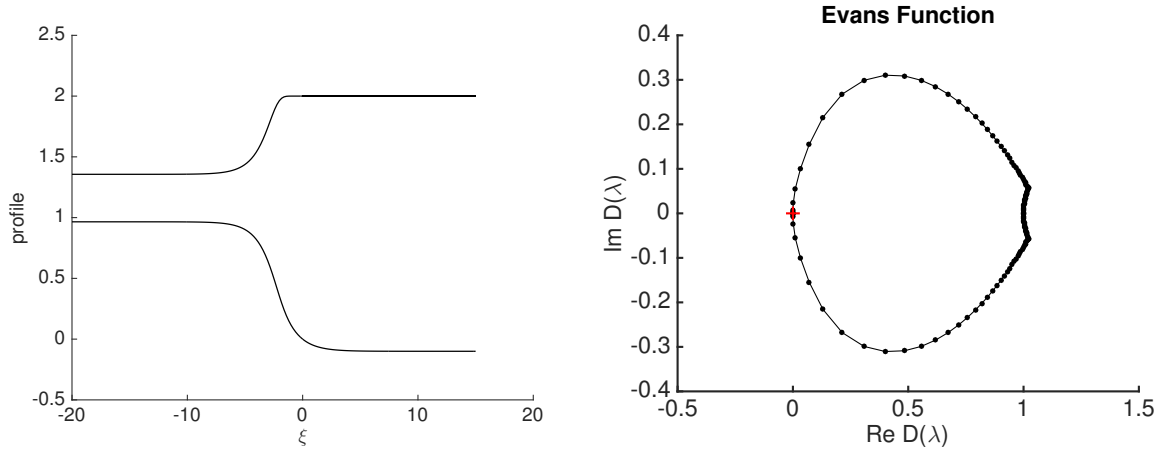

Figure 6.3 Profile for the system (4.2)–(4.3) (left) and Evans function output for a semi-circular contour of radius 250 (right). We have $Y^+ = 1.5$.

As Y^+ reaches its minimum value at Y^+_{**}, the curve of Figure 4.8 turns and solutions labeled from 21 to 47 stay in region 2 that corresponds to $OC \xrightarrow{c_f} TC$ wave. Now we decrease Y^+ to 1.2 and compute Evans function. These parameters yield the output shown in the left of the Figure 6.5. The picture in the right of the Figure 6.5 has winding number two about 0 indicating the simple eigenvalue at 0 and a positive eigenvalue in the right half plane. Figure 6.6 shows that the Evans function output winds around 0. We

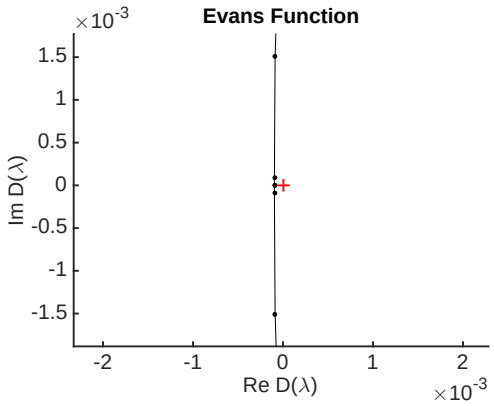

Figure 6.4 Evans function of Figure 6.3, zoom in near 0, showing that 0 is inside the curve.

also computed the Evans function for the solutions labeled from 21 to 47 by increasing Y^+ until solution labeled 47. We saw that they have similar result. Therefore solutions labeled after 21 are not stable since they have a positive eigenvalue in $\{\lambda : Re\lambda \geq 0\}$.

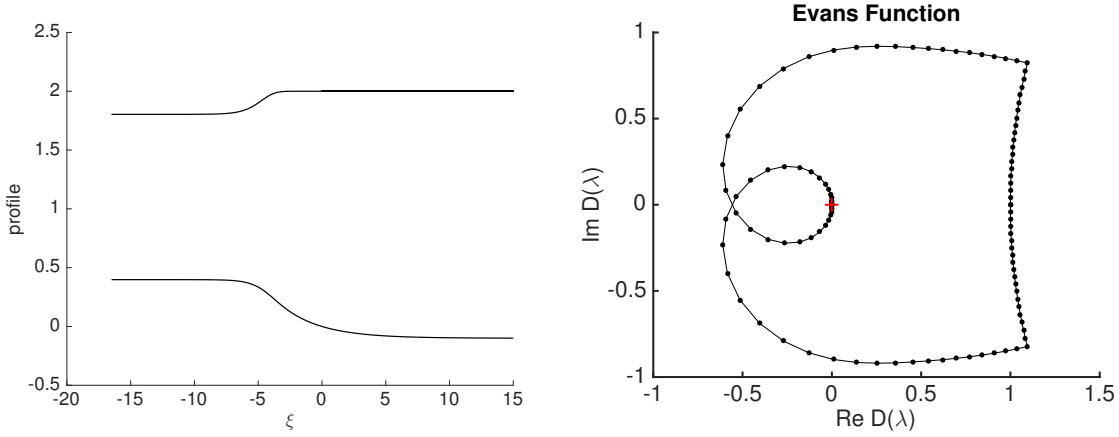

Figure 6.5 Profile for the system (4.2)–(4.3) (left) and Evans function output for a semi-circular contour of radius 2 (right). We have $Y^+ = 1.2$.

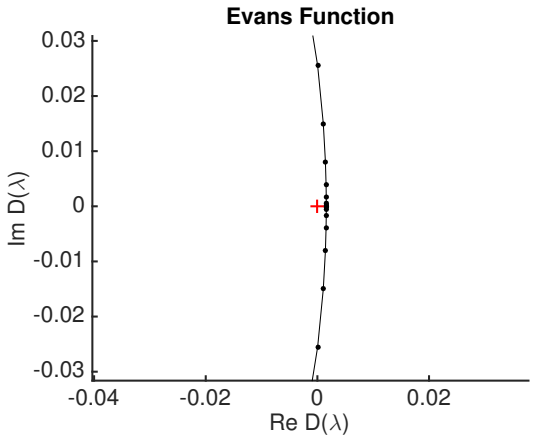

Figure 6.6 Evans function of Figure 6.5, zoom in near 0, showing that the curve winds twice around 0.

Chapter 7

Stability analysis of combustion waves

In this section, we focus on the stability of a given traveling wave. Previously the existence of combustion waves was proved in section 4.1, 4.2 and 4.3. Then we study the spectrum of the operator obtained by the linearization of the combustion system about the wave. Since the essential spectrum of each type of combustion waves touches the imaginary axis, a weight function is needed to be introduced. Such study is done extensively in chapter 5. Concerning the discrete spectrum, in previous chapter we compute the Evans functions. From these computations it is reasonable to conclude that certain waves have no eigenvalues in the half–plane $Re\lambda \geq 0$ other than a simple eigenvalue zero. Although we have not proved this, we will assume it in this chapter.

Even though the discrete spectrum is stable, it does not imply either linear stability or nonlinear stability. We encounter some difficulties.

1. The essential spectrum of the operator (5.7) touches the imaginary axis so it is marginally stable. We overcome this issue by introducing a weight function $\gamma_\alpha(\xi)$. Unfortunately there is no such α that shifts these spectra to the left of the imaginary axis for slow and intermediate combustion waves. On the other hand we are able to find weight function $\gamma_\alpha(\xi)$ with $0 < \alpha_- < c_f - a$ and $0 < \alpha_+ < c_f - a$ for only fast combustion waves. In the weighted space with a positive growth rate, we study the fast traveling waves to prove their linear and nonlinear stability.

2. Since the system (2.7)-(2.9) is partially parabolic, the linearized operator has a vertical line in its spectrum so it is not a sectorial operator.Therefore the linearized system generates a C^0-semigroup, not an analytic semigroup. This difficulty is typical for systems with no diffusion in some equations.

By using recently obtained results about partially parabolic systems [34, 15], these difficulties can be cured. In [34], more general result states that sometimes spectral stability implies linear stability even when the spectrum has vertical lines. In Appendix A the theorem in [34] is stated and note that the assumption of Theorem A.0.1 holds in the weighted space $\mathcal{X}_\alpha$ for the system (2.7)-(2.9). Therefore linear stability follows from the spectral stability for the fast traveling waves.

Nonlinear stability does not necessarily follow from the linear stability. The semigroup estimates which follows from the Theorem A.0.1 are not sufficient to conclude the nonlinear stability. The system (5.1)-(5.3) and the traveling wave solution T^* have some properties that satisfy the hypotheses of Theorem 3.14 in [15] which allow us to obtain nonlinear stability.

Let $\mathcal{X}_0$ denote one of the standard Banach spaces $L^2(\mathbb{R})^n$,$H^1(\mathbb{R})^n$ or $BUC(\mathbb{R})^n$. We denote the norm in $\mathcal{X}_0$ by $\|\ \|_0$. Recall the weight functions $\gamma_\alpha(\xi)$ introduced in section 5. Let $\mathcal{X}_\alpha$ denote the weighted space for a fixed weight γ_α such that $\mathcal{X}_\alpha = \{x : \gamma_\alpha(\xi)x(\xi) \in \mathcal{X}_0\}$ with norm $\|x\|_\alpha = \|\gamma_\alpha(\xi)x(\xi)\|_0$.

We assume α_- and α_+ are nonnegative. Let $\beta = (\min(0, \alpha_-), \max(0, \alpha_+)) = (0, \alpha_+)$ and $\gamma_\beta(\xi)$ be a fixed weight function such that $\max(1, \gamma_\alpha(\xi)) \leq \gamma_\beta(\xi)$. Let $\mathcal{X}_\beta$ denote the weighted space for a fixed weight γ_β such that $\mathcal{X}_\beta = \{x : \gamma_\beta(\xi)x(\xi) \in \mathcal{X}_0\}$ with norm $\|x\|_\beta = \|\gamma_\beta(\xi)x(\xi)\|_0$.

Consider the system (5.1)-(5.3) and let $T^*(\xi)$ be a stationary solution of it, i.e, a traveling wave solution of (2.7)-(2.9) with speed $c > 0$, with $T^- = (\theta^-, 0, Y^-)$ and $T^+ = (0, \rho^+, Y^+)$ that corresponds to a fast traveling wave which has temperature controlled right state and fuel controlled left state. Following work can be easily done for a fast traveling wave which has temperature controlled right state and oxygen controlled left state.

The change of variables $u_1 = \theta - \theta^-$, $u_2 = \rho$, and $u_3 = Y - Y^-$ converts (5.1)-(5.3) to the system

$$\partial_t u_1 = \partial_{\xi\xi} u_1 + (c-a)\partial_\xi u_1 + u_2(u_3 + Y^-)\Phi(u_1 + \theta^-), \tag{7.1}$$

$$\partial_t u_2 = c\partial_\xi u_2 - u_2(u_3 + Y^-)\Phi(u_1 + \theta^-), \tag{7.2}$$

$$\partial_t u_3 = (c-b)\partial_\xi u_3 - u_2(u_3 + Y^-)\Phi(u_1 + \theta^-). \tag{7.3}$$

Let $U^*(\xi) = (u_1^*(\xi), u_2^*(\xi), u_3^*(\xi))$ be stationary solution of (7.1)-(7.3) that corresponds to $T^*(\xi)$ so that $U^- = (0,0,0)$ and $U^+ = (-\theta^-, \rho^+, Y^+ - Y^-)$.

Let

$$R(U) = (u_2(u_3+Y^-)\Phi(u_1+\theta^-), -u_2(u_3+Y^-)\Phi(u_1+\theta^-), -u_2(u_3+Y^-)\Phi(u_1+\theta^-)), \tag{7.4}$$

then the linearization of (7.1)-(7.3) at $U^*(\xi)$ is

$$\begin{pmatrix} \tilde{u}_{1t} \\ \tilde{u}_{2t} \\ \tilde{u}_{3t} \end{pmatrix} = \begin{pmatrix} \partial_{\xi\xi} + (c-a)\partial_\xi & 0 & 0 \\ 0 & c\partial_\xi & 0 \\ 0 & 0 & (c-b)\partial_\xi \end{pmatrix} \begin{pmatrix} \tilde{u}_1 \\ \tilde{u}_2 \\ \tilde{u}_3 \end{pmatrix} + DR(U^*(\xi))\tilde{U} \tag{7.5}$$

where

$$DR(U^*(\xi)) = \begin{pmatrix} u_2^*(u_3^*+Y^-)\Phi'(u_1^*+\theta^-) & (u_3^*+Y^-)\Phi(u_1^*+\theta^-) & u_2^*\Phi(u_1^*+\theta^-) \\ -u_2^*(u_3^*+Y^-)\Phi'(u_1^*+\theta^-) & -(u_3^*+Y^-)\Phi(u_1^*+\theta^-) & -u_2^*\Phi(u_1^*+\theta^-) \\ -u_2^*(u_3^*+Y^-)\Phi'(u_1^*+\theta^-) & -(u_3^*+Y^-)\Phi(u_1^*+\theta^-) & -u_2^*\Phi(u_1^*+\theta^-) \end{pmatrix}. \tag{7.6}$$

Then the following statement follows from Theorem 3.14 in [15].

Theorem 7.0.1. *Consider the system* (5.1)-(5.3) *with the constants* a, b *and* $c > 0$ *that are chosen so that there is a stationary solution* $T^*(\xi)$ *of type FC to TC. Let* $\alpha = (\alpha_-, \alpha_+)$ *with* $0 < \alpha_- < c-a$ *and* $0 < \alpha_+ < c-a$. *Assume the Evans function for the traveling wave* $T^*(\xi)$ *has no zeros in the half-plane* $Re\lambda \geq 0$ *other than a simple zero at the origin. Let* $\beta = (0, \alpha_+)$. *Choose* $\nu > 0$ *as in Corollary A.0.2. Suppose* $T^0 \in T^* + \mathcal{X}^3_\beta$ *with* $\|T^0 - T^*\|_\beta$ *small and let* $T(t)$ *be the solution of* (5.1)-(5.3) *with* $T(0) = T^0$. *Then :*

1. $T(t)$ *is defined for all* $t \geq 0$
2. $T(t) = \tilde{T}(t) + T^*(\xi - q(t))$ *with* $\tilde{T}(t)$ *in a fixed subspace of* $\mathcal{X}^3_\alpha$ *complementary to the span of* $T^{*\prime}$

3. $\|\tilde{T}(t)\|_\beta + |q(t)|$ *is small for all* $t \geq 0$

4. $\|\tilde{T}(t)\|_\alpha \leq Ce^{-\nu t}\|\tilde{T}^0\|_\alpha$

5. *There exists* q^* *such that* $|q(t) - q^*| \leq Ce^{-\nu t}\|\tilde{T}^0\|_\alpha$
   Let $\tilde{U} = (\tilde{M}, \tilde{N})$ *with* $\tilde{M} = (\tilde{u}_1, \tilde{u}_3)$ *and* $\tilde{N} = \tilde{u}_2$.

6. $\|(\tilde{M}(t)\|_0 \leq C\|\tilde{T}^0\|_\beta$

7. $\|\tilde{N}(t)\|_0 \leq Ce^{-\nu t}\|\tilde{T}^0\|_\beta$

For a fast traveling wave which has temperature controlled right state and oxygen controlled left state, the only changes in Theorem 7.0.1 are in the $(\tilde{M}, \tilde{N})$ decomposition: $\tilde{M} = (\tilde{u}_1, \tilde{u}_2)$ and $\tilde{N} = \tilde{u}_3$.

The results of Theorem 7.0.1 (6) and (7) have a physical interpretation. In the case of FC left state, combustion front moves to the right by leaving the high temperature zone behind. Behind the combustion front fuel is exhausted and oxygen is present. If we make a perturbation behind the front by adding

- fuel ($\tilde{u}_2$), it immediately burns because of the high temperature and presence of oxygen.
- oxygen ($\tilde{u}_3$), it simply sits there since there is no fuel.
- heat ($\tilde{u}_1$), it simply diffuses.

On the other hand, in the case of OC left state, behind the combustion front temperature is high, oxygen is exhausted and fuel is present. If we make a perturbation behind the front by adding

- fuel ($\tilde{u}_2$), it simply sits there since there is no oxygen.
- oxygen ($\tilde{u}_3$), it immediately reacts with the fuel until it is exhausted.
- heat ($\tilde{u}_1$), it simply diffuses.

In order to prove Theorem 7.0.1, we need to verify hypotheses of Theorem 3.14 in [15]. We do this in the remainder of this chapter.

7.1 Assumptions

The linearization of (7.1)-(7.3) at the end state $U^- = (0, 0, 0)$ is

$$\begin{pmatrix} \tilde{u}_{1t} \\ \tilde{u}_{2t} \\ \tilde{u}_{3t} \end{pmatrix} = \mathcal{L}^- \begin{pmatrix} \tilde{u}_1 \\ \tilde{u}_2 \\ \tilde{u}_3 \end{pmatrix} = \begin{pmatrix} \partial_{\xi\xi} + (c-a)\partial_\xi & Y^-\Phi(\theta^-) & 0 \\ 0 & c\partial_\xi - Y^-\Phi(\theta^-) & 0 \\ 0 & -Y^-\Phi(\theta^-) & (c-b)\partial_\xi \end{pmatrix} \begin{pmatrix} \tilde{u}_1 \\ \tilde{u}_2 \\ \tilde{u}_3 \end{pmatrix}. \quad (7.7)$$

If $(\tilde{u}_1, \tilde{u}_2, \tilde{u}_3)$ is in a weighted space L^2 with weight function $e^{\alpha\xi}$, then $(\tilde{u}_1, \tilde{u}_2, \tilde{u}_3) = (e^{-\alpha\xi}\tilde{w}_1, e^{-\alpha\xi}\tilde{w}_2, e^{-\alpha\xi}\tilde{w}_3)$ is in $L^2(\mathbb{R})^3$. Substitute them into $\mathcal{L}^-$ and multiply by $e^{\alpha_-\xi}$. We obtain the following linear differential expression

$$\hat{\mathcal{L}}^-\tilde{W} = \begin{pmatrix} \partial_{\xi\xi} + (c-a-2\alpha_-)\partial_\xi + \alpha_-^2 + (a-c)\alpha_- & Y^-\Phi(\theta^-) & 0 \\ 0 & c\partial_\xi - \alpha_- c - Y^-\Phi(\theta^-) & 0 \\ 0 & -Y^-\Phi(\theta^-) & (c-b)\partial_\xi - (c-b)\alpha_- \end{pmatrix} \begin{pmatrix} \tilde{w}_1 \\ \tilde{w}_2 \\ \tilde{w}_3 \end{pmatrix}. \quad (7.8)$$

We find the spectrum of $\hat{\mathcal{L}}^-$ by using the Fourier transform.

$$\lambda = -\mu^2 + (c-a-2\alpha_-)i\mu + \alpha_-^2 + (a-c)\alpha_-,$$

$$\lambda = i\mu c - \alpha_- c - Y^-\Phi(\theta^-),$$

$$\lambda = (c-b)i\mu - (c-b)\alpha_-.$$

Then

$$\begin{aligned} \sup\{Re\lambda : \lambda \in Sp(\mathcal{L}^-_{\alpha_-})\} &= \sup\{Re\lambda : \lambda \in Sp(\hat{\mathcal{L}}^-)\} \quad (7.9) \\ &= \max(\alpha_-^2 + (a-c)\alpha_-, -\alpha_- c - Y^-\Phi(\theta^-), -(c-b)\alpha_-) \end{aligned}$$

which is negative for $0 < \alpha_- < c - a$.

Similarly, the linearization of of (7.1)-(7.3) at the end state $U^+ = (-\theta^-, \rho^+, Y^+ - Y^-)$ is

$$\begin{pmatrix} \tilde{u}_{1t} \\ \tilde{u}_{2t} \\ \tilde{u}_{3t} \end{pmatrix} = \mathcal{L}^+ \begin{pmatrix} \tilde{u}_1 \\ \tilde{u}_2 \\ \tilde{u}_3 \end{pmatrix} = \begin{pmatrix} \partial_{\xi\xi} + (c-a)\partial_\xi & 0 & 0 \\ 0 & c\partial_\xi & 0 \\ 0 & 0 & (c-b)\partial_\xi \end{pmatrix} \begin{pmatrix} \tilde{u}_1 \\ \tilde{u}_2 \\ \tilde{u}_3 \end{pmatrix}. \quad (7.10)$$

Substitute $(\tilde{u}_1, \tilde{u}_2, \tilde{u}_3) = (e^{-\alpha_+\xi}\tilde{w}_1, e^{-\alpha_+\xi}\tilde{w}_2, e^{-\alpha_+\xi}\tilde{w}_3)$ into $\mathcal{L}^+$ and multiply by $e^{\alpha_+\xi}$ to obtain the following linear differential expression

$$\hat{\mathcal{L}}^+\tilde{W} = \begin{pmatrix} \partial_{\xi\xi} + (c-a-2\alpha_+)\partial_\xi + \alpha_+^2 + (a-c)\alpha_+ & 0 & 0 \\ 0 & c\partial_\xi - \alpha_+ & 0 \\ 0 & 0 & (c-b)\partial_\xi - (c-b)\alpha_+ \end{pmatrix} \begin{pmatrix} \tilde{w}_1 \\ \tilde{w}_2 \\ \tilde{w}_3 \end{pmatrix}. \tag{7.11}$$

Using the Fourier transform, we find that the spectrum of $\mathcal{L}^+$ is the set of the λ such that

$$\lambda = -\mu^2 + (c-a-2\alpha_+)i\mu + \alpha_+^2 + (a-c)\alpha_+,$$

$$\lambda = i\mu c - \alpha_+ c,$$

$$\lambda = (c-b)i\mu - (c-b)\alpha_+.$$

Then

$$\begin{aligned} \sup\{Re\lambda : \lambda \in Sp(\mathcal{L}^+_{\alpha_+})\} &= \sup\{Re\lambda : \lambda \in Sp(\hat{\mathcal{L}}^+)\} \\ &= \max(\alpha_+^2 + (a-c)\alpha_+, -\alpha_+ c, -(c-b)\alpha_+) \end{aligned} \tag{7.12}$$

which is negative for $0 < \alpha_+ < c - a$.

7.2 Eigenvalue problem

The eigenvalue problem for (7.5) reads

$$\lambda \begin{pmatrix} \tilde{u}_1 \\ \tilde{u}_2 \\ \tilde{u}_3 \end{pmatrix} = \begin{pmatrix} \partial_{\xi\xi} + (c-a)\partial_\xi & 0 & 0 \\ 0 & c\partial_\xi & 0 \\ 0 & 0 & (c-b)\partial_\xi \end{pmatrix} \begin{pmatrix} \tilde{u}_1 \\ \tilde{u}_2 \\ \tilde{u}_3 \end{pmatrix} + DR(U^*(\xi))\tilde{U}. \tag{7.13}$$

We can write (7.13) as a first order system, for simplification let $k_1 = u_2^*(u_3^* + Y^-)\Phi'(u_1^* + \theta^-)$, $k_2 = (u_3^* + Y^-)\Phi(u_1^* + \theta^-)$, $k_3 = u_2^*\Phi(u_1^* + \theta^-)$ and let $\tilde{v} = \partial_\xi \tilde{u}_1$

$$\begin{pmatrix} \partial_\xi \tilde{v} \\ \partial_\xi \tilde{u}_1 \\ \partial_\xi \tilde{u}_2 \\ \partial_\xi \tilde{u}_3 \end{pmatrix} = \begin{pmatrix} a-c & \lambda - k_1 & -k_2 & -k_3 \\ 1 & 0 & 0 & 0 \\ 0 & \frac{k_1}{c} & \frac{\lambda+k_2}{c} & \frac{k_3}{c} \\ 0 & \frac{k_1}{c-b} & \frac{k_2}{c-b} & \frac{\lambda+k_3}{c-b} \end{pmatrix} \begin{pmatrix} \tilde{v} \\ \tilde{u}_1 \\ \tilde{u}_2 \\ \tilde{u}_3 \end{pmatrix}. \tag{7.14}$$

As $\xi \to \pm\infty$ the linear system (7.14) approaches the constant coefficient linear system.

Let μ be the eigenvalues of the constant coefficient system at U^-, then we obtain

$$\begin{pmatrix} a-c-\mu & \lambda & -Y^-\Phi(\theta^-) & 0 \\ 1 & -\mu & 0 & 0 \\ 0 & 0 & \frac{\lambda+Y^-\Phi(\theta^-)}{c} - \mu & 0 \\ 0 & 0 & \frac{Y^-\Phi(\theta^-)}{c-b} & -\mu \end{pmatrix} \begin{pmatrix} \tilde{v} \\ \tilde{u}_1 \\ \tilde{u}_2 \\ \tilde{u}_3 \end{pmatrix} = 0. \tag{7.15}$$

Therefore the eigenvalues at U^- are

$$\mu_{-1} = \frac{\lambda}{c-b}, \quad \mu_{-2} = \frac{\lambda + Y^-\Phi(\theta^-)}{c}, \quad \mu_{-3\pm} = \frac{-(c-a) \pm \sqrt{(c-a)^2 + 4\lambda}}{2}.$$

Similarly, the eigenvalues at U^+ are

$$\mu_{+1} = \frac{\lambda}{c-b}, \quad \mu_{+2} = \frac{\lambda}{c}, \quad \mu_{+3\pm} = \frac{-(c-a) \pm \sqrt{(c-a)^2 + 4\lambda}}{2}.$$

Note that for $\lambda = 0$, at U^- there are two zero, one negative and one positive eigenvalues; at U^+ there are three zero and one negative eigenvalues. The eigenvalues $\mu_{-1}, \mu_{-2}, \mu_{-3\pm}$ (respectively $\mu_{+1}, \mu_{+2}, \mu_{+3\pm}$) are also the eigenvalues of the linearization of (5.1)-(5.3) at the equilibrium $(T^-, 0)$ (respectively, $(T^+, 0)$).

7.3 Hypotheses and proof of Theorem 7.0.1

In this subsection we give the hypotheses of Theorem 3.4 in [15] and verify these hypotheses to prove the Theorem 7.0.1.

Hypothesis 1. The function R is C^3.

The function R defined by (7.4) is C^∞, so Hypothesis 1 is satisfied.

Hypothesis 2. The system (2.7)-(2.9) has a traveling wave solution $T^*(\xi)$, $\xi = x - ct$, for which there exist numbers $K > 0$ and $\omega_- < 0 < \omega_+$ such that for $\xi \leq 0$, $\|T^*(\xi)\| \leq$

$Ke^{-\omega_-\xi}$, and for $\xi \geq 0$, $\|T^*(\xi) - T^+\| \leq Ke^{-\omega_+\xi}$.

Let $-\omega_-$ be the minimum of the positive eigenvalues of the linearization of (5.1)-(5.3) at $(T^-, 0)$ and let $-\omega_+$ be the maximum of the negative eigenvalues of the linearization of (5.1)-(5.3) at $(T^+, 0)$. Since there is only one positive eigenvalue at $(T^-, 0)$ and only one negative eigenvalue at $(T^+, 0)$, we have

$$\omega_- = -\min\left(\frac{1}{c}Y^-\Phi(\theta^-)\right), \qquad \omega_+ = \min\left(c - a\right).$$

The values ω_- and ω_+ satisfy the Hypothesis 2.

Hypothesis 3. There exist $\alpha = (\alpha_-, \alpha_+) \in \mathbb{R}^2$ such that the following are true

1. $0 < \alpha_- < -\omega_-$
2. $0 \leq \alpha_+ < \omega_+$
3. For the system (7.5) and $\mathcal{X}_0 = L^2(\mathbb{R})$,
   (a) $\sup\{Re\lambda : \lambda \in Sp_{ess}(\mathcal{L}_\alpha)\} < 0$
   (b) the only element of $Sp(\mathcal{L}_\alpha)$ in $\{\lambda : Re\lambda \geq 0\}$ is a simple eigenvalue 0.

Let $\alpha = (\alpha_-, \alpha_+)$ with $0 < \alpha_- < \min(c-a, -\omega_-)$ and $0 < \alpha_+ < \omega_+$ so that Hypothesis 3 (1) and (2) are satisfied. (7.12) is negative since we have $0 < \alpha_+ < \omega_+$. Also (7.9) is negative since $0 < \alpha_- < \min\left(c - a, \frac{1}{c}Y^-\Phi(\theta^-)\right)$. Hence Hypothesis 3 (3a) is satisfied with

$$\begin{aligned}\sup\{Re\lambda : \lambda \in Sp_{ess}(\mathcal{L}_\alpha)\} &= \max(\alpha_-^2 + (a-c)\alpha_-, -\alpha_- c - Y^-\Phi(\theta^-), -(c-b)\alpha_-, \\ &\quad \alpha_+^2 + (a-c)\alpha_+, -\alpha_+ c, -(c-b)\alpha_+). \qquad (7.16)\end{aligned}$$

Hypothesis 3 (3b) requires a numerical study of Evans function. In chapter 6, numerically we showed that for a large semi-circle a simple eigenvalue 0 is the only element in $\{\lambda : Re\lambda \geq 0\}$. Therefore Hypothesis 3 (3b) holds.

By using Corollary A.0.2, there exists $K > 0$ such that for $t \geq 0$, $\|e^{t\mathcal{L}_\alpha \mathcal{P}_\alpha^s}\|_{R(\mathcal{L}_\alpha)\to R(\mathcal{L}_\alpha)} \leq Ke^{-\nu t}$. This result says that every solution of the linearized system about the traveling wave $T^*(\xi)$ in the weighted space decays exponentially to a multiple of $T^{*\prime}(\xi)$. This linear result is needed to use in the proof of nonlinear Theorem 7.0.1.

Hypothesis 4. There is a 2×2 matrix A such that $R(M, 0) = (AM, 0)$.

Decompose $\tilde{U}$-space such that $\tilde{U} = (\tilde{M}, \tilde{N})$ with $\tilde{M} = (\tilde{u}_1, \tilde{u}_3)$ and $\tilde{N} = \tilde{u}_2$. Since $R(u_1, 0, u_3) = (0, 0, 0)$ from (7.4), Hypothesis 4 is satisfied with $A = 0$.

From (7.7) we have

$$\mathcal{L}^{(1)} = \begin{pmatrix} \partial_{\xi\xi} + (c-a)\partial_\xi & 0 \\ 0 & (c-b)\partial_\xi \end{pmatrix}, \qquad \mathcal{L}^{(2)} = c\partial_\xi - Y^- \Phi(\theta^-). \tag{7.17}$$

Hypothesis 5.

1. For $\mathcal{X}_0 = L^2(\mathbb{R})$ or $BUC(\mathbb{R})$, the operator $\mathcal{L}^{(1)}$ on $\mathcal{X}_0^2$ generates a bounded semigroup.

2. For $\mathcal{X}_0 = L^2(\mathbb{R})$, the operator $\mathcal{L}^{(2)}$ on $\mathcal{X}_0$ satisfies $\sup\{Re\lambda : \lambda \in Sp(\mathcal{L}^{(2)})\} < 0$.

The operator $\mathcal{L}^{(1)}$ defined by (7.17) on $L^2(\mathbb{R})$ or $BUC(\mathbb{R})$ generates a bounded semigroup. Indeed, the operator $(c-b)\partial_\xi$ generates a C^0-semigroup and the operator $\partial_{\xi\xi} + (c-a)\partial_\xi$ is sectorial. Also the spectrum of the operator $c\partial_\xi - Y^-\Phi(\theta^-)$ on $L^2(\mathbb{R})$ is contained in $Re\lambda \leq -Y^-\Phi(\theta^-) < 0$. Therefore Hypothesis 5 is satisfied.

Chapter 8

Contact discontinuities and wave sequences

For the definition of contact discontinuities see [9]. In this paper we assume the oxygen is transported faster than the temperature. Therefore we have contact discontinuity of velocity 0, a or b. Only fuel concentration, temperature and oxygen concentration can vary across the wave with velocity 0, a and b respectively.

Wave dimension number of a contact discontinuity is the dimension of the set of the right states that can be reached from a fixed left state. For example, by speed 0, only fuel concentration of the right state can be changed therefore dimension number is 1.

$$OC \xrightarrow{0} OC \quad \text{(dimension 1)}$$

If the fuel concentration is 0 at the right state than dimension number is 0.

$$OC \xrightarrow{0} OC \cap FC \quad \text{(dimension 0)}$$

We find six types of combustion waves and they are listed below with their dimension numbers.

- $FC \xrightarrow{c_f} TC$ (dimension 1)
- $OC \xrightarrow{c_f} TC$ (dimension 1)
- $FC \xrightarrow{c_m} OC$ (dimension 1)

- $FC \xrightarrow{c_m} TC$ (dimension 1)
- $FC \xrightarrow{c_s} OC$ (dimension 1)
- $TC \xrightarrow{c_s} OC$ (dimension 0)

Theorem 2.0.4 and 2.0.6(3) define a smooth mapping from three dimensional space of temperature controlled right states to two dimensional space of oxygen controlled or fuel controlled left states. By Sard's Theorem, almost every FC or OC left state would correspond to a one dimensional set of right states.
Theorem 2.0.5(1) and 2.0.6(1) say that there is a one-parameter family of right states of type OC for each left state of type FC to which the left state can be connected by a slow combustion wave or intermediate combustion wave.
Theorem 2.0.5(2) says that the set of points in $(\theta^-, \rho^-, Y^-, \theta^+, \rho^+, c_s)$–space that corresponds to temperature controlled to oxygen controlled slow waves should be a three dimensional manifold. By Sard's Theorem, almost every left state corresponds to a set of isolated right states (which may be empty).

For a wave sequence that solves the boundary value problem, the velocity of the waves must be in increasing order. Only generic wave sequences are considered. These are the wave sequences that satisfy the following properties;

1. Left end state must be of type TC, FC or OC.
2. Right end state must be of type TC, FC or OC.
3. If the right end state is of type TC, then the wave dimension numbers must sum to at least three.
4. If the right end state is of type FC or OC, then the wave dimension numbers must sum to at least two.

Contact discontinuities that begin or end at states of type $TC \cap FC$, $TC \cap OC$, $FC \cap OC$ or $TC \cap FC \cap OC$ can not be the first or last in the wave sequences. However they can occur as intermediate waves in the generic wave sequences. An example of generic wave sequence; $OC \xrightarrow{0} FC \cap OC \xrightarrow{a} FC \cap OC \xrightarrow{b} FC$ (dimension number= 0+1+1=2)

Theorem 8.0.1. *Contact discontinuities with velocity 0, other than the following can not appear in generic wave sequences*

1. $TC \xrightarrow{0} TC$ *(dimension 1)*

2. $TC \xrightarrow{0} TC \cap FC$ *(dimension 0)*

3. $OC \xrightarrow{0} OC$ *(dimension 1)*

4. $OC \xrightarrow{0} OC \cap FC$ *(dimension 0)*

By the generic wave sequence properties, a contact discontinuity with velocity 0 is the first wave in the sequence and has left state TC, OC or FC. FC is not allowed to be the first state since only fuel concentration can vary across the wave with velocity 0. Therefore the new right is not allowed. However if the left is TC or OC, then only fuel concentration can vary across the wave. Therefore the new right state is the same as the left state or left state intersected with FC.

Theorem 8.0.2. *Contact discontinuities with velocity b, other than the following can not appear in generic wave sequences*

1. $TC \xrightarrow{b} TC$ *(dimension 1)*

2. $FC \xrightarrow{b} FC$ *(dimension 1)*

3. $TC \cap OC \xrightarrow{b} TC$ *(dimension 1)*

4. $FC \cap OC \xrightarrow{b} FC$ *(dimension 1)*

There are two possibilities that a contact discontinuity of speed b is the last wave in the sequence or followed by a fast combustion wave. If it is the last wave then by the generic wave sequence properties, the right state is of type TC, OC or FC. If it is followed by a fast combustion wave then the right state is of type OC or FC. Therefore we have seven possible left sates (TC, OC, FC, $TC \cap FC$, $TC \cap OC$, $FC \cap OC$, $TC \cap FC \cap OC$) and three possible right state (TC, OC, FC). There are 21 possible contact discontinuities of speed b and only four which are listed above can appear since only oxygen concentration can vary across the wave with velocity b. The rest of the waves cannot occur.

Theorem 8.0.3. *Contact discontinuities with velocity a, other than the following can not appear in generic wave sequences*

1. $TC \xrightarrow{a} TC$ *(dimension 1)*

2. $TC \cap FC \xrightarrow{a} FC$ *(dimension 1)*

3. $OC \xrightarrow{a} OC \cap TC$ *(dimension 1)*

4. $OC \xrightarrow{a} OC$ *(dimension 1)*

5. $FC \xrightarrow{a} FC$ *(dimension 1)*

6. $OC \cap FC \xrightarrow{a} OC \cap FC$ *(dimension 1)*

There are four possibilities that a contact discontinuity of speed a is the last wave in the sequence or followed by a fast combustion wave or followed by a contact discontinuity of speed b or followed by an intermediate combustion wave. If it is the last wave then by the generic wave sequence properties, the right state is of type TC, OC or FC. If it is followed by a fast combustion wave then the right state is of type OC or FC. If it is followed by a contact discontinuity of speed b then by Theorem (8.0.2) the right state is of type TC, FC, $TC \cap OC$, $FC \cap OC$. If it is followed by an intermediate combustion wave then the right state is of type TC or FC. Therefore we have seven possible left sates (TC, OC, FC, $TC \cap FC$, $TC \cap OC$, $FC \cap OC$, $TC \cap FC \cap OC$) and five possible right state (TC, OC, FC, $TC \cap OC$, $FC \cap OC$). There are 35 possible contact discontinuities of speed a and only six which are listed above can appear since only temperature concentration can vary across the wave with velocity a. The rest of the waves cannot occur.

Using Figure 8.1, we can list all possible generic wave sequences that satisfy above four properties. These wave sequences are classified according to their right state of type FC, OC and TC. We provide more detailed description of these wave sequences below.

8.1 Right state of type FC

- TC to FC BVPs ($\theta^L \leq 0$ and $\rho^R = 0$).

  $TC \xrightarrow{0} TC \cap FC \xrightarrow{a} FC \xrightarrow{b} FC$ is the only generic wave sequence of type TC to FC, in detail,

$$(\theta^L, \rho^L, Y^L) \xrightarrow{0} (\theta^L, 0, Y^L) \xrightarrow{a} (\theta^R, 0, Y^L) \xrightarrow{b} (\theta^R, 0, Y^R).$$

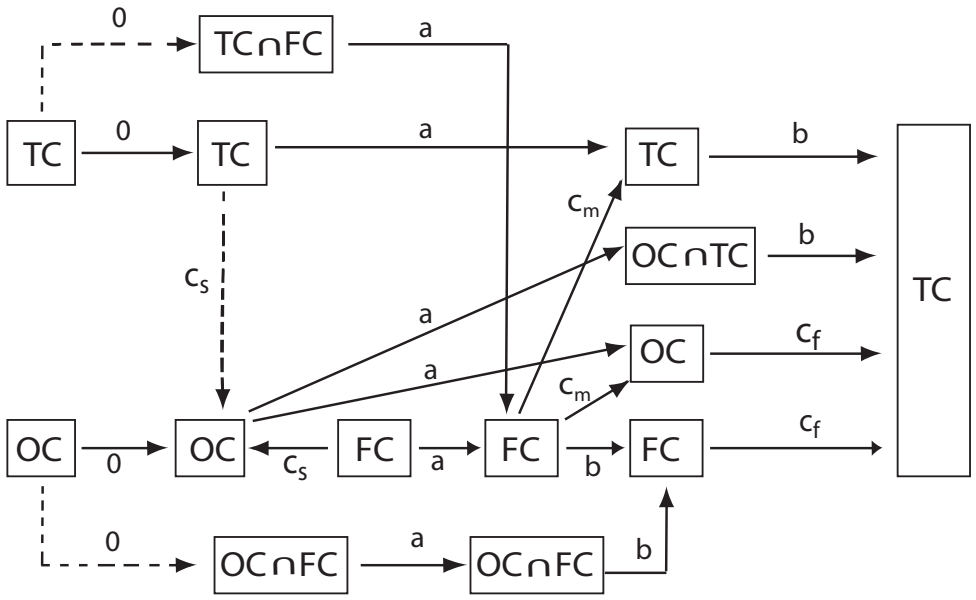

Figure 8.1 All possible generic wave sequences. Dashed and black arrows indicate dimension number 0 and 1 respectively.

See the simulation result in Figure 8.2. Notice that there is no combustion wave. We only have three contact discontinuities with speed 0, a and b.

- OC to FC BVPs ($Y^L = 0$ and $\rho^R = 0$).

  $OC \xrightarrow{0} FC \cap OC \xrightarrow{a} FC \cap OC \xrightarrow{b} FC$ is the only generic wave sequence of type OC to FC, more precisely, $(\theta^L, \rho^L, 0) \xrightarrow{0} (\theta^L, 0, 0) \xrightarrow{a} (\theta^R, 0, 0) \xrightarrow{b} (\theta^R, 0, Y^R)$.

- FC to FC BVPs ($\rho^L = \rho^R = 0$).

  $FC \xrightarrow{a} FC \xrightarrow{b} FC$ is the only generic wave sequence of type FC to FC, more precisely, $(\theta^L, 0, Y^L) \xrightarrow{a} (\theta^R, 0, Y^L) \xrightarrow{b} (\theta^R, 0, Y^R)$.

8.2 Right state of type OC

- FC to OC BVPs ($\rho^L = 0$, $Y^R = 0$).

  There are two generic wave sequences. If $(a - b)Y^L + a\rho^R > 0$, then by Theorem 2.0.5(1), θ^L, Y^L, and ρ^R determine θ^N such that there is a slow $FC \xrightarrow{c_s} OC$

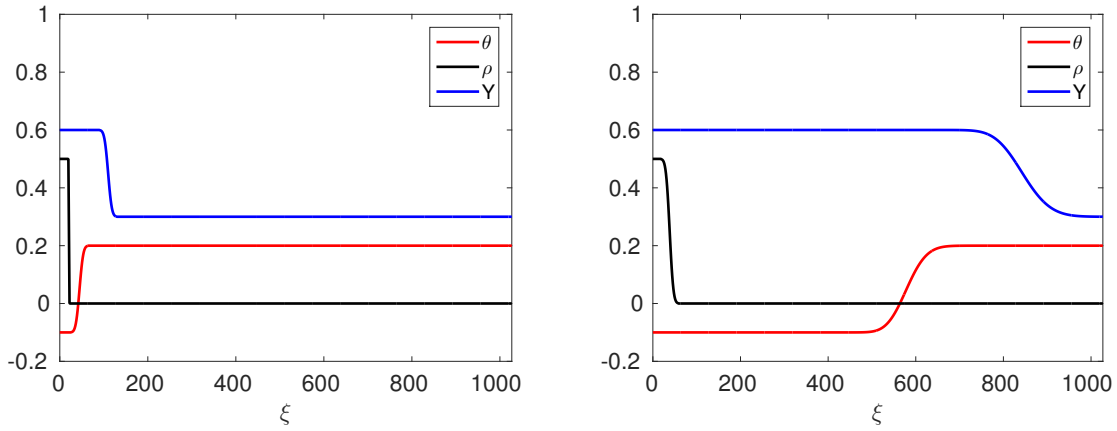

Figure 8.2 Result of numerical simulation for the wave sequence $TC \xrightarrow{0} TC \cap FC \xrightarrow{a} FC \xrightarrow{b} FC$ with $a = 0.5$ and $b = 0.7$, demonstrating contact discontinuities of speed 0, a and b. Initial conditions (left) and simulation time 1000 (right).

combustion wave from $(\theta^L, 0, Y^L)$ to $(\theta^N, \rho^R, 0)$ and for $(a-b)Y^L + a\rho^R < 0$ by Theorem 2.0.6(1), θ^R, ρ^R and Y^L determine θ^N such that there is an intermediate $FC \xrightarrow{c_m} OC$ combustion wave from $(\theta^N, 0, Y^L)$ to $(\theta^R, \rho^R, 0)$

1. $FC \xrightarrow{c_s} OC \xrightarrow{a} OC$; more precisely $(\theta^L, 0, Y^L) \xrightarrow{c_s} (\theta^N, \rho^R, 0) \xrightarrow{a} (\theta^R, \rho^R, 0)$.
   See the result of numerical simulation in Figure 8.3.
2. $FC \xrightarrow{a} FC \xrightarrow{c_m} OC$; more precisely $(\theta^L, 0, Y^L) \xrightarrow{a} (\theta^N, 0, Y^L) \xrightarrow{c_m} (\theta^R, \rho^R, 0)$.
   See the result of numerical simulation in Figure 8.4.

Note that there is a bifurcation from FC to OC wave sequences and fixing θ^L and ρ^R and altering the amount of Y^L determine which wave sequence we get. Increasing Y^L enough in the wave sequence $FC \xrightarrow{c_s} OC \xrightarrow{a} OC$ changes the wave sequence to $FC \xrightarrow{a} FC \xrightarrow{c_m} OC$. Similarly, fixing θ^L and Y^L and decreasing the amount of ρ^R enough gives the same result.

- OC to OC BVPs ($Y^L = Y^R = 0$).

  $OC \xrightarrow{0} OC \xrightarrow{a} OC$ is the only generic wave sequence of type OC to OC, more precisely, $(\theta^L, \rho^L, 0) \xrightarrow{0} (\theta^L, \rho^R, 0) \xrightarrow{a} (\theta^R, \rho^R, 0)$.

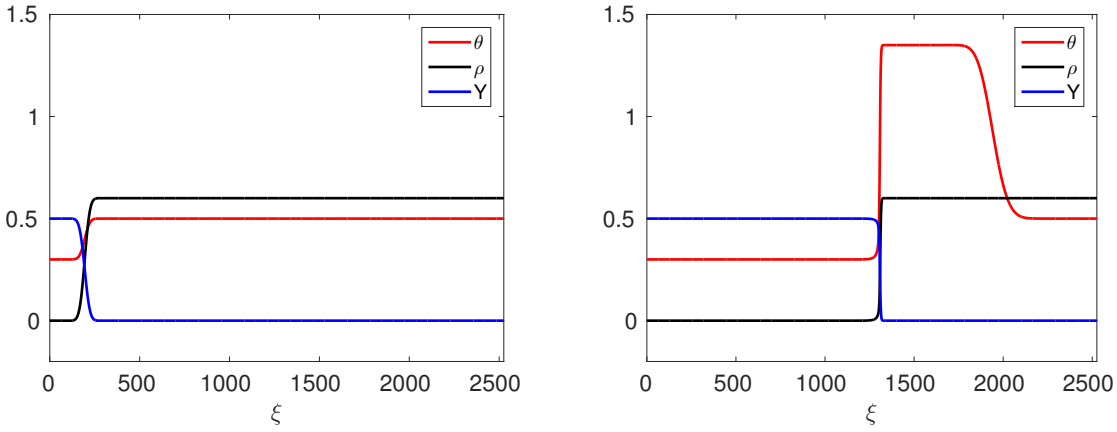

Figure 8.3 Result of numerical simulation for the wave sequence $FC \xrightarrow{c_s} OC \xrightarrow{a} OC$ with $a = 0.5$, demonstrating a fuel-controlled to oxygen-controlled slow combustion wave followed by a contact discontinuity of speed a. Initial conditions (left) and simulation time 3500 (right).

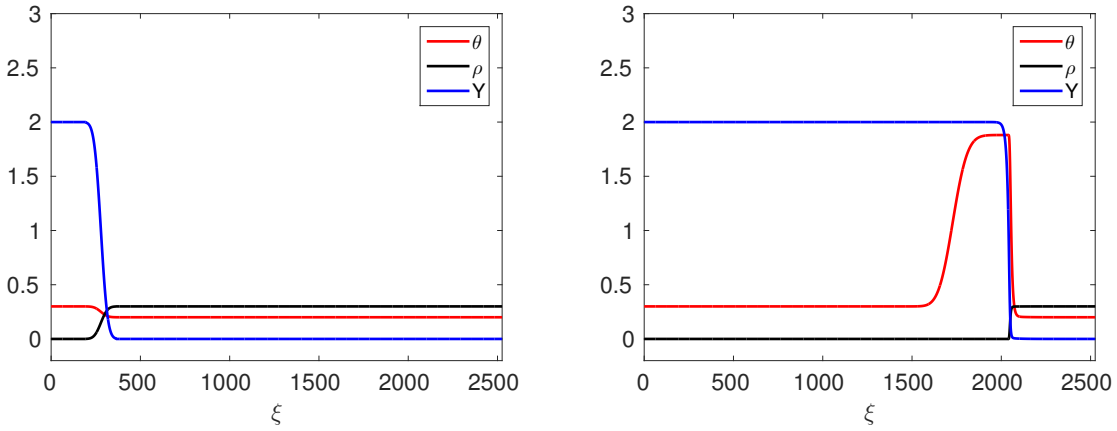

Figure 8.4 Result of numerical simulation for the wave sequence $FC \xrightarrow{a} FC \xrightarrow{c_m} OC$ with $a = 0.5$, demonstrating a fuel-controlled to oxygen-controlled intermediate combustion wave that moves ahead of a contact discontinuity of speed 0. Initial conditions (left) and simulation time 3000 (right).

- TC to OC BVPs ($\theta^L \leq 0$, $Y^R = 0$).

  We have two generic wave sequences of type TC to OC.

  1. For $\theta^L + \frac{b}{a}Y^L > 0$, $TC \xrightarrow{0} TC \xrightarrow{c_s} OC \xrightarrow{a} OC$ is a generic wave sequence. if $\theta^L + \frac{b}{a}Y^L > 0$, then by Theorem 2.0.5(2), θ^L, Y^L, and ρ^R determine θ^N and ρ^M such that there is a slow $TC \xrightarrow{c_s} OC$ combustion wave from (θ^L, ρ^M, Y^L) to $(\theta^N, \rho^R, 0)$.

     $$(\theta^L, \rho^L, Y^L) \xrightarrow{0} (\theta^L, \rho^M, Y^L) \xrightarrow{c_s} (\theta^N, \rho^R, 0) \xrightarrow{a} (\theta^R, \rho^R, 0).$$

     See the result of numerical simulation in Figure 8.5.

  2. For $(a-b)Y^L + a\rho^R < 0$, $TC \xrightarrow{0} TC \cap FC \xrightarrow{a} FC \xrightarrow{c_m} OC$ is a generic wave sequence. If $(a-b)Y^L + a\rho^R < 0$, then by Theorem 2.0.6(1), θ^R, Y^L, and ρ^R determine θ^N such that there is an intermediate $FC \xrightarrow{c_m} OC$ combustion wave from $(\theta^L, 0, Y^L)$ to $(\theta^N, \rho^R, 0)$.

     $$(\theta^L, \rho^L, Y^L) \xrightarrow{0} (\theta^L, 0, Y^L) \xrightarrow{a} (\theta^N, 0, Y^L) \xrightarrow{c_m} (\theta^R, \rho^R, 0).$$

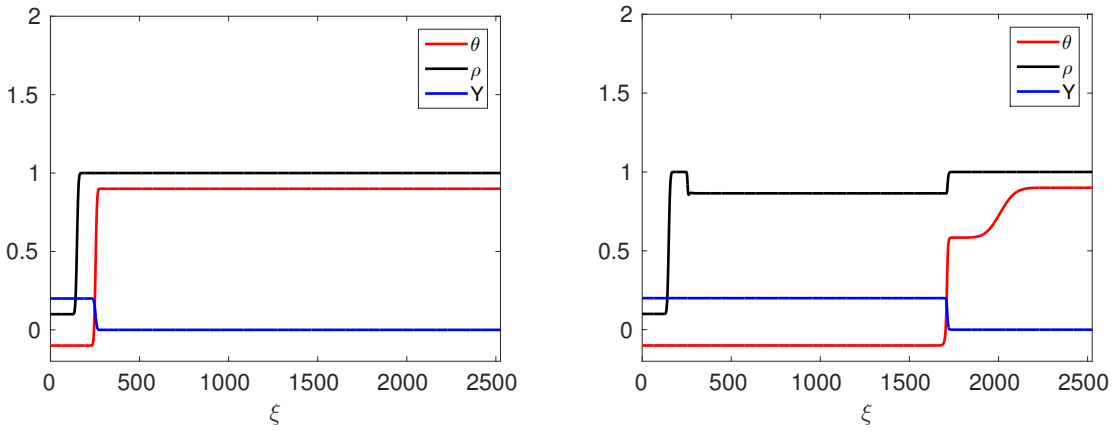

Figure 8.5 Result of numerical simulation for the wave sequence $TC \xrightarrow{0} TC \xrightarrow{c_s} OC \xrightarrow{a} OC$ with $a = 0.5$, demonstrating a temperature-controlled to oxygen-controlled slow combustion wave that moves ahead of a contact discontinuity of speed 0 and followed a contact discontinuity of speed a. Initial conditions (left) and simulation time 3500 (right).

8.3 Right state of type TC

- TC to TC BVPs ($\theta^L \le 0$ and $\theta^R \le 0$).

  We have six generic wave sequences of type TC to TC.

  1. $TC \xrightarrow{0} TC \xrightarrow{a} TC \xrightarrow{b} TC$; more precisely,

  $$(\theta^L, \rho^L, Y^L) \xrightarrow{0} (\theta^L, \rho^R, Y^L) \xrightarrow{a} (\theta^R, \rho^R, Y^L) \xrightarrow{b} (\theta^R, \rho^R, Y^R).$$

  2. $TC \xrightarrow{0} TC \xrightarrow{c_s} OC \xrightarrow{a} OC \cap TC \xrightarrow{b} TC$. If $\theta^L + \frac{b}{a} Y^L > 0$, then by Theorem 2.0.5(2), θ^L, Y^L, and ρ^R determine θ^N and ρ^M such that there is a slow $TC \xrightarrow{c_s} OC$ combustion wave from (θ^L, ρ^M, Y^L) to $(\theta^N, \rho^R, 0)$.

  $$(\theta^L, \rho^L, Y^L) \xrightarrow{0} (\theta^L, \rho^M, Y^L) \xrightarrow{c_s} (\theta^N, \rho^R, 0) \xrightarrow{a} (\theta^R, \rho^R, 0) \xrightarrow{b} (\theta^R, \rho^R, Y^R)$$

  See the result of numerical simulation in Figure 8.6.

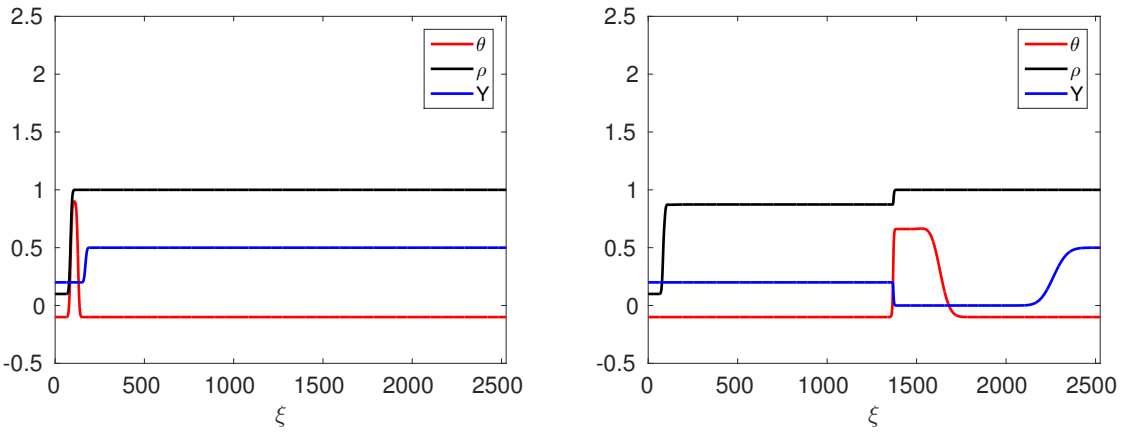

Figure 8.6 Result of numerical simulation for the wave sequence $TC \xrightarrow{0} TC \xrightarrow{c_s} OC \xrightarrow{a} OC \cap TC \xrightarrow{b} TC$ with $a = 0.5$ and $b = 0.7$, demonstrating a temperature-controlled to oxygen-controlled slow combustion wave that moves ahead of a contact discontinuity of speed 0 and followed contact discontinuities of speed a and b. Initial conditions (left) and simulation time 3000 (right).

3. $TC \xrightarrow{0} TC \cap FC \xrightarrow{a} FC \xrightarrow{b} FC \xrightarrow{c_f} TC$. By Theorem 2.0.4(2), for given θ^R, ρ^R and if $Y^R > Y^R_*$, there exists a left state (θ^N, ρ^N, Y^N), with $\theta^N > 0$, $\rho^N = 0$ and $Y^N > 0$, such that there is a fast $FC \xrightarrow{c_f} TC$ combustion wave from (θ^N, ρ^N, Y^N) to (θ^R, ρ^R, Y^R). More precisely

$$(\theta^L, \rho^L, Y^L) \xrightarrow{0} (\theta^L, 0, Y^L) \xrightarrow{a} (\theta^N, 0, Y^L) \xrightarrow{b} (\theta^N, 0, Y^N) \xrightarrow{c_f} (\theta^R, \rho^R, Y^R).$$

See the result of numerical simulation in Figure 8.7.

4. According to our numerical results in section 6, for given θ^R, ρ^R and if $Y^R_* > Y^R > Y^R_{**}$, there exists a left state (θ^N, ρ^N, Y^N), with $\theta^N > 0$, $\rho^N > 0$ and $Y^N = 0$, such that there is a stable fast $OC \xrightarrow{c_f} TC$ combustion wave from (θ^N, ρ^N, Y^N) to (θ^R, ρ^R, Y^R).

   (a) $TC \xrightarrow{0} TC \xrightarrow{c_s} OC \xrightarrow{a} OC \xrightarrow{c_f} TC$. if $\theta^L + \frac{b}{a} Y^L > 0$, then by Theorem 2.0.5(2), θ^L, Y^L, and ρ^N determine ρ^M and θ^M such that there is a slow $TC \xrightarrow{c_s} OC$ combustion wave from (θ^L, ρ^M, Y^L) to $(\theta^M, \rho^N, 0)$.

   $$(\theta^L, \rho^L, Y^L) \xrightarrow{0} (\theta^L, \rho^M, Y^L) \xrightarrow{c_s} (\theta^M, \rho^N, 0) \xrightarrow{a} (\theta^N, \rho^N, 0) \xrightarrow{c_f} (\theta^R, \rho^R, Y^R).$$

   (b) $TC \xrightarrow{0} TC \cap FC \xrightarrow{a} FC \xrightarrow{c_m} OC \xrightarrow{c_f} TC$. If $(a-b)Y^L + a\rho^R < 0$, then by Theorem 2.0.6(1), θ^N, Y^L, and ρ^N determine θ^M such that there is an intermediate $FC \xrightarrow{c_m} OC$ combustion wave from $(\theta^M, 0, Y^L)$ to $(\theta^N, \rho^N, 0)$.

   $$(\theta^L, \rho^L, Y^L) \xrightarrow{0} (\theta^L, 0, Y^L) \xrightarrow{a} (\theta^M, 0, Y^L) \xrightarrow{c_m} (\theta^N, \rho^N, 0) \xrightarrow{c_f} (\theta^R, \rho^R, Y^R).$$

   See the result of numerical simulation in Figure 8.8.

5. $TC \xrightarrow{0} TC \cap FC \xrightarrow{a} FC \xrightarrow{c_m} TC \xrightarrow{b} TC$. If $(a-b)Y^L + a\rho^R < 0$, then by Theorem 2.0.6(3), θ^R, ρ^R, and Y^L determine θ^N and Y^N such that there is an intermediate $FC \xrightarrow{c_m} TC$ combustion wave from $(\theta^N, 0, Y^L)$ to (θ^R, ρ^R, Y^N).

$$(\theta^L, \rho^L, Y^L) \xrightarrow{0} (\theta^L, 0, Y^L) \xrightarrow{a} (\theta^N, 0, Y^L) \xrightarrow{c_m} (\theta^R, \rho^R, Y^N) \xrightarrow{b} (\theta^R, \rho^R, Y^R).$$

See the result of numerical simulation in Figure 8.9.

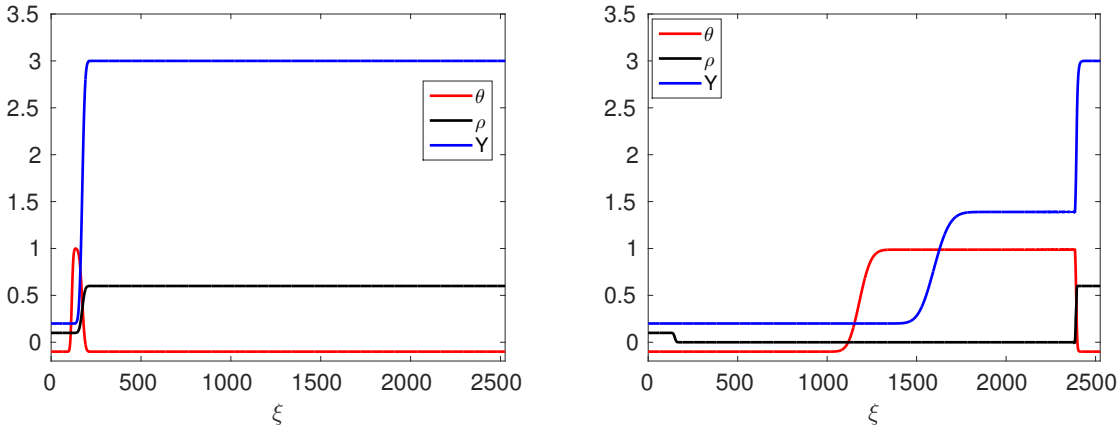

Figure 8.7 Result of numerical simulation for the wave sequence $TC \xrightarrow{0} TC \cap FC \xrightarrow{a} FC \xrightarrow{b} FC \xrightarrow{c_f} TC$ with $a = 0.5$ and $b = 0.7$, demonstrating a fuel-controlled to temperature-controlled fast combustion wave that moves ahead of contact discontinuities of speed a and b. Initial conditions (left) and simulation time 1900 (right). We take $Y^+ > Y_*^+$ to have FC to TC fast combustion wave as stated in Theorem 2.0.4(2). Once combustion starts, the produced high temperature zone remains behind the combustion front.

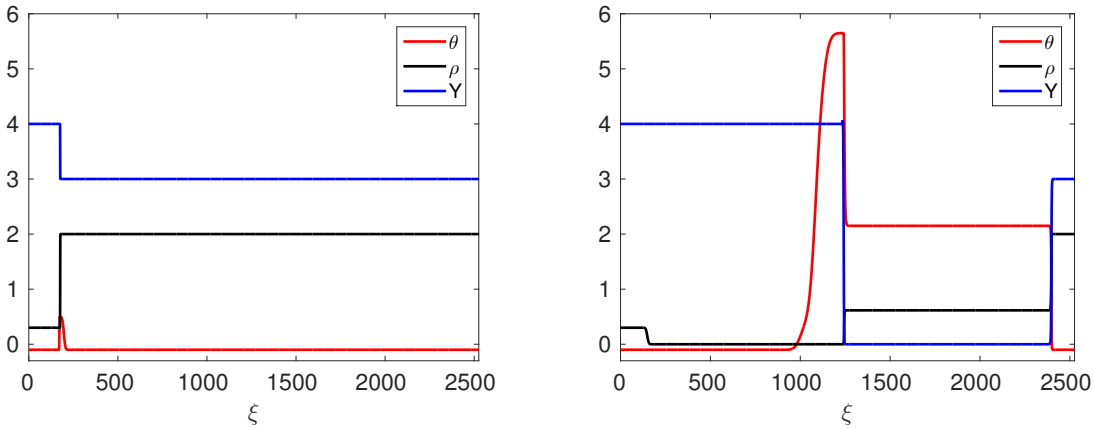

Figure 8.8 Result of numerical simulation for the wave sequence $TC \xrightarrow{0} TC \cap FC \xrightarrow{a} FC \xrightarrow{c_m} OC \xrightarrow{c_f} TC$ with a=0.5, demonstrating a fuel-controlled to oxygen-controlled intermediate combustion wave and oxygen controlled to temperature-controlled fast combustion wave that move ahead of contact discontinuities of speed 0 and a. Initial conditions (left) and simulation time 1600 (right).

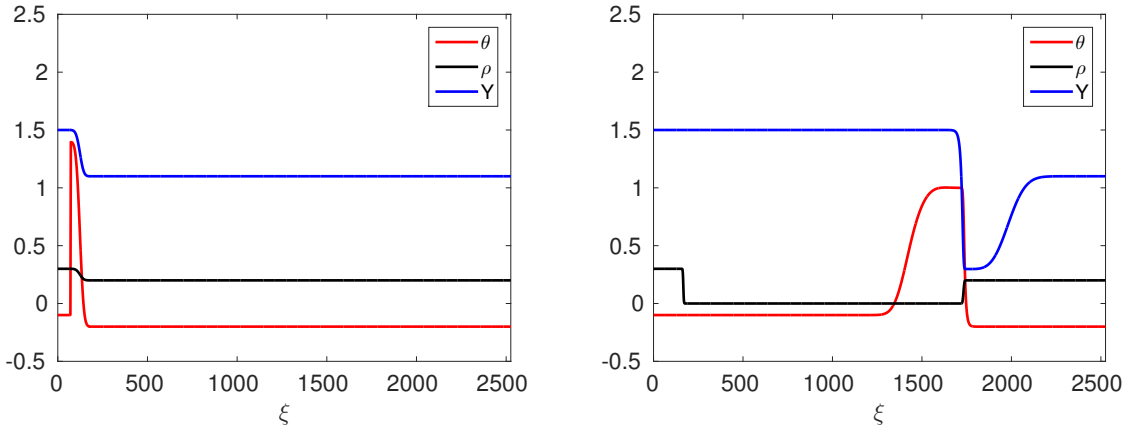

Figure 8.9 Result of numerical simulation for the wave sequence $TC \xrightarrow{0} TC \cap FC \xrightarrow{a} FC \xrightarrow{c_m} TC \xrightarrow{b} TC$ with $a = 0.5$ and $b = 0.7$, demonstrating a fuel-controlled to temperature-controlled intermediate combustion wave that is preceded and followed by contact discontinuities of speed 0, a and b. Initial conditions (left) and simulation time 2500 (right).

- FC to TC BVPs ($\rho^L = 0$, $\theta^R \leq 0$).

  1. For $(a-b)Y^L + a\rho^R > 0$, there is a generic wave sequence. If $(a-b)Y^L + a\rho^R > 0$, then by Theorem 2.0.5(1), θ^L, Y^L, and ρ^R determine θ^N such that there is a slow $FC \xrightarrow{c_s} OC$ combustion wave from $(\theta^L, 0, Y^L)$ to $(\theta^N, \rho^R, 0)$.
  $FC \xrightarrow{c_s} OC \xrightarrow{a} OC \cap TC \xrightarrow{b} TC$; more precisely

  $$(\theta^L, 0, Y^L) \xrightarrow{c_s} (\theta^N, \rho^R, 0) \xrightarrow{a} (\theta^R, \rho^R, 0) \xrightarrow{b} (\theta^R, \rho^R, Y^R).$$

  2. By Theorem 2.0.4(2), for given θ^R, ρ^R and if $Y^R > Y^R_*$, there exists (θ^N, ρ^N, Y^N), with $\theta^N > 0$, $\rho^N = 0$ and $Y^N > 0$, such that there is a fast $FC \xrightarrow{c_f} TC$ combustion wave from (θ^N, ρ^N, Y^N) to (θ^R, ρ^R, Y^R). $FC \xrightarrow{a} FC \xrightarrow{b} FC \xrightarrow{c_f} TC$; more precisely,

  $$(\theta^L, 0, Y^L) \xrightarrow{a} (\theta^N, 0, Y^L) \xrightarrow{b} (\theta^N, 0, Y^N) \xrightarrow{c_f} (\theta^R, \rho^R, Y^R).$$

  3. According to our numerical results in section 6, for given θ^R, ρ^R and if $Y^R_* > Y^R > Y^R_{**}$, there exists a left state (θ^N, ρ^N, Y^N), with $\theta^N > 0$, $\rho^N > 0$ and $Y^N = 0$, such that there is a stable fast $OC \xrightarrow{c_f} TC$ combustion wave from (θ^N, ρ^N, Y^N) to (θ^R, ρ^R, Y^R).

(a) $FC \xrightarrow{c_s} OC \xrightarrow{a} OC \xrightarrow{c_f} TC$. To construct the wave sequence, note that by Theorem 2.0.5(1), θ^L, Y^L, and ρ^N determine θ^M such that there is a slow $FC \xrightarrow{c_s} OC$ combustion wave from $(\theta^L, 0, Y^L)$ to $(\theta^M, \rho^N, 0)$. Between slow and fast combustion wave there is a wave of velocity a:

$$(\theta^L, 0, Y^L) \xrightarrow{c_s} (\theta^M, \rho^N, 0) \xrightarrow{a} (\theta^N, \rho^N, 0) \xrightarrow{c_f} (\theta^R, \rho^R, Y^R).$$

See the result of numerical simulation in Figure 8.10.

(b) For $(a-b)Y^L + a\rho^N < 0$, there is a generic wave sequence. If $(a-b)Y^L + a\rho^N < 0$, then by Theorem 2.0.6(1), θ^M, Y^L, and ρ^N determine θ^N such that there is a slow $FC \xrightarrow{c_s} OC$ combustion wave from $(\theta^N, 0, Y^L)$ to $(\theta^M, \rho^N, 0)$. $FC \xrightarrow{a} FC \xrightarrow{c_m} OC \xrightarrow{c_f} TC$; more precisely,

$$(\theta^L, 0, Y^L) \xrightarrow{a} (\theta^N, 0, Y^L) \xrightarrow{c_m} (\theta^M, \rho^N, 0) \xrightarrow{c_f} (\theta^R, \rho^R, Y^R).$$

See the result of numerical simulation in Figure 8.11.

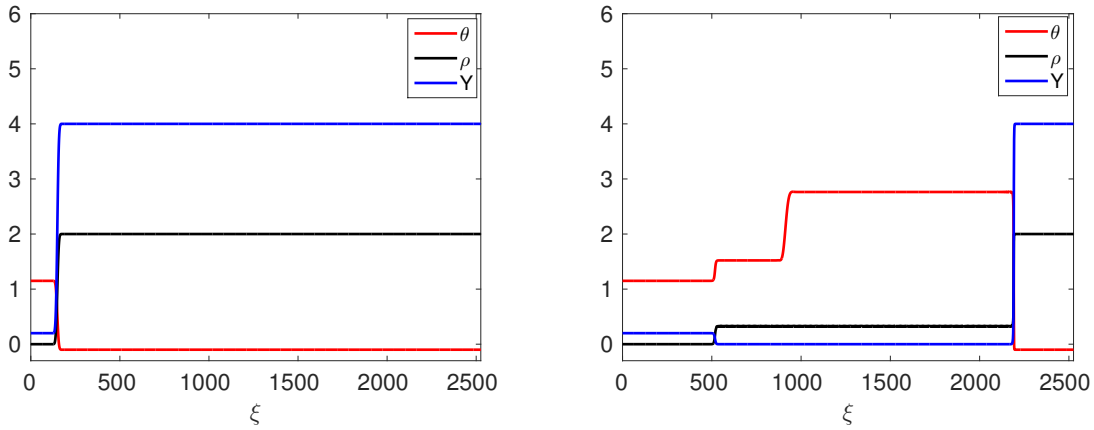

Figure 8.10 Result of numerical simulation for the wave sequence $FC \xrightarrow{c_s} OC \xrightarrow{a} OC \xrightarrow{c_f} TC$. with $a = 0.5$, demonstrating a fuel-controlled to oxygen-controlled slow combustion wave and oxygen-controlled to temperature-controlled fast combustion wave. Between these combustion waves there is a contact discontinuity of speed a. Initial conditions (left) and simulation time 1800 (right).

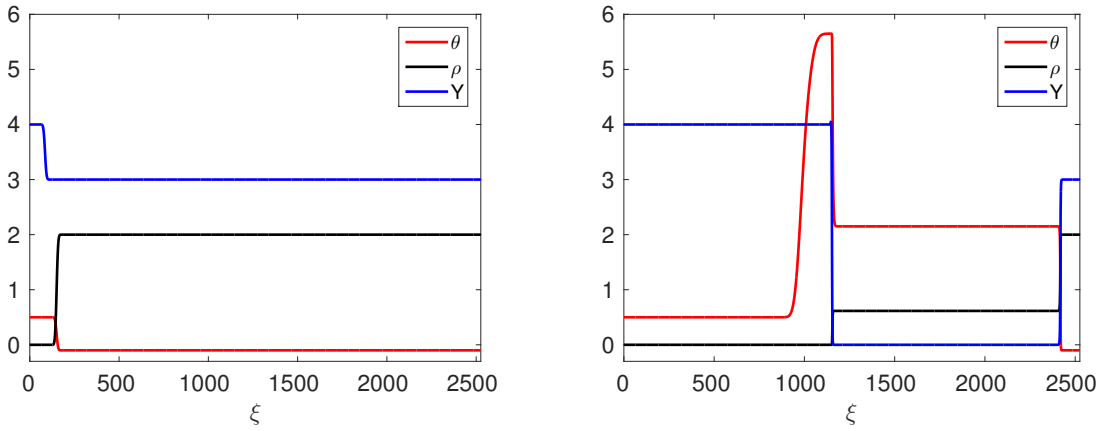

Figure 8.11 Result of numerical simulation for the wave sequence $FC \xrightarrow{a} FC \xrightarrow{c_m} OC \xrightarrow{c_f} TC$ with $a = 0.5$, demonstrating a fuel-controlled to oxygen-controlled intermediate combustion wave and oxygen-controlled to temperature controlled fast combustion wave that move ahead of contact discontinuity of speed a. Initial conditions (left) and simulation time 1750 (right).

4. $FC \xrightarrow{a} FC \xrightarrow{c_m} TC \xrightarrow{b} TC$. If $(a-b)Y^L + a\rho^R < 0$, then by Theorem 2.0.6(3), θ^R, ρ^R, and Y^L determine θ^N and Y^M such that there is an intermediate $FC \xrightarrow{c_m} TC$ combustion wave from $(\theta^N, 0, Y^L)$ to (θ^R, ρ^R, Y^N) .

$$(\theta^L, 0, Y^L) \xrightarrow{a} (\theta^N, 0, Y^L) \xrightarrow{c_m} (\theta^R, \rho^R, Y^M) \xrightarrow{b} (\theta^R, \rho^R, Y^R).$$

See the result of numerical simulation in Figure 8.12.

- OC to TC BVPs ($Y^L = 0$, $\theta^R \leq 0$).

1. $OC \xrightarrow{0} OC \xrightarrow{a} TC \cap OC \xrightarrow{b} TC$; more precisely, $(\theta^L, \rho^L, 0) \xrightarrow{0} (\theta^L, \rho^R, 0) \xrightarrow{a} (\theta^R, \rho^R, 0) \xrightarrow{b} (\theta^R, \rho^R, Y^R)$.
2. $OC \xrightarrow{0} FC \cap OC \xrightarrow{a} FC \cap OC \xrightarrow{b} FC \xrightarrow{c_f} TC$ .By Theorem 2.0.4(2), for given θ^R, ρ^R and if $Y^R > Y^R_*$, there exists (θ^N, ρ^N, Y^N), with $\theta^N > 0$, $\rho^N = 0$ and $Y^N > 0$, such that there is a fast $FC \xrightarrow{c_f} TC$ combustion wave from (θ^N, ρ^N, Y^N) to (θ^R, ρ^R, Y^R). More precisely,

$$(\theta^L, \rho^L, 0) \xrightarrow{0} (\theta^L, 0, 0) \xrightarrow{a} (\theta^N, 0, 0) \xrightarrow{b} (\theta^N, 0, Y^N) \xrightarrow{c_f} (\theta^R, \rho^R, Y^R).$$

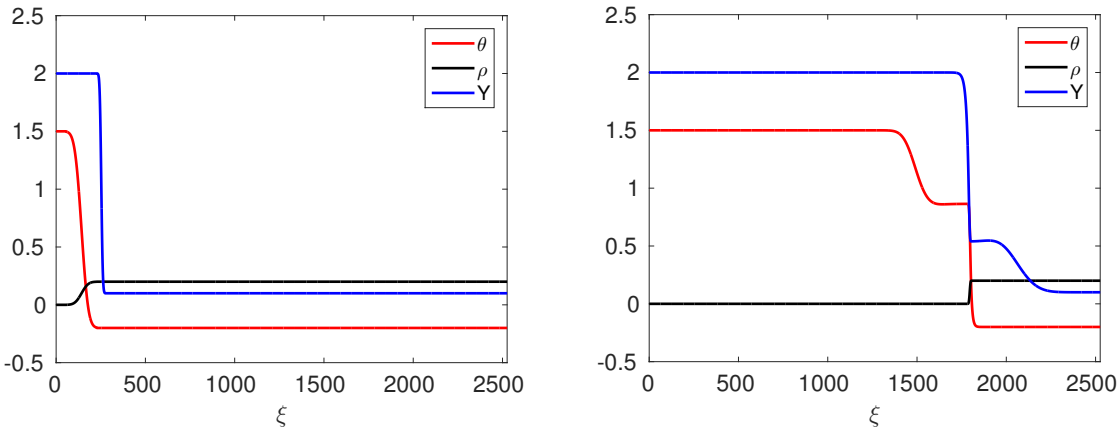

Figure 8.12 Result of numerical simulation for the wave sequence $FC \xrightarrow{a} FC \xrightarrow{c_m} TC \xrightarrow{b} TC$ with $a = 0.5$ and $b = 0.7$, demonstrating a fuel-controlled to temperature-controlled intermediate combustion wave that is preceded and followed by contact discontinuities of speed a and b. Initial conditions (left) and simulation time 2500 (right).

3. $OC \xrightarrow{0} OC \xrightarrow{a} OC \xrightarrow{c_f} TC$. According to our numerical results in section 6, for given θ^R, ρ^R and if $Y_*^R > Y^R > Y_{**}^R$, there exists a left state (θ^N, ρ^N, Y^N), with $\theta^N > 0$, $\rho^N > 0$ and $Y^N = 0$, such that there is a stable fast $OC \xrightarrow{c_f} TC$ combustion wave from (θ^N, ρ^N, Y^N) to (θ^R, ρ^R, Y^R). More precisely,

$$(\theta^L, \rho^L, 0) \xrightarrow{0} (\theta^L, \rho^N, 0) \xrightarrow{a} (\theta^N, \rho^N, 0) \xrightarrow{c_f} (\theta^R, \rho^R, Y^R).$$

See the result of numerical simulation in Figure 8.13.

For all numerical simulations shown in this section we use nonlinear Crank-Nicolson implicit finite difference scheme and Newton's method in each time-step with $a = 0.5$ and $b = 0.7$.

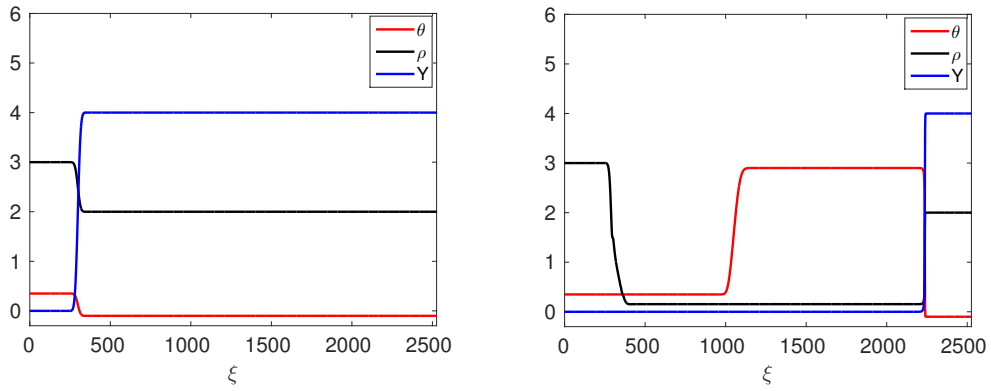

Figure 8.13 Result of numerical simulation for the wave sequence $OC \xrightarrow{0} OC \xrightarrow{a} OC \xrightarrow{c_f} TC$ with $a = 0.5$, demonstrating an oxygen-controlled to temperature-controlled fast combustion wave that move ahead of contact discontinuities of speed 0 and a. Initial conditions (left) and simulation time 1500 (right).

Chapter 9

Adding small diffusion to the model

In this section we add small diffusion term $\epsilon\partial_{xx}Y$ ($\epsilon > 0$ small) to the oxygen equation (2.9) and show the traveling waves have not changed. Although the traveling waves do not change, continuous spectrum and weight function may change. We also show how the continuous spectrum and weight function change for each type of combustion waves.

We consider the combustion system with small diffusion on the oxygen equation that is defined by

$$\partial_t\theta + a\partial_x\theta = \partial_{xx}\theta + \rho Y\Phi, \tag{9.1}$$

$$\partial_t\rho = -\rho Y\Phi, \tag{9.2}$$

$$\partial_t Y + b\partial_x Y = \epsilon\partial_{xx}Y - \rho Y\Phi. \tag{9.3}$$

In the moving coordinate frame $\xi = x - ct$, the PDE is

$$\partial_t\theta = \partial_{\xi\xi}\theta + (c-a)\partial_\xi\theta + \rho Y\Phi, \tag{9.4}$$

$$\partial_t\rho = c\partial_\xi - \rho Y\Phi, \tag{9.5}$$

$$\partial_t Y = \epsilon\partial_{\xi\xi}Y + (c-b)\partial_\xi Y - \rho Y\Phi. \tag{9.6}$$

We can identify traveling wave solution of (9.1)-(9.3) by looking for steady-state solutions of (9.4)-(9.6). Steady-state solutions satisfy the ordinary differential system

$$0 = \partial_{\xi\xi}\theta + (c-a)\partial_\xi\theta + \rho Y\Phi, \tag{9.7}$$

$$0 = c\partial_\xi - \rho Y\Phi, \tag{9.8}$$

$$0 = \epsilon\partial_{\xi\xi}Y + (c-b)\partial_\xi Y - \rho Y\Phi. \tag{9.9}$$

Let $v_1 = \partial_\xi\theta$ and $v_2 = \partial_\xi Y$, then we have

$$\partial_\xi\theta = v_1, \tag{9.10}$$

$$\partial_\xi v_1 = (a-c)v_1 - \rho Y\Phi, \tag{9.11}$$

$$\partial_\xi\rho = \frac{1}{c}\rho Y\Phi, \tag{9.12}$$

$$\partial_\xi Y = v_2, \tag{9.13}$$

$$\epsilon\partial_\xi v_2 = (b-c)v_2 + \rho Y\Phi. \tag{9.14}$$

This is a slow-fast system. The critical manifold ($\epsilon = 0$) is $v_2 = \frac{1}{c-b}\rho Y\Phi$. It is normally hyperbolic $\frac{\partial}{\partial v_2}\epsilon\partial_\xi v_2 = b - c \neq 0$. Therefore any compact portion persists for small ϵ. To lowest order in ϵ, the flow on it is given by the first four equations (9.10)-(9.13) with $v_2 = \frac{1}{c-b}\rho Y\Phi$. These are exactly the traveling wave equations we get when $\epsilon = 0$, hence the traveling waves have not changed. When $\epsilon > 0$, at least things that are stable to perturbation have not changed.

Fast traveling waves involve a connection to a non-hyperbolic equilibrium, so it is not clear that they persist for $\epsilon > 0$. Therefore we have to study them explicitly. We shall show that the fast traveling waves have not changed. As in section 3.1 we begin by reducing the system in a more convenient form.

First we add equation (9.5) to (9.4), then replace (9.5). Next we substract equation (9.5) from (9.6), then replace (9.6). We obtain

$$\partial_t\theta = (c-a)\partial_\xi\theta + \partial_{\xi\xi}\theta + \rho Y\Phi(\theta), \tag{9.15}$$

$$\partial_t(\theta+\rho) = (c-a)\partial_\xi\theta + \partial_{\xi\xi}\theta + c\partial_\xi\rho, \tag{9.16}$$

$$\partial_t(Y-\rho) = (c-b)\partial_\xi Y + \epsilon\partial_{\xi\xi}Y - c\partial_\xi\rho. \tag{9.17}$$

Stationary solutions of (9.15)–(9.17) satisfy the system of ODEs

$$0 = (c-a)\partial_\xi\theta + \partial_{\xi\xi}\theta + \rho Y\Phi(\theta), \tag{9.18}$$

$$0 = (c-a)\partial_\xi\theta + \partial_{\xi\xi}\theta + c\partial_\xi\rho, \tag{9.19}$$

$$0 = (c-b)\partial_\xi Y + \epsilon\partial_{\xi\xi}Y - c\partial_\xi\rho. \tag{9.20}$$

In (9.18) and (9.20), let $v_1 = \partial_\xi\theta$ and $v_2 = \partial_\xi Y$ respectively, and integrate (9.19)–(9.20). Note that dot denotes the derivative with respect to ξ. Then we obtain the system

$$\dot{\theta} = v_1, \tag{9.21}$$

$$\dot{v}_1 = (a-c)v_1 - \rho Y\Phi(\theta), \tag{9.22}$$

$$\dot{Y} = v_2, \tag{9.23}$$

$$w_1 = (c-a)\theta + v_1 + c\rho, \tag{9.24}$$

$$w_2 = (c-b)Y + \epsilon v_2 - c\rho, \tag{9.25}$$

where w_1 and w_2 are constants. In (9.21) and (9.22) we substitute for v_1 using (9.24). In (9.22) and (9.23) we substitute for Y using (9.25). We obtain the reduced traveling wave system

$$\dot{\theta} = (a-c)\theta - c\rho + w_1, \tag{9.26}$$

$$\dot{\rho} = \frac{c\rho + w_2 - \epsilon v_2}{c(c-b)}\rho\Phi(\theta), \tag{9.27}$$

$$\epsilon\dot{v}_2 = \frac{w_2 + c\rho - \epsilon v_2}{c-b}\rho\Phi(\theta) - (c-b)v_2, \tag{9.28}$$

where (w_1, w_2) is a vector of parameters. The critical manifold ($\epsilon = 0$) is $v_2 = \frac{w_2+c\rho}{(c-b)^2}\rho\Phi(\theta)$. We substitute $v_2 = \frac{w_2+c\rho}{(c-b)^2}\rho\Phi(\theta) + \epsilon F(\theta,\rho,\epsilon)$ (the lowest order in ϵ) into the (9.26)–(9.27). The new system still has the invariant line $\rho = 0$ and the nullcline H defined by $(a-c)\theta - c\rho + w_1$ which contains all equilibria.

Since fast traveling waves have TC right state that is (θ^+, ρ^+, Y^+) with $\theta^+ \le 0$, $\rho^+ > 0$ and $Y^+ > 0$, we still have the degenerate equilibria which lie in H. Also the invariant line $\rho = 0$ has one equilibrium which also lies in H. The proof of existence of fast traveling waves goes through as before.

To show the changes on the spectrum, we use same calculation from chapter 5. Only

difference is on the oxygen equation.

- Spectrum of fast combustion waves ($a < b < c_f$)

  They have TC right state. We compute the spectrum of $\mathcal{L}_+$ at the right end state.

$$\mathcal{L}_+ = \begin{pmatrix} -\mu^2 + i\mu(c_f - a) & 0 & 0 \\ 0 & i\mu c_f & 0 \\ 0 & 0 & -\epsilon\mu^2 + i\mu(c_f - b) \end{pmatrix}. \tag{9.29}$$

  The spectrum of $\mathcal{L}_+$ is the set of the λ that are eigenvalues of (9.29) for some μ in $\mathbb{R}$.

$$\lambda(\mu) = -\mu^2 + i\mu(c_f - a), \quad \lambda(\mu) = i\mu c_f, \quad \lambda(\mu) = -\epsilon\mu^2 + i\mu(c_f - b).$$

  The spectrum of the linearization is two parabolas in the left-half plane that touch the imaginary axis at the origin and the imaginary axis.

  Similarly, for

  1. FC left state

$$\lambda(\mu) = -\mu^2 + i\mu(c_f - a), \quad \lambda(\mu) = i\mu c_f - Y^-\Phi(\theta^-), \quad \lambda(\mu) = -\epsilon\mu^2 + i\mu(c_f - b).$$

     The spectrum of the linearization is two parabolas in the left-half plane that touch the origin and a vertical line in the left-half plane.

  2. OC left state

$$\lambda(\mu) = -\mu^2 + i\mu(c_f - a), \quad \lambda(\mu) = -\epsilon\mu^2 + i\mu(c_f - b) - \rho^-\Phi(\theta^-), \quad \lambda(\mu) = i\mu c_f.$$

     The spectrum consists of a parabola in the left half plane, another parabola that touches the origin and imaginary axis.

- Spectrum of slow combustion waves ($c_s < a < b$)

  1. OC right state

$$\lambda(\mu) = -\mu^2 + i\mu(c_s - a), \quad \lambda(\mu) = i\mu c_s, \quad \lambda(\mu) = -\epsilon\mu^2 + i\mu(c_s - b) - \rho^+\Phi(\theta^+).$$

The spectrum of the linearization is a parabola in the left-half plane that touches the origin, another parabola in the left-half plane and the imaginary axis.

2. FC left state

$$\lambda(\mu) = -\mu^2 + i\mu(c_s - a), \quad \lambda(\mu) = i\mu c_s - Y^-\Phi(\theta^-), \quad \lambda(\mu) = -\epsilon\mu^2 + i\mu(c_s - b).$$

The spectrum of the linearization is two parabolas in the left-half plane that touch the origin and a vertical line in the left-half plane.

3. TC left state

$$\lambda(\mu) = -\mu^2 + i\mu(c_s - a), \quad \lambda(\mu) = i\mu c_s, \quad \lambda(\mu) = -\epsilon\mu^2 + i\mu(c_s - b).$$

The spectrum of the linearization is two parabolas in the left-half plane that touch the imaginary axis at the origin and the imaginary axis.

- Spectrum of intermediate combustion waves ($a < c_m < b$)

1. FC left state

$$\lambda(\mu) = -\mu^2 + i\mu(c_m - a), \quad \lambda(\mu) = i\mu c_m - Y^-\Phi(\theta^-), \quad \lambda(\mu) = -\epsilon\mu^2 + i\mu(c_m - b).$$

The spectrum of the linearization is two parabolas in the left-half plane that touch the imaginary axis at the origin and a vertical line in the left half-plane.

2. TC right state

$$\lambda(\mu) = -\mu^2 + i\mu(c_m - a), \quad \lambda(\mu) = i\mu c_m, \quad \lambda(\mu) = -\epsilon\mu^2 + i\mu(c_m - b).$$

The spectrum of the linearization is two parabolas in the left-half plane that touch the imaginary axis at the origin and the imaginary axis.

3. OC right state

$$\lambda(\mu) = -\mu^2 + i\mu(c_m - a), \quad \lambda(\mu) = i\mu c_m, \quad \lambda(\mu) = -\epsilon\mu^2 + i\mu(c_m - b) - \rho^+\Phi(\theta^+).$$

The spectrum of the linearization is a parabola in the left-half plane that touches the origin, another parabola in the left-half plane and the imaginary axis.

Adding small diffusion to the oxygen equation only changes a vertical line to a parabola in the spectrum for every type of combustion waves. The spectrum of fast, slow and intermediate combustion waves still touches the imaginary axis. We determine weight functions for the new system (9.1)-(9.3) by using the same idea from previous section.

- Weight function for fast combustion waves ($a < b < c_f$)
  1. TC right state : if $0 < \alpha_+ < \min\{c_f - a, \frac{c_f - b}{\epsilon}\}$ is provided, then the spectra lies in the left half plane.
  2. FC left state : we require $0 < \alpha_- < \min\{c_f - a, \frac{c_f - b}{\epsilon}\}$ to move the spectra to the left half plane.
  3. OC left state : we require $0 < \alpha_- < \min\{c_f - a, \frac{c_f - b + \sqrt{(b-c)^2 + 4\epsilon\rho_-\Phi(\theta^-)}}{2\epsilon}\}$ to move the spectra to the left half plane.
- Weight function for slow combustion waves ($c_s < a < b$)
  1. OC right state : there is still no weight function to move the spectrum to the left half plane.
  2. FC left state : if $0 > \alpha_- > \max\{c_s - a, \frac{c_s - b}{\epsilon}, \frac{-Y^-\Phi(\theta^-)}{\epsilon}\}$ is provided, then the spectra lies in the left half plane.
  3. TC left state : there is no α_- which moves the spectra to the left half plane.
- Weight function for intermediate combustion waves ($a < c_m < b$)
  1. FC left state : there is no α_- which moves the spectra to the left half plane.
  2. TC right state : there is no α_+ which moves the spectra to the left half plane.
  3. OC right state : we require $0 < \alpha_+ < \min\{c_m - a, \frac{c_m - b + \sqrt{(b-c_m)^2 + 4\epsilon\rho_-\Phi(\theta^-)}}{2\epsilon}\}$ to move the spectra to the left half plane.

9.1 Spectral Energy Estimates

By spectral energy estimates, we try to find bounds on the unstable eigenvalues for the system when we add small diffusion. Consider the system (9.1)-(9.3) and linearize it about the combustion front $(\hat{\theta}, \hat{\rho}, \hat{Y})$, we obtain

$$\partial_t \theta = \partial_{\xi\xi}\theta + (c-a)\partial_\xi \theta + h_1\theta + h_2 Y + h_3\rho, \tag{9.30}$$

$$\partial_t \rho = c\partial_\xi \rho - h_1\theta - h_2 Y - h_3\rho, \tag{9.31}$$

$$\partial_t Y = \epsilon\partial_{\xi\xi} Y + (c-b)\partial_\xi Y - h_1\theta - h_2 Y - h_3\rho, \tag{9.32}$$

where

$$h_1(\xi) = \frac{\hat{\rho}(\xi)\hat{Y}(\xi)}{\hat{\theta}(\xi)^2}\exp(-\frac{1}{\hat{\theta}(\xi)}), \quad h_2(\xi) = \hat{\rho}(\xi)\exp(-\frac{1}{\hat{\theta}(\xi)}), \quad h_3(\xi) = \hat{Y}(\xi)\exp(-\frac{1}{\hat{\theta}(\xi)}).$$

We introduce the weight function to move the spectrum to the left half-plane. Note that we were able to find weight function $e^{\alpha\xi}$ only for the fast combustion waves with $\alpha = (\alpha_-, \alpha_+)$, $0 < \alpha_\pm < c - a$.

If $(\theta(\xi), \rho(\xi), Y(\xi))$ is in a weighted space $\mathcal{X}_\alpha$ with weight function $e^{\alpha\xi}$, then $(\theta(\xi), \rho(\xi), Y(\xi)) = e^{-\alpha\xi}(u(\xi), v(\xi), z(\xi))$ with $(u(\xi), v(\xi), z(\xi))$ in $\mathcal{X}_0$. Substitute them into (9.30)–(9.32) and multiply by $e^{\alpha\xi}$. We obtain

$$\partial_t u = \partial_{\xi\xi}u + (c - a - 2\alpha)\partial_\xi u + (h_1 + \alpha^2 + a\alpha - c\alpha)u + h_2 z + h_3 v, \tag{9.33}$$

$$\partial_t v = c\partial_\xi v - h_1 u - h_2 z - (h_3 + c\alpha)v, \tag{9.34}$$

$$\partial_t z = \epsilon\partial_{\xi\xi} z + (c - b - 2\epsilon\alpha)\partial_\xi z - h_1 u + (\epsilon\alpha^2 + b\alpha - c\alpha - h_2)z - h_3 v. \tag{9.35}$$

The eigenvalue problem reads

$$\lambda u = \partial_{\xi\xi}u + (c - a - 2\alpha)\partial_\xi u + (h_1 + \alpha^2 + a\alpha - c\alpha)u + h_2 z + h_3 v, \tag{9.36}$$

$$\lambda v = c\partial_\xi v - h_1 u - h_2 z - (h_3 + c\alpha)v, \tag{9.37}$$

$$\lambda z = \epsilon\partial_{\xi\xi} z + (c - b - 2\epsilon\alpha)\partial_\xi z - h_1 u + (\epsilon\alpha^2 + b\alpha - c\alpha - h_2)z - h_3 v. \tag{9.38}$$

Lemma 9.1.1. *If (u, v, z) satisfies (9.36)-(9.38) for some nonzero λ, then the following two inequalities hold for all $\epsilon_1 > 0$ and $\epsilon_2 > 0$:*

$$Re(\lambda)\int|u|^2 \le \int(h_1+\alpha^2+a\alpha-c\alpha)|u|^2+\epsilon_1\int h_2|u|^2+\frac{1}{4\epsilon_1}\int h_2|z|^2+\epsilon_2\int h_3|u|^2+\frac{1}{4\epsilon_2}\int h_3|v|^2 \tag{9.39}$$

and

$$\begin{aligned}(Re(\lambda)+|Im(\lambda)|)\int|u|^2 \;\;\le\;\; & \int(h_1+\alpha^2+a\alpha-c\alpha)|u|^2+\frac{(c-a-2\alpha)^2}{4}\int|u|^2+\epsilon_1\int h_2|u|^2\\ & +\frac{1}{2\epsilon_1}\int h_2|z|^2+\epsilon_2\int h_3|u|^2+\frac{1}{2\epsilon_2}\int h_3|v|^2. \end{aligned}\tag{9.40}$$

Proof. We multiply (9.36) by the conjugate $\bar{u}$ and integrate from $-\infty$ to ∞. We have

$$\lambda\int|u|^2=(c-a-2\alpha)\int u'\bar{u}+\int(h_1+\alpha^2+a\alpha-c\alpha)|u|^2+\int h_2z\bar{u}+\int h_3v\bar{u}-\int|u'|^2. \tag{9.41}$$

Since $Re\int_{-\infty}^{\infty}u'\bar{u}d\xi=\int_{-\infty}^{\infty}(u'\bar{u}+\bar{u}'u)d\xi/2=\int_{-\infty}^{\infty}(u\bar{u})'d\xi/2=0$, taking the real and imaginary parts of (9.41), we have

$$Re(\lambda)\int|u|^2=\int(h_1+\alpha^2+a\alpha-c\alpha)|u|^2+Re\int h_2z\bar{u}+Re\int h_3v\bar{u}-\int|u'|^2, \tag{9.42}$$

$$|Im(\lambda)|\int|u|^2\le(c-a-2\alpha)\int|u'||\bar{u}|+|Im\int h_2z\bar{u}|+|Im\int h_3v\bar{u}|. \tag{9.43}$$

The inequality (9.39) follows by using Young's inequality on (9.42). We use Young's inequality in the form that $ab\le\epsilon a^2+\frac{1}{4\epsilon}b^2$ where a,b are any real numbers and $\epsilon>0$. In Lemma 10.1 ϵ_1 and ϵ_2 come from this inequality.

The inequality (9.40) follows by adding (9.42) and (9.43) together and using the fact that $|Re(x\bar{y})|+|Im(x\bar{y})|\le\sqrt{2}|x||y|$ where x,y are complex numbers and using Young's inequality to get $(c-a-2\alpha)|u'||u|\le\frac{(c-a-2\alpha)^2|u|^2}{4}+|u'^2|$.

$$
\begin{aligned}
(Re(\lambda)+|Im(\lambda)|)\int|u|^2 &\leq \int(h_1+\alpha^2+a\alpha-c\alpha)|u|^2+\frac{(c-a-2\alpha)^2}{4}\int|u|^2 \\
&\quad +\sqrt{2}\int h_2|z||u|+\sqrt{2}\int h_3|v||u| \\
&\leq \int(h_1+\alpha^2+a\alpha-c\alpha)|u|^2+\frac{(c-a-2\alpha)^2}{4}\int|u|^2+\epsilon_1\int h_2|u|^2 \\
&\quad +\frac{1}{2\epsilon_1}\int h_2|z|^2+\epsilon_2\int h_3|u|^2+\frac{1}{2\epsilon_2}\int h_3|v|^2.
\end{aligned}
$$

□

Lemma 9.1.2. *If (u,v,z) satisfies (9.36)-(9.38) for some nonzero λ, then the following two inequalities hold for all $\epsilon_3>0$ and $\epsilon_4>0$:*

$$
Re(\lambda)\int|v|^2\leq\epsilon_3\int h_1|v|^2+\frac{1}{4\epsilon_3}\int h_1|u|^2+\epsilon_4\int h_2|v|^2+\frac{1}{4\epsilon_4}\int h_2|z|^2-\int(h_3+c\alpha)|v|^2. \tag{9.44}
$$

Proof. We multiply (9.37) by the conjugate $\bar{v}$ and integrate from $-\infty$ to ∞. We have

$$
\lambda\int|v|^2=c\int v'\bar{v}-\int h_1u\bar{v}-\int h_2z\bar{v}-\int(h_3+c\alpha)|v|^2. \tag{9.45}
$$

Taking the real part of (9.45), we have

$$
Re(\lambda)\int|v|^2=-Re\int h_1u\bar{v}-Re\int h_2z\bar{v}-\int(h_3+c\alpha)|v|^2. \tag{9.46}
$$

The inequality (9.44) follows by using Young's inequality on (9.46). □

Lemma 9.1.3. *If (u,v,z) satisfies (9.36)-(9.38) for some nonzero λ, then the following two inequalities hold for all $\epsilon_5>0$ and $\epsilon_6>0$:*

$$
Re(\lambda)\int|z|^2\leq\epsilon_5\int h_1|u|^2+\frac{1}{4\epsilon_5}\int h_1|z|^2+\epsilon_6\int h_3|v|^2+\frac{1}{4\epsilon_6}\int h_3|z|^2+\int(\epsilon\alpha^2+b\alpha-c\alpha-h_2)|z|^2 \tag{9.47}
$$

and

$$
\begin{aligned}
(Re(\lambda)+|Im(\lambda)|)\int|z|^2 &\leq \frac{(c-b-2\epsilon\alpha)^2}{4\epsilon}\int|z|^2+\epsilon_5\int h_1|u|^2+\frac{1}{2\epsilon_5}\int h_1|z|^2 \\
&\quad +\epsilon_6\int h_3|v|^2+\frac{1}{2\epsilon_6}\int h_3|z|^2+\int(\epsilon\alpha^2+b\alpha-c\alpha-h_2)|z|^2.
\end{aligned} \tag{9.48}
$$

Proof. We multiply (9.38) by the conjugate $\bar{z}$ and integrate from $-\infty$ to ∞. We have

$$\lambda \int |z|^2 = (c-b-2\epsilon\alpha)\int z'\bar{z} - \int h_1 u\bar{z} - \int h_3 \bar{z} v + \int (\epsilon\alpha^2 + b\alpha - c\alpha - h_2)|z|^2 - \epsilon \int |z'|^2. \tag{9.49}$$

Taking the real and imaginary parts of (9.49), we have

$$Re(\lambda)\int |z|^2 = -Re\int h_1 u\bar{z} - Re\int h_3\bar{z}v + \int (\epsilon\alpha^2 + b\alpha - c\alpha - h_2)|z|^2 - \epsilon\int |z'|^2, \tag{9.50}$$

$$|Im(\lambda)|\int |z|^2 \leq (c-b-2\epsilon\alpha)\int |z'||\bar{z}| + |Im\int h_1 u\bar{z}| + |Im\int h_3 v\bar{z}|. \tag{9.51}$$

The inequality (9.47) follows by using Young's inequality on (9.50).

The inequality (9.48) follows by adding (9.50) and (9.51) together and using the fact that $|Re(x\bar{y})| + |Im(x\bar{y})| \leq \sqrt{2}|x||y|$ where x, y are complex numbers and using Young's inequality to get $(c-b-2\epsilon\alpha)|z'||z| \leq \frac{(c-b-2\epsilon\alpha)^2|z|^2}{4} + |z'^2|$.

$$\begin{aligned}
(Re(\lambda) + |Im(\lambda)|)\int |z|^2 &\leq \frac{(c-b-2\epsilon\alpha)^2}{4\epsilon}\int |z|^2 + \int (\epsilon\alpha^2 + b\alpha - c\alpha - h_2)|z|^2 \\
&\quad + \sqrt{2}\int h_1|z||u| + \sqrt{2}\int h_3|v||z| \\
&\leq \frac{(c-b-2\epsilon\alpha)^2}{4\epsilon}\int |z|^2 + \int (\epsilon\alpha^2 + b\alpha - c\alpha - h_2)|z|^2 + \epsilon_5\int h_1|u|^2 \\
&\quad + \frac{1}{2\epsilon_5}\int h_1|z|^2 + \epsilon_6\int h_3|v|^2 + \frac{1}{2\epsilon_6}\int h_3|z|^2.
\end{aligned}$$

□

Theorem 9.1.4. *If (u, v, z) satisfies* (9.36)-(9.38) *for some nonzero λ, then the following inequality holds for all $0 < \delta < 1$:*

$$Re(\lambda) \leq \frac{1}{1-\delta}\sup_{\xi} h_1 + \frac{(1-\delta)^2 + 2\delta}{8\delta}\sup_{\xi}\{h_2 + h_3\} + \max\{\alpha^2 + a\alpha, \epsilon\alpha^2 + b\alpha\}. \tag{9.52}$$

Proof. First we multiply (9.39) by $k > 0$ and add to (9.44) and (9.47). We obtain,

$$\begin{aligned} Re(\lambda)\int(k|u|^2+|v|^2+|z|^2) &\leq (k+\epsilon_5+\frac{1}{4\epsilon_3})\int h_1u^2+\epsilon_3\int h_1v^2+\frac{1}{4\epsilon_5}\int h_1z^2 \\ &\quad +k\epsilon_1\int h_2u^2+\epsilon_4\int h_2v^2+(\frac{k}{4\epsilon_1}+\frac{1}{4\epsilon_4}-1)\int h_2z^2 \\ &\quad +k\epsilon_2\int h_3u^2+(\frac{k}{4\epsilon_2}+\epsilon_6-1)\int h_3v^2+\frac{1}{4\epsilon_6}\int h_3z^2 \\ &\quad +\max\{\alpha^2+a\alpha,\epsilon\alpha^2+b\alpha\}\int(ku^2+z^2)-c\alpha\int(ku^2+v^2+z^2). \end{aligned}$$

Set $\frac{k}{4\epsilon_1}+\frac{1}{4\epsilon_4}=1$, $\frac{k}{4\epsilon_2}+\epsilon_6=1$ and take $\epsilon_4=\epsilon_1$ and $\epsilon_6=\frac{1}{4\epsilon_2}$. Therefore $\epsilon_1=\epsilon_2=\epsilon_4=\frac{k+1}{4}$ and $\epsilon_6=\frac{1}{k+1}$. Also set $\epsilon_3=\frac{1}{1-\delta}$, $\epsilon_5=\frac{1-\delta}{4}$ and $k=\frac{(1-\delta)^2}{2\delta}$. Thus we get,

$$\begin{aligned} Re(\lambda)\int(k|u|^2+|v|^2+|z|^2) &\leq \frac{1}{1-\delta}\int h_1(k|u|^2+|v|^2+|z|^2) \\ &\quad +\frac{(1-\delta)^2+2\delta}{8\delta}\int h_2(k|u|^2+|v|^2)+\frac{(1-\delta)^2+2\delta}{8\delta}\int h_3(k|u|^2+|z|^2) \\ &\quad +\max\{\alpha^2+a\alpha,\epsilon\alpha^2+b\alpha\}\int(ku^2+z^2)-c\alpha\int(ku^2+v^2+z^2). \end{aligned}$$

Therefore,

$$Re(\lambda)\leq\frac{1}{1-\delta}\sup_\xi h_1+\frac{(1-\delta)^2+2\delta}{8\delta}\sup_\xi\{h_2+h_3\}+\max\{\alpha^2+a\alpha,\epsilon\alpha^2+b\alpha\}. \quad (9.53)$$

□

Theorem 9.1.5. *If (u,v,z) satisfies (9.36)-(9.38) for some nonzero λ, then the following inequality holds for all $0<\delta<1$:*

$$\begin{aligned} Re(\lambda)+|Im(\lambda)| &\leq \max_\xi\{\alpha^2+a\alpha-c\alpha+\frac{(c-a-2\alpha)^2}{4}+(1-\delta)h_2+\frac{h_3}{1-\delta}+\frac{(2-\delta)}{4\delta(1-\delta)}\frac{\hat v^2}{\hat u^4}h_3+\frac{5h_1}{4} \\ &\quad \epsilon\alpha^2+b\alpha-c\alpha+\frac{(c-b-2\epsilon\alpha)^2}{4\epsilon}+\frac{h_1}{1-\delta}+\frac{h_3}{2(1-\delta)}+\frac{(2-\delta)}{2\delta}\frac{\hat v^2}{\hat z^2}h_3\}. \end{aligned} \quad (9.54)$$

Proof. To prove (9.54), we need to revise Lemma 9.1.2. First we replace $(\hat\theta,\hat\rho,\hat Y)$ in $h_1(\xi),h_2(\xi)$ and $h_3(\xi)$ with $(\hat u,\hat v,\hat z)$. Note that we can write h_1 and h_2 in terms of h_3 such that $h_1=\frac{\hat v}{\hat u^2}h_3$ and $h_2=\frac{\hat v}{\hat z}h_3$. In (9.46) we replace $h_1u\bar v$ and $h_2z\bar v$ with $\frac{\hat v}{\hat u^2}h_3u\bar v$ and

$\frac{\hat{v}}{\hat{z}}h_3 z\bar{v}$ and apply Young's inequality, we have

$$h_1 u\bar{v} = \frac{\hat{v}}{\hat{u}^2}h_3 u\bar{v} \leq \epsilon_3 h_3|v|^2 + \frac{\hat{v}^2}{4\epsilon_3\hat{u}^4}h_3|u|^2$$

and

$$h_2 z\bar{v} = \frac{\hat{v}}{\hat{z}}h_3 z\bar{v} \leq \epsilon_4 h_3|v|^2 + \frac{\hat{v}^2}{4\epsilon_4\hat{z}^2}h_3|z|^2.$$

Substitute them in (9.46) and it yields

$$Re(\lambda)\int|v|^2 \leq \epsilon_3\int h_3|v|^2 + \frac{1}{4\epsilon_3}\int\frac{\hat{v}^2}{\hat{u}^4}h_3|u|^2 + \epsilon_4\int h_3|v|^2 + \frac{1}{4\epsilon_4}\int\frac{\hat{v}^2}{\hat{z}^2}h_3|z|^2 - \int(h_3+c\alpha)|v|^2. \tag{9.55}$$

We multiply (9.40) and (9.48) by k_1 and k_2 respectively then add to (9.55).

$(Re(\lambda)+|Im(\lambda)|)\int(k_1u^2+k_2z^2) + Re(\lambda)\int v^2$

$$\leq \int\left(h_1+\alpha^2+a\alpha-c\alpha+\epsilon_1h_2+\epsilon_2h_3+\frac{(c-a-2\alpha)^2}{4}+\frac{h_3}{4\epsilon_3k_1}\frac{\hat{v}^2}{\hat{u}^4}+\frac{\epsilon_5k_2h_1}{k_1}\right)k_1|u|^2$$
$$+\int\left(\epsilon\alpha^2+b\alpha-c\alpha+\frac{(c-b-2\epsilon\alpha)^2}{4\epsilon}+\frac{h_1}{2\epsilon_5}+\frac{h_3}{2\epsilon_6}+\frac{h_3}{4\epsilon_4k_2}\frac{\hat{v}^2}{\hat{z}^2}\right)k_2|z|^2$$
$$+(\epsilon_3+\epsilon_4+\frac{k_1}{2\epsilon_2}+k_2\epsilon_6-1)\int h_3|v|^2+(\frac{k_1}{2\epsilon_1}-k_2)\int h_2|z|^2.$$

Take $\epsilon_1=\epsilon_6=1-\delta$, $\epsilon_3=\epsilon_4=\epsilon_5=\frac{1-\delta}{2}$, $\epsilon_2=\frac{1}{1-\delta}$ and $k_1=\frac{2\delta}{2-\delta}$. Then $\epsilon_3+\epsilon_4+\frac{k_1}{2\epsilon_2}+k_2\epsilon_6=1$ and $\frac{k_1}{2k_2\epsilon_1}=1$. Thus we get,

$(Re(\lambda)+|Im(\lambda)|)\int(k_1u^2+k_2z^2) + Re(\lambda)\int v^2$

$$\leq \int\left(\alpha^2+a\alpha-c\alpha+\frac{(c-a-2\alpha)^2}{4}+(1-\delta)h_2+\frac{h_3}{1-\delta}+\frac{(2-\delta)}{4\delta(1-\delta)}\frac{\hat{v}^2}{\hat{u}^4}h_3+\frac{5h_1}{4}\right)k_1|u|^2$$
$$+\int\left(\epsilon\alpha^2+b\alpha-c\alpha+\frac{(c-b-2\epsilon\alpha)^2}{4\epsilon}+\frac{h_1}{1-\delta}+\frac{h_3}{2(1-\delta)}+\frac{(2-\delta)}{2\delta}\frac{\hat{v}^2}{\hat{z}^2}h_3\right)k_2|z|^2.$$

Thus we have a contradiction when

$$\begin{aligned}Re(\lambda)+|Im(\lambda)| \quad \geq \quad & \max_{\xi}\{\alpha^2+a\alpha-c\alpha+\frac{(c-a-2\alpha)^2}{4}+(1-\delta)h_2+\frac{h_3}{1-\delta}+\frac{(2-\delta)}{4\delta(1-\delta)}\frac{\hat{v}^2}{\hat{u}^4}h_3+\frac{5h_1}{4},\\ & \epsilon\alpha^2+b\alpha-c\alpha+\frac{(c-b-2\epsilon\alpha)^2}{4\epsilon}+\frac{h_1}{1-\delta}+\frac{h_3}{2(1-\delta)}+\frac{(2-\delta)}{2\delta}\frac{\hat{v}^2}{\hat{z}^2}h_3\}.\end{aligned}$$

□

The inequalities (9.52) and (9.54) form a trapezoidal region of admissible unstable spectrum. After we find the bound on the eigenvalues for the system with small diffusion added to the oxygen equation, we could use it to compute the Evans function and rigorously rule out the large eigenvalues.

Chapter 10

Conclusion

In our combustion model we assumed the oxygen is transported faster than the temperature. A consequence is that we have more complicated existence theory of fast traveling waves. For certain parameter values, we find two fast combustion waves or there is no fast combustion wave. More precisely, if the right state has small amount of oxygen, then the reaction cannot occur; if it has moderate amount of oxygen, then there is a stable combustion wave in which all the oxygen is consumed (OC to TC); if it has lots of oxygen, then there is a stable a combustion wave in which all the fuel is consumed in the reaction (FC to TC); and in both cases there also exists an OC to TC wave that is unstable.

Moreover, stability theory of fast traveling waves requires using weight function, performing numerical computation of Evans function and using the linear and the nonlinear theorem. The results of nonlinear theorem have physical interpretation which makes sense for FC to TC and OC to TC fast traveling waves. We found that FC to TC waves are stable and OC to TC waves are sometimes stable and sometimes unstable.

Another consequence is the intermediate waves which make the model more fully reproduce waves seen numerically in more elaborate models such as smoldering combustion system which is studied in [2]. The intermediate combustion waves have been called "reaction-leading smolder waves". These are the combustion waves when the velocity of the combustion front propagates more slowly than the velocity of the oxygen but faster than the velocity of the temperature.

We constructed possible generic wave sequences that could be observed for large time. Identifying generic wave sequences is more complex when $a < b$ is assumed. Also the number of wave sequences increased by four. The wave sequences which include both

an intermediate and a fast combustion wave or a slow and a fast combustion wave are the most complicated wave sequences. List of possible wave sequences omitting unstable waves corresponds well to the numerical solutions.

Lastly, we looked at the extension of the combustion model by adding small diffusion term to the oxygen equation. This allowed us to find a bound on the unstable eigenvalues by spectral energy estimates.

BIBLIOGRAPHY

[1] I.Y. Akkutlu and Y.C. Yortsos. The dynamics of in-situ combustion fronts in porous media. *J. of Combustion and Flame*, 134:229–247, 2003.

[2] A.P. Aldushin, I.E. Rumanov, and B.J Matkowsky. Maximal energy accumulation in a superadiabatic filtration combustion wave. *J. of Combustion and Flame*, 118:76–90, 1999.

[3] B. Barker, J. Humpherys, and K. Zumbrun. STABLAB: A MATLAB-Based Numerical Library for Evans Function Computation. *http://www.impact.byu.edu/stablab/*, 2009.

[4] H. Berestycki, B. Nicolaenko, and B. Scheurer. Phase plane analysis of one-dimensional reaction diffusion waves with degenerate reaction terms. *SIAM J. Math. Anal.*, 16:1207–1242, 1985.

[5] J. Billingham. Phase plane analysis of one-dimensional reaction diffusion waves with degenerate reaction terms. *Dyn. Stab. Syst.*, 15:23–33, 2000.

[6] G. Chapiro. *Gas-Solid Combustion in Insulated Porous Media*. PhD thesis, IMPA, 2009.

[7] G. Chapiro, A. A. Mailybaev, A.J. Souza, D. Marchesin, and J. Bruining. Asymptotic approximation of long-time solution for low-temperature filtration combustion. *Comput. Geosciences*, 16:799–808, 2012.

[8] G. Chapiro and D. Marchesin. Non-diffusive combustion waves in insulated porous media. *BJPG*, 2:18–28, 2008.

[9] G. Chapiro, D. Marchesin, and S. Schecter. Combustion waves and riemann solutions in light porous foam. *Journal of Hyperbolic Differential Equations*, 11:295, 2014.

[10] A. Ghazaryan. Nonlinear stability of high Lewis number combustion fronts. *Indiana Univ. Math. J.*, 58:181–212, 2009.

[11] A. Ghazaryan, P. Gordon, and C. Jones. Traveling waves in porous media combustion: Uniqueness of waves for small thermal diffusivity. *J. of Dynam. Differential Equations*, 19:951–966, 2007.

[12] A. Ghazaryan, J. Humpherys, and J. Lytle. Spectral behavior of combustion fronts with high exothermicity. *SIAM J. Appl. Math.*, 73:422–437, 2013.

[13] A. Ghazaryan and C. Jones. On the existence of high Lewis number combustion fronts. *J. of Mathematics and Computers in Simulation*, 82:1133–1141, 2012.

[14] A. Ghazaryan, S. Lafortuna, and P. McLarnan. Stability analysis for combustion fronts traveling in hydraulically resistant porous media. *SIAM J.Appl. Math.*, 75:1225–1244, 2015.

[15] A. Ghazaryan, Y. Latushkin, and S. Schecter. Stability of traveling waves for a class of reaction diffusion systems that arise in chemical reaction models. *SIAM J.Math. Anal.*, 42:2434–2472, 2010.

[16] A. Ghazaryan, Y. Latushkin, and S. Schecter. Stability of traveling waves for degenerate systems of reaction dffusion equations. *Indiana Univ. Math. J.*, 60:443–472, 2011.

[17] A. Ghazaryan, Y. Latushkin, S. Schecter, and Aparecido J.de Souza. Stability of gasless combustion fronts in one-dimensional solids. *Arch. Rational Mech. Anal.*, 198:981–1030, 2010.

[18] A. Ghazaryan, S. Schecter, and P. Simon. Gasless combustion fronts with heat loss. *SIAM J.Appl. Math.*, 73:1303–1326, 2013.

[19] P. Gordon and L. Ryzhik. Traveling fronts in porous media: existence and a singular limit. *Proc. Roy. Soc. London Ser. A*, 462:1965–1985, 2006.

[20] V. Gubernov, G.N. Mercer, H.S. Sidhu, and R.O. Weber. Evan function stability of combustion waves. *SIAM J.Appl. Math.*, 63(4):1259–1275, 2003.

[21] Y.I. Kanel. On steady state solutions to systems of equations arising in combustion theory. *Dokl. Akad. Nauk SSSR*, 149:367–369, 1963.

[22] T. Kapitula. The Evans function and generalized Melnikov integrals. *SIAM J. Math. Anal.*, 30:273–297, 1998.

[23] Todd Kapitula and Keith Promislow. *Spectral and dynamical stability of nonlinear waves*. Springer, 2013.

[24] B. Kazmierczak and V. Volpert. Traveling waves in partially degenerate reaction–diffusion systems. *Math. Model. Nat. Phenom.*, 2:106–125, 2007.

[25] D. Marchesin and S. Schecter. Oxidation heat pulses in two-phase expansive flow in porous media. *Z. Angew. Math. Phys.*, 54:48–83, 2003.

[26] J.C.D. Mota and S. Schecter. Combustion fronts in a porous medium with two layers. *Journal of dynamics and differential equations*, 18(3):615–665, 2006.

[27] J. Rottman-Matthes. Linear stability of traveling waves in first-order hyperbolic PDEs. *J. Dynam. Differential Equations*, 23:365–393, 2011.

[28] J. Rottman-Matthes. Stability of parabolic–hyperbolic traveling waves. *J. Dynam. Differential Equations*, 9:29–62, 2012.

[29] B. Sandstede. Stability of traveling waves. *in Handbook of Dynamical Systems*, 2:983–1055, 2002.

[30] S. Schecter and D. Marchesin. Geometric singular perturbation analysis of oxidation heat pulses for two-phase flow in porous media. *Bull. Braz. Math. Soc.*, 32:237–270, 2001.

[31] D.A. Schult, B.J. Matkowsky, V.A. Volpert, and A.C. Fernandez-Pello. Forced forward smolder combustion. *Combustion and Flame*, 104(1–2):1–26, 1996.

[32] Gerald Teschl. *Ordinary differential equations and dynamical systems*. AMS, 2012.

[33] F. Varas and J.M. Vega. Linear stability of a plane front in solid combustion at large heat of reaction. *SIAM J.Appl. Math.*, 62:1810–1822, 2006.

[34] V. Yurov. *Stability estimates for semigroups and partly parabolic reaction diffusion equation*. PhD thesis, University of Missouri, 2013.

[35] Y. B. Zeldovich, G. I. Barenblatt, V. B. Librovich, and G. M. Makhviladze. *The mathematical theory of combustion and explosion*. Consultants Bureau, New York, 1985.

APPENDIX

Appendix A

Linear stability theorem

Consider the differential operator $\mathcal{L}$ on $L^2(\mathbb{R};\mathbb{C}^N)$ of the following type:

$$\mathcal{L} = \begin{pmatrix} \mathcal{A} & R_{12} \\ R_{21} & \mathcal{G} \end{pmatrix}, \qquad \mathcal{A} = d\partial_{\xi\xi} + a\partial_\xi + R, \qquad \mathcal{G} = B\partial_\xi + D \tag{A.1}$$

where $N = N_1 + N_2$, $d = diag\{d_1, ..., d_{N_1}\}$ and $a = diag\{a_1, ..., a_{N_1}\}$ are constant diagonal matrices with positive entries, $R = R(\xi)$ is a bounded continuous $N_1 \times N_1$ matrix valued function on $\mathbb{R}$, $B = diag\{b_1, ..., b_{N_2}\}$ is a constant diagonal matrix with positive entries, $D = D(\xi)$ is a bounded continuous $N_2 \times N_2$ matrix valued function on $\mathbb{R}$, and $R_{12} = R_{12}(\xi)$, $R_{21} = R_{21}(\xi)$ are bounded continuous $N_1 \times N_2$ and $N_2 \times N_1$ matrix valued functions on $\mathbb{R}$. We assume the existence of limiting values as $\xi \to \pm\infty$, denoted by $\lim_{\xi\to\pm\infty} R(\xi) = R^\pm$, $\lim_{\xi\to\pm\infty} D(\xi) = D^\pm$, $\lim_{\xi\to\pm\infty} R_{12}(\xi) = R_{12}^\pm$, and $\lim_{\xi\to\pm\infty} R_{21}(\xi) = R_{21}^\pm$.

Theorem A.0.1. *[34] Let $0 < \nu$, $Sp(\mathcal{L}) \subset Re\lambda < -\nu \Rightarrow \exists\ K$ such that for all $t \geq 0$, $\|e^{t\mathcal{L}}\| \leq Ke^{-\nu t}$.*

It is important to note that for the system (2.7)–(2.9), Theorem A.0.1 holds in the weighted space $\mathcal{X}_\alpha$.

Next corollary follows from Theorem A.0.1 in the case that the spectrum of $\mathcal{L}_\alpha$ with $\alpha = (\alpha_-, \alpha_+)$, $0 < \alpha_\pm < c - a$ has simple eigenvalue zero at the origin and there is $\nu > 0$ such that $\sup\{Re\lambda : \lambda \in Sp(\mathcal{L}_\alpha)\ and\ \lambda \neq 0\} < -\nu$.

Since 0 is isolated in the spectrum of $\mathcal{L}_\alpha$, we can define the Riesz spectral projection $\mathcal{P}_\alpha^c$ of $\mathcal{X}_\alpha^n$ onto the $N(\mathcal{L}_\alpha)$. Let $\mathcal{P}_\alpha^s = I - \mathcal{P}_\alpha^c$. $\mathcal{P}_\alpha^s$ is projection onto $R(\mathcal{L}_\alpha)$, with kernel $N(\mathcal{L}_\alpha)$.

Corollary A.0.2. *Choose $\nu > 0$, such that $\sup\{Re\lambda : \lambda \in Sp(\mathcal{L}_\alpha)$ and $\lambda \neq 0\} < -\nu$. Then there exists $K > 0$ such that for $t \geq 0$, $\|e^{t\mathcal{L}_\alpha}\mathcal{P}^s_\alpha\|_{R(\mathcal{L}_\alpha)\to R(\mathcal{L}_\alpha)} \leq Ke^{-\nu t}$.*